

**MODIFICATION OF THE DYKSTRA-PARSONS METHOD TO
INCORPORATE BUCKLEY-LEVERETT DISPLACEMENT THEORY FOR
WATERFLOODS**

A Thesis

by

RUSTAM RAUF GASIMOV

Submitted to the Office of Graduate Studies of
Texas A&M University
in partial fulfillment of the requirements for the degree of

MASTER OF SCIENCE

August 2005

Major Subject: Petroleum Engineering

**MODIFICATION OF THE DYKSTRA-PARSONS METHOD TO
INCORPORATE BUCKLEY-LEVERETT DISPLACEMENT THEORY FOR
WATERFLOODS**

A Thesis

by

RUSTAM RAUF GASIMOV

Submitted to the Office of Graduate Studies of
Texas A&M University
in partial fulfillment of the requirements for the degree of

MASTER OF SCIENCE

Approved by:

Chair of Committee, Daulat D. Mamora

Committee Members, Bryan J. Maggard

Robert R. Berg

Head of Department, Stephen A. Holditch

August 2005

Major Subject: Petroleum Engineering

ABSTRACT

Modification of the Dykstra-Parsons Method to Incorporate Buckley-Leverett

Displacement Theory for Waterfloods. (August 2004)

Rustam Rauf Gasimov, B.S., Azerbaijan State Oil Academy

Chair of Advisory Committee: Dr. Daulat D. Mamora

The Dykstra-Parsons model describes layer 1-D oil displacement by water in multilayered reservoirs. The main assumptions of the model are: piston-like displacement of oil by water, no crossflow between the layers, all layers are individually homogeneous, constant total injection rate, and injector-producer pressure drop for all layers is the same. Main drawbacks of Dykstra-Parsons method are that it does not take into account Buckley-Leverett displacement and the possibility of different oil-water relative permeability for each layer.

A new analytical model for layer 1-D oil displacement by water in multilayered reservoir has been developed that incorporates Buckley-Leverett displacement and different oil-water relative permeability and water injection rate for each layer (layer injection rate varying with time). The new model employs an extensive iterative procedure, thus requiring a computer program.

To verify the new model, calculations were performed for a two-layered reservoir and the results compared against that of numerical simulation. Cases were run, in which layer thickness, permeability, oil-water relative permeability and total water injection rate were varied.

Main results for the cases studied are as follows. First, cumulative oil production up to 20 years based on the new model and simulation are in good agreement. Second, model water breakthrough times in the layer with the highest permeability-thickness product

(kh) are in good agreement with simulation results. However, breakthrough times for the layer with the lowest kh may differ quite significantly from simulation results. This is probably due to the assumption in the model that in each layer the pressure gradient is uniform behind the front, ahead of the front, and throughout the layer after water breakthrough. Third, the main attractive feature of the new model is the ability to use different oil-water relative permeability for each layer. However, further research is recommended to improve calculation of layer water injection rate by a more accurate method of determining pressure gradients between injector and producer.

DEDICATION

I wish to dedicate my thesis:

To my daughter, Nezin, the person I love the most, and my wife, Sabina, for her love and support.

To my parents, Rauf and Zulfiya, for all their support, encouragement, sacrifice, and especially for their unconditional love; I love you both.

ACKNOWLEDGEMENTS

I wish to express my sincere gratitude and appreciation to:

Dr. Daulat D. Mamora, chair of my advisory committee, for his continued help and support throughout my research. It was great to work with him.

Dr. J. Bryan Maggard, member of my advisory committee, for his enthusiastic and active participation and guidance during my investigation.

Dr. Robert Berg, member of my advisory committee, for his encouragement to my research, his motivation to continue studying and his always-good mood.

Finally, I want to express my gratitude and appreciation to all my colleagues in Texas A&M University: Marylena Garcia, Anar Azimov, and Adedayo Oyerinde.

TABLE OF CONTENTS

	Page
ABSTRACT.....	iii
DEDICATION.....	v
ACKNOWLEDGEMENTS	vi
TABLE OF CONTENTS	vii
LIST OF FIGURES.....	ix
LIST OF TABLES... ..	xv
 CHAPTER	
I INTRODUCTION	1
1.1 Buckley-Leverett Model.....	1
1.2 Dykstra-Parsons Model.....	2
1.3 Problem Description	4
1.4 Objectives	5
II LITERATURE REVIEW	6
2.1 Buckley-Leverett Frontal Advance Theory	6
2.2 Stiles Method	11
2.3 Dykstra-Parsons Approach	12
III NEW ANALYTICAL METHOD	18
3.1 Calculation Procedure	18
3.2 Case 1.....	29
3.3 Case 2.....	36
3.4 Case 3.....	46
3.5 Case 4.....	53
3.6 Case 5.....	59
3.7 Case 6.....	65
3.8 Case 7.....	72
3.9 Case 8.....	77
3.9 Case 9.....	83

CHAPTER	Page
IV SIMULATION MODEL OVERVIEW	90
V SUMMARY, CONCLUSIONS AND RECOMMENDATIONS	99
5.1 Summary	99
5.2 Conclusions	99
5.3 Recommendations	100
NOMENCLATURE.....	102
REFERENCES.....	104
APPENDIX A.....	106
APPENDIX B.....	108
APPENDIX C.....	116
VITA.....	172

LIST OF FIGURES

FIGURE	Page
1.1 Oil production: comparison of results based on Dykstra-Parsons model, and numerical simulation for 2-layered model, $i_w = 800$ STB/D.....	4
2.1 Typical fractional flow curve as a function of water saturation	7
2.2 Water saturation distribution as a function of distance, before breakthrough in the producing well.....	8
2.3 Water saturation distribution at, and after breakthrough in the producing well...	10
2.4 Schematic piston-like displacement in a layer in the Dykstra-Parsons model....	14
3.1 Corey type relative permeability curves for Case 1	19
3.2 Fractional flow curve for Case 1.....	21
3.3 Schematic representation of the waterflood process at the moment of breakthrough in layer 1	24
3.4 Comparison of oil production rate of new analytical model vs. simulation (Case 1).....	31
3.5 Comparison of water injection rate of new analytical model vs. simulation by layers (Case 1)	32
3.6 Comparison of cumulative oil produced calculated with new analytical model vs. simulation (Case 1)	33
3.7 Oil production rates by layers, new analytical model vs. simulation (Case 1) ...	34
3.8 Water production rate by layers, new analytical model vs. simulation (Case 1)	35
3.9 Total water production rate comparison of new analytical model vs. simulation (Case 1).....	36

FIGURE	Page
3.10 Sets of relative permeabilities for layers one and two (Case 2)	39
3.11 Fractional flow curves for layers one and two respectively (Case 2)	40
3.12 Oil production rate of new analytical model vs. simulation, different sets of relative permeabilities are applied (Case 2)	41
3.13 Water injection rates by layers of new analytical model vs. simulation, different sets of relative permeabilities are applied(Case 2).....	42
3.14 Cumulative oil produced comparison of new analytical model vs. simulation, two sets of relative permeability are provided for each layer (Case 2).....	43
3.15 Oil production rate by layers comparison of new analytical model vs. simulation, two sets of relative permeability are provided for each layer (Case 2).....	44
3.16 Water production rate by layers, comparison of new analytical model vs. simulation, two sets of relative permeability are provided for each layer (Case 2).....	45
3.17 Total water production rate, comparison of new analytical model vs. simulation, two sets of relative permeability are provided for each layer (Case 2).....	46
3.18 Oil production comparison of new analytical model to the simulation, variable kh is applied (Case 3)	48
3.19 Water injection rate comparison of new analytical model versus simulation, variable kh is applied (Case 3)	49
3.20 Cumulative oil produced comparison of new analytical model to the simulation, variable kh is applied (Case 3)	50
3.21 Oil production layer by layer comparison of new analytical model to the simulation, variable kh is applied (Case 3)	51
3.22 Water production layer by layer comparison of new analytical model to the simulation, variable kh is applied (Case 3)	52
3.23 Total water production comparison of new analytical model to the simulation, variable kh is applied (Case 3)	53

FIGURE	Page
3.24 Total oil production comparison of new analytical model versus simulation, variable kh and relative permeability sets are applied (Case 4)	54
3.25 Water injection layer by layer comparison of new analytical model to simulation, variable kh and relative permeability sets are applied (Case 4)	55
3.26 Cumulative oil produced, comparison of new analytical model to simulation, variable kh and relative permeability sets are applied (Case 4)	56
3.27 Oil production layer by layer, comparison of new analytical model to simulation, variable kh and relative permeability sets are applied (Case 4).....	57
3.28 Water production layer by layer, comparison of new analytical model to simulation, variable kh and relative permeability sets are applied (Case 4)	58
3.29 Water production rate, comparison of new analytical model to the simulation, variable kh and relative permeability sets are applied (Case 4)	59
3.30 Oil production rate, comparison of new analytical model to the simulation, injection rate of 1600 STB/D is applied (Case 5)	60
3.31 Water injection rate by layers, comparison of new analytical model to simulation, injection rate of 1600 STB/D is applied (Case 5)	61
3.32 Cumulative oil production, comparison of new analytical model to simulation, injection rate of 1600 STB/D is applied (Case 5)	62
3.33 Oil production rate on layer basis, comparison of new analytical model to simulation, injection rate of 1600 STB/D is applied (Case 5)	63
3.34 Water production on layer basis, comparison of new analytical model to simulation, injection rate of 1600 STB/D is applied (Case 5)	64
3.35 Water production rate, comparison of new analytical model to simulation, injection rate of 1600 STB/D is applied (Case 5)	65
3.36 Oil production rate, comparison of new analytical model to simulation, 2 relative permeability sets and injection rate of 1600 STB/D are applied (Case 6).....	66

FIGURE	Page
3.37 Water injection rate by layers, comparison of new analytical model to simulation, 2 relative permeability sets and injection rate of 1600 STB/D are applied (Case 6).....	67
3.38 Cumulative oil produced, comparison of new analytical model to simulation, 2 relative permeability sets and injection rate of 1600 STB/D are applied (Case 6).....	68
3.39 Oil production rate by layers, comparison of new analytical model to simulation, 2 relative permeability sets and injection rate of 1600 STB/D are applied (Case 6).....	69
3.40 Water production rate by layers, comparison of new analytical model to simulation, 2 relative permeability sets and injection rate of 1600 STB/D are applied (Case 6).....	70
3.41 Total water production rate, comparison of new analytical model to simulation, 2 relative permeability sets and injection rate of 1600 STB/D are applied (Case 6).....	71
3.42 Oil production rate, comparison of new analytical model to simulation, different kh and injection rate of 1600 STB/D are applied (Case 7).....	72
3.43 Water injection rate by layers, comparison of new analytical model to simulation, different kh and injection rate of 1600 STB/D are applied (Case 7).....	73
3.44 Cumulative oil produced, comparison of new analytical model to simulation, different kh and injection rate of 1600 STB/D are applied.	74
3.45 Oil production by layers, comparison of new analytical model to simulation, different kh and injection rate of 1600 STB/D are applied (Case 7).....	75
3.46 Water production by layers, comparison of new analytical model to simulation, different kh and injection rate of 1600 STB/D are applied (Case 7).....	76
3.47 Total water production, comparison of new analytical model to simulation, different kh and injection rate of 1600 STB/D are applied (Case 7).....	77
3.48 Total oil production rate, comparison of new analytical model to simulation, 2 relative permeability sets and injection rate of 1600 STB/D are applied (Case 8).....	78

FIGURE	Page
3.49 Water injection rate by layers, comparison of new analytical model to simulation, 2 relative permeability sets and injection rate of 1600 STB/D are applied (Case 8).....	79
3.50 Cumulative oil, comparison of new analytical model to simulation, 2 relative permeability sets and injection rate of 1600 STB/D are applied (Case 8)	80
3.51 Oil production by layers, comparison of new analytical model to simulation, 2 relative permeability sets and injection rate of 1600 STB/D are applied (Case 8).....	81
3.52 Water production by layers, comparison of new analytical model to simulation, 2 relative permeability sets and injection rate of 1600 STB/D are applied (Case 8).....	82
3.53 Water production rate, comparison of new analytical model to simulation, 2 relative permeability sets and injection rate of 1600 STB/D are applied (Case 8).....	83
3.54 Oil production rate, comparison of new analytical model to simulation, for 2 identical layers (Case 9)	84
3.55 Water injection rate by layers, comparison of new analytical model to simulation, for 2 identical layers (Case 9).....	85
3.56 Cumulative oil produced, comparison of new analytical model to simulation, for 2 identical layers (Case 9)	86
3.57 Oil production by layers, comparison of new analytical model to simulation, for 2 identical layers (Case 9)	87
3.58 Water production by layers, comparison of new analytical model to simulation, for 2 identical layers (Case 9)	88
3.59 Water production rate, comparison of new analytical model to simulation, for 2 identical layers (Case 9)	89
4.1 Simulation results indicate cumulative oil production with and without grid refinement is practically identical.....	91
4.2 Simulation results for Case 1 at 274 days, showing earlier water breakthrough in layer that has a higher kh	93

FIGURE	Page
4.3 Simulation results for Case 2 at 274 days, showing faster waterflood displacement in lower layer, which has different oil-water relative permeability.....	94
4.4 Simulation results for Case 3 at 274 days, showing faster water front propagation in upper layer that has a higher kh value.....	94
4.5 Simulation results for Case 4 at 274 days, showing faster oil displacement in upper layer that has a higher kh value.....	95
4.6 Simulation results for Case 5 at 274 days, showing that flood front advanced more than that in Case 1, as water injection rate was doubled.....	95
4.7 Simulation results for Case 6 at 274 days, showing similarity to Case 2 except that lower layer broke through.....	96
4.8 Simulation results for Case 7 at 274 days, showing faster front propagation than that in Case 3 due to increased injection rate	96
4.9 Simulation results for Case 8 at 274 days, showing faster front propagation than that in Case 4 due to increased injection rate	97
4.10 Simulation results for Case 9 at 274 days, showing identical displacement in both layers, as both layers have identical reservoir properties.....	97
4.11 Injector-producer pressure drop for simulation model on example of Case 3.....	98

LIST OF TABLES

TABLE	Page
3.1 Reservoir Properties for Case 1.....	30
3.2 Reservoir Properties of Layer 1 for Case2.....	37
3.3 Reservoir Properties of Layer 2 for Case 2.....	38
3.4 Height and Permeability Variation in Layers 1 and 2.....	47
4.1 Summary of Reservoir Properties for Each Case.....	92
4.2 Oil-Water Relative Permeability Set Parameters.....	92

CHAPTER I

INTRODUCTION

1.1 Buckley-Leverett Model

In 1941, Leverett¹ in his pioneering paper presented the concept of fractional flow. Beginning with the Darcy's law for water and oil 1-D flow, he formulated the following fractional flow equation:

$$f_w = \frac{1 + \frac{k k_{ro}}{q_t \mu_o} \left(\frac{\partial P_c}{\partial x} - g \Delta \rho \sin \alpha \right)}{1 + \frac{\mu_w k_{ro}}{\mu_o k_{rw}}}, \dots \dots \dots (1.1)$$

where f_w is the fractional flow of water, q_t is the total flow rate of oil and water, k_{ro} and k_{rw} are relative permeabilities of oil and water respectively, μ_o and μ_w are viscosities of oil and water respectively, $\frac{\partial P_c}{\partial x}$ is the capillary pressure gradient, $\Delta \rho$ is the density difference ($\rho_o - \rho_w$), α is the reservoir dip angle, and g is the gravitational constant.

For the case where the reservoir is horizontal ($\alpha = 0$), **Eq. 1.1** reduces to:

This thesis follows the style of the *Journal of Petroleum Technology*.

$$f_w = \frac{1}{1 + \frac{\mu_w k_{ro}}{\mu_o k_{rw}}} \dots\dots\dots(1.2)$$

In 1946, Buckley and Leverett² presented the frontal advance equation. Applying mass balance to a small element within the continuous porous medium, they expressed the difference at which the displacing fluid enters this element and the rate at which it leaves it in terms of the accumulation of the displacing fluid.

This led to a description of the saturation profile of the displacing fluid as a function of time and distance from the injection point. The most remarkable outcome of their displacement theory was the presence of a shock front. The frontal advance equation obtained was:

$$\left(\frac{\partial x}{\partial t}\right)_{S_w} = \frac{q_t}{A\phi} \left(\frac{\partial f_w}{\partial S_w}\right)_t \dots\dots\dots(1.3)$$

where q_t is a total volumetric liquid rate, equal to $q_w + q_o$, A is the cross-sectional area of flow, ϕ is porosity, S_w is water saturation.

1.2 Dykstra-Parsons Model

An early paper by Dykstra and Parsons³ presented a correlation between waterflood recovery and both mobility ratio and permeability distribution. This correlation was based on calculations applied to a layered linear model with no crossflow.

This first work on vertical stratification with inclusion of mobility ratios other than unity was presented in the work of Dykstra and Parsons who have developed an approach for handling stratified reservoirs, which allows calculating waterflood performance in multi-

layered systems. But their method requires the assumption that the saturation behind the flood front is uniform, i.e. only water moves behind the waterflood front. There are other assumptions involved such as: linear flow, incompressible fluid, piston-like displacement, no cross flow, homogeneous layers, constant injection rate, and the pressure drop (ΔP) between injector and producer across all layers is the same.

Governing equation for Dykstra-Parsons front propagation is as follows:

$$\frac{x_j}{x_n} = \frac{M - \sqrt{M^2 + \left(\frac{k_j}{k_n}\right) [(1-M)^2]}}{(1-M)}, \dots \dots \dots (1.4)$$

where M is the end point mobility ratio, x_n is the distance of front propagation of the layer in which water just broke through, which is equal to L the total layer length; x_j is the distance of water front of the next layer to be flooded after layer n .

Generalizing **Eq. 1.4** for N -number of layers, the coverage (vertical sweep efficiency) can be obtained:

$$C_n = \frac{n}{N} + \sum_{n+1}^N \left[\frac{M - \sqrt{M^2 + \left(\frac{k_j}{k_n}\right) [(1-M)^2]}}{(1-M)N} \right], \dots \dots \dots (1.5)$$

where C_n is the vertical coverage after n layers have been flooded, n is the layer in which water just broke through.

1.3 Problem Description

For many years analytical models have been used to estimate performance of waterflood projects. The Buckley-Leverett frontal advance theory and Dykstra-Parsons method for stratified reservoirs have been used for this purpose, but not in combination for stratified reservoirs with different kh and oil-water relative permeability.

The Dykstra-Parsons method has a major drawback in that it assumes the displacement of oil by water is piston-like. As illustration, I have compared oil production rate estimated by Dykstra-Parsons method against that from numerical simulation (GeoQuest Eclipse 100). For the comparison, I used a 2-layered reservoir with the following parameters: length L -1200 ft., width w -400 ft., height h -35 ft. each layer, with total injection rate i_{wr} -800 STB/D. The results are shown in **Fig. 1.1** The following observation can be made.

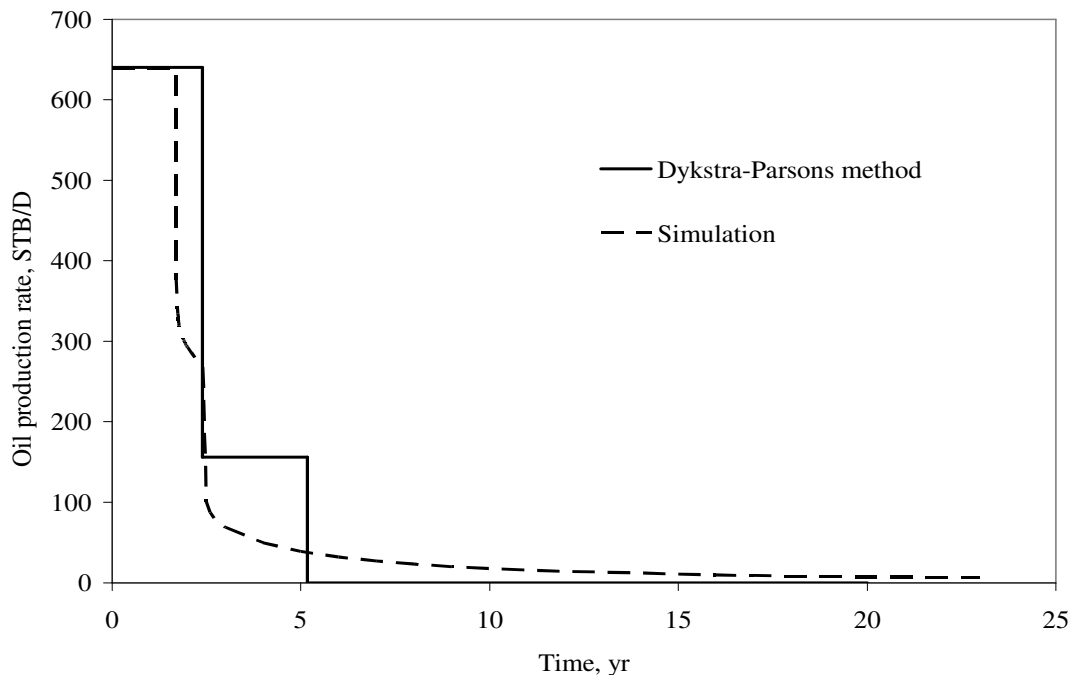


Figure 1.1 Oil production: comparison of results based on Dykstra-Parsons model, and numerical simulation for 2-layered model, $i_w = 800$ STB/D.

First, the water breakthrough time based on simulation is significantly earlier compared to that from Dykstra-Parsons method. Second, cumulative oil produced at the moment of breakthrough in layer 1, is more for the Dykstra-Parsons analytical model compared to simulation. This is because Dykstra-Parsons model assumes that at breakthrough, all moveable oil has been swept from layer 1, whereas in the simulation model at breakthrough, there is still moveable oil behind the front.

1.4 Objectives

The goal of this research is to modify the Dykstra-Parsons method for 1-D oil displacement by water in such a manner that it would be possible to incorporate the Buckley-Leverett frontal advance theory. This would require modeling fractional flow behind the waterflood front instead of assuming piston-like displacement. By incorporating Buckley-Leverett displacement, a more accurate analytical model of oil displacement by water is expected. Permeability-thickness and oil-water relative permeability will be different for each layer, with no crossflow between the layers. The analytical model results (injection rate, water and oil production rate) will be compared against simulation results to ensure the validity of the analytical model.

CHAPTER II

LITERATURE REVIEW

2.1 Buckley-Leverett Frontal Advance Theory

Since the original paper of Dykstra-Parsons, a great number of papers have suggested some modifications to the basic approach. The literature review gives the reader an overview of these modifications.

Buckley and Leverett (1946): The Buckley-Leverett frontal advance theory considers the mechanism of oil displacement by water in a linear 1-D system. An equation was developed for calculating the frontal advance rate. In the Buckley-Leverett approach oil displacement occurred under so-called diffuse flow condition, which means that fluid saturations at any point in the linear displacement path are uniformly distributed with respect to thickness.

The fractional flow of water, at any point in the reservoir, is defined as

$$f_w = \frac{q_w}{q_o + q_w}, \dots\dots\dots(2.1)$$

where q_w is water flow rate, and q_o is oil flow rate.

Using Darcy's law for linear one dimensional flow of oil and water, considering the displacement in a horizontal reservoir, and neglecting the capillary pressure gradient we get the following expression:

$$f_w = \frac{1}{1 + \frac{\mu_w k_{ro}}{k_{rw} \mu_o}} \dots\dots\dots(2.2)$$

Provided the oil displacement occurs at a constant temperature then the oil and water viscosities have fixed values and **Eq. 2.2** is strictly a function of the water saturation. This is illustrated in **Fig. 2.1** for typical oil-water relative permeability and properties.

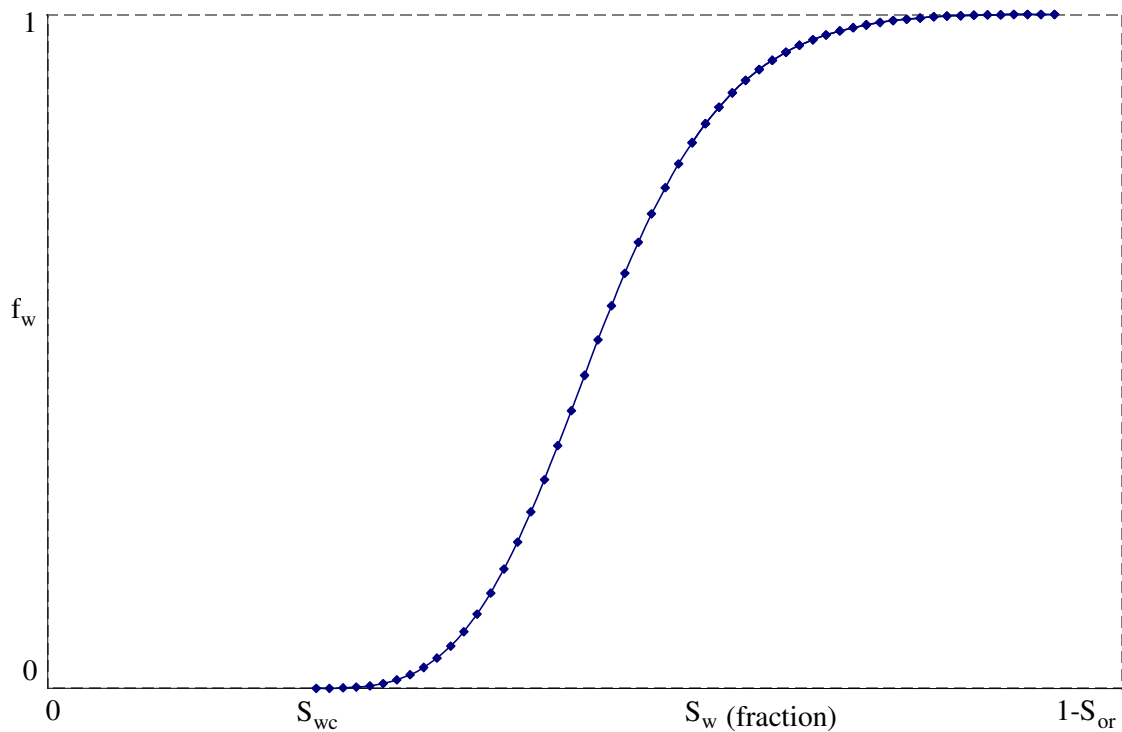


Figure 2.1 Typical fractional flow curve as a function of water saturation.

In their paper Buckley and Leverett presented what is recognized as the basic equation describing immiscible displacement in one dimension. For water displacing oil, the equation describes the velocity of a plane of constant water saturation traveling through

the linear system. Assuming the diffuse flow conditions and conservation of mass of water flowing through volume element Adx :

$$x_{S_w} = \frac{W_i}{A\phi} \frac{df_w}{dS_w} \Big|_{S_w}, \dots\dots\dots(2.3)$$

where W_i is the cumulative water injected and it is assumed, as an initial condition, that $W_i = 0$ when $t = 0$.

There is a mathematical difficulty encountered in applying this technique, which exists due to the nature of the fractional flow curve creating a saturation discontinuity or a shock front.

In 1952 Welge⁴ presented the simplified method to the frontal advance equation. This method consists of integrating the saturation distribution over the distance from the injection point to the front, obtaining the average water saturation behind the front $\overline{S_w}$.

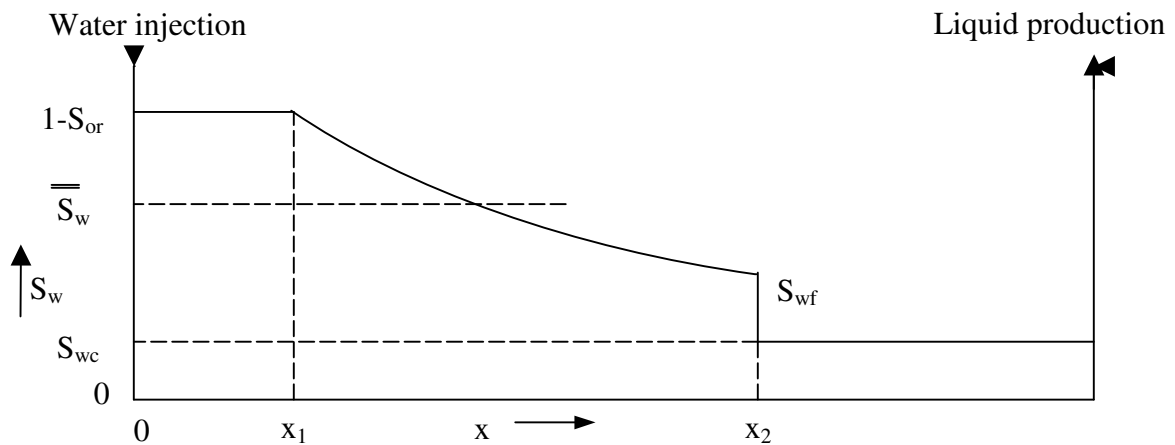


Figure 2.2 Water saturation distribution as a function of distance, before breakthrough in the producing well⁵.

Fig. 2.2 presents water saturation profile as a function of distance.

Applying the simple material balance:

$$W_i = x_2 A \phi (\overline{S_w} - S_{wc}), \dots \dots \dots (2.4)$$

where $\overline{S_w}$ is average water saturation behind the front, x_1 is distance in the reservoir totally flooded by water, x_2 is distance of waterflood front location.

Eqs. 2.3 and **2.4** yield the following solution to $\overline{S_w}$:

$$\overline{S_w} - S_{wc} = \frac{W_i}{x_2 A \phi} = \frac{1}{\left. \frac{df_w}{dS_w} \right|_{S_{wf}}} \dots \dots \dots (2.5)$$

The expression for the average water saturation behind the front can also be obtained by direct integration of the saturation profile as

$$\overline{S_w} = \frac{(1 - S_{or})x_1 + \int_{x_1}^{x_2} S_w dx}{x_2} \dots \dots \dots (2.6)$$

And since $x_{S_w} \propto \left. \frac{df}{dS_w} \right|_{S_w}$ the **Eq. 2.6** can be expressed as

$$\overline{S_w} = \frac{(1 - S_{or}) \left. \frac{df_w}{dS_w} \right|_{1-S_{or}} + \int_{x_1}^{x_2} S_w d \left(\frac{df_w}{dS_w} \right)}{\left. \frac{df_w}{dS_w} \right|_{S_{wf}}} \dots \dots \dots (2.7)$$

After rearranging **Eq. 2.7**,

$$\overline{S_w} = S_{wf} + (1 - f_w|_{S_{wf}}) \left/ \frac{df_w}{dS_w} \right|_{S_{wf}} \dots\dots\dots(2.8)$$

Note that for $f_w = 0$, **Eq. 2.8** reduces to **Eq. 2.5**.

Cumulative oil production at the breakthrough can be expressed by following equation:

$$N_{pDbt} = W_{iDbt} = q_{iD} t_{bt} = (\overline{S_w} - S_{wc}) = \frac{1}{\left. \frac{df_w}{dS_w} \right|_{S_{wbt}}} \dots\dots\dots(2.9)$$

where N_{pDbt} is dimensionless cumulative oil produced at the moment of breakthrough,

W_{iDbt} is dimensionless cumulative water injected at the moment of breakthrough.

Eq. 2.5 is true only for the waterflood before and at the point of breakthrough.

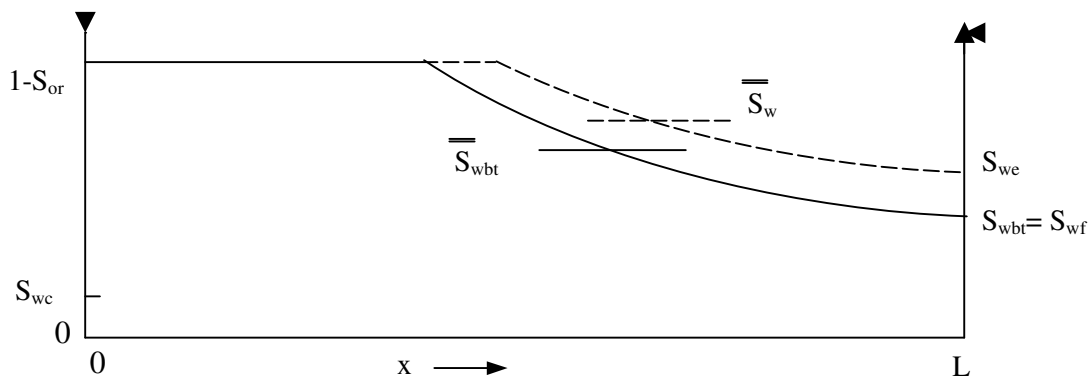


Figure 2.3 Water saturation distributions at, and after breakthrough in the producing well⁵.

From the **Fig. 2.3**, S_{we} is the current value of the water saturation at the producing well after water breakthrough. Water saturation by the Welge technique gives:

$$\overline{S}_w = S_{we} + (1 - f_{we}) \frac{1}{\left. \frac{df_w}{dS_w} \right|_{S_{we}}} \dots \dots \dots (2.10)$$

Following **Eq. 2.9** oil recovery after water breakthrough can be expressed as:

$$N_{pD} = \overline{S}_w - S_{wc} = (S_{we} - S_{wc}) + (1 - f_{we}) W_{iD} \dots \dots \dots (2.11)$$

2.2 Stiles Method

Stiles⁶ (1949): This method for predicting the performance of waterflood operations basically involves accounting for permeability variations, vertical distribution of flow capacity kh . Most important assumption was that within the reservoir of various permeabilities injected water sweeps first the zones of higher permeability and that first breakthrough occurs in these layers. The different flood-front positions in liquid-filled, linear layers having different permeabilities, each layer insulated from the others. Stiles assumes that the rate of water injected into each layer depends only upon the kh of that layer. This is equivalent to assuming a mobility ratio of unity. Also it is assumed that fluid flow is linear and the distance of penetration of the flood front is proportional to permeability-thickness product.

The Stiles method assumes that there is piston-like displacement of oil, so that after water breakthrough in a layer, only water is produced from that layer. After water breakthrough, the producing WOR is found as follows:

$$WOR = \frac{\kappa k_{rw} \mu_o}{1 - \kappa \mu_w k_{ro}} B_o, \dots \dots \dots (2.12)$$

where κ is the fraction of the total flow capacity represented by layers having water breakthrough. In addition, the Stiles method assumes a unit mobility ratio. In his work Stiles rearranged the layers depending on their permeability in descending manner.

Later Johnson⁷ developed a graphical approach that simplified the consideration of layer permeability and porosity variations. Layer properties were chosen such that each had equal flow capacities so that the volumetric injection rate into each layer was the same.

2.3 Dykstra-Parsons Approach

Dykstra and Parsons (1950): An early paper presented a correlation between waterflood recovery and both mobility ratio and permeability distribution. This correlation was based on calculations applied to a layered linear model with no crossflow.

More than 200 flood pot tests were made on more than 40 California core samples in which initial fluid saturations, mobility ratios, producing *WOR*'s, and fractional oil recoveries were measured. The permeability distribution was measured by the coefficient of permeability variation.

The correlations presented by Dykstra-Parsons related oil recovery at producing *WOR*'s of 1, 5, 25, and 100 as a fraction of the oil initially in place to the permeability variation, mobility ratio, and the connate-water and flood-water saturations. The values obtained assume a linear flood since they are based upon linear flow tests.

The Dykstra-Parsons method considers the effect of vertical variations of horizontal permeabilities for the waterflood performance calculation. Similar to the Stiles method, permeabilities are arranged in descending order. Following is a full list of assumptions for Dykstra-Parsons approach.

- (1) Linear flow

- (2) Incompressible displacement
- (3) Piston-like displacement
- (4) Each layer is a homogenous layer
- (5) No crossflow between layers
- (6) Pressure drop for all layers is the same
- (7) Constant water injection rate
- (8) Velocity of the front is proportional to absolute permeability and end point mobility ratio of the layer

As there is a piston-like displacement in each layer, flow velocity of oil and water in any layer can be expressed as:

$$v_o = -\frac{k_o}{\mu_o} \frac{dP}{dx}, \dots\dots\dots(2.13)$$

$$v_w = -\frac{k_w}{\mu_w} \frac{dP}{dx}, \dots\dots\dots(2.14)$$

where k_o is effective oil permeability and k_w effective water permeability. **Fig. 2.4** shows the sample of piston-like displacement.

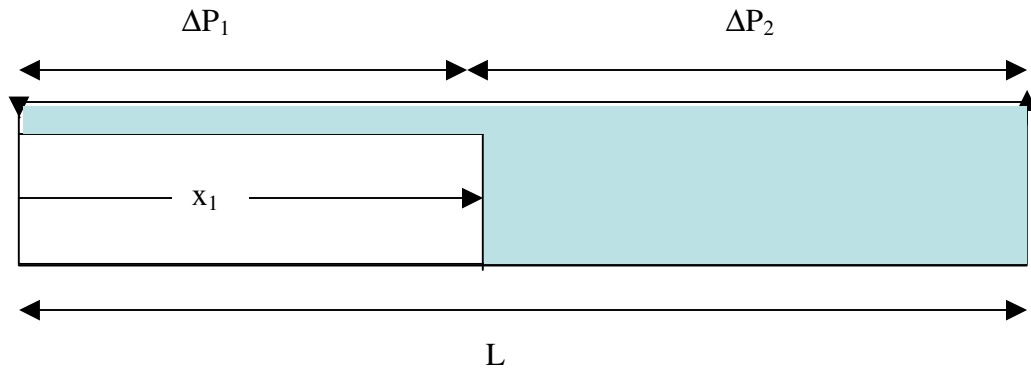


Figure 2.4 Schematic piston-like displacement in a layer in the Dykstra-Parsons model.

From assumption 6,

$$\Delta P = \Delta P_1 + \Delta P_2 \dots\dots\dots(2.15)$$

Subsequently **Eqs. 2.13** and **2.14** can be presented as:

$$v_w = -\frac{k_w}{\mu_w} \frac{\Delta P_1}{x_1} \dots\dots\dots(2.16)$$

$$v_o = -\frac{k_o}{\mu_o} \frac{\Delta P_2}{(L - x_1)} \dots\dots\dots(2.17)$$

Assuming incompressible flow, $v_o = v_w$. After rearranging **Eqs. 2.16** and **2.17** and substitute in **Eq. 2.15**:

$$v_w \left(\frac{x_1 \mu_w}{k_w} \right) + v_o \left(\frac{\mu_o (L - x_1)}{k_o} \right) = -\Delta P \dots\dots\dots(2.18)$$

Rearranging **Eq. 2.18**,

$$v_o = \frac{-\Delta P}{\frac{\mu_w}{k_w} x_1 + \frac{\mu_o}{k_o} (L - x_1)} \dots\dots\dots(2.19)$$

Effective permeability for oil and water can be expressed as $k_o = kk_{ro}$, $k_w = kk_{rw}$, which on substituting into **Eq. 2.19** yields:

$$v_o = \frac{-k_1 \Delta P}{\frac{\mu_w}{k_{rw}} x_1 + \frac{\mu_o}{k_{ro}} (L - x_1)} \dots\dots\dots(2.20)$$

Using assumption that k_{rw} and k_{ro} are the same for all layers:

$$\frac{v_{oi}}{v_o} = \frac{k_i \left(\frac{\mu_w}{k_{rw}} x_1 + \frac{\mu_o}{k_{ro}} (L - x_1) \right)}{k_1 \left(\frac{\mu_w}{k_{rw}} x_i + \frac{\mu_o}{k_{ro}} (L - x_i) \right)} \dots\dots\dots(2.21)$$

The end point mobility ratio is defined as:

$$M_{ep} = \frac{k_{rwe} \mu_o}{\mu_w k_{roe}} \dots\dots\dots(2.22)$$

Eq. 2.21 may be rearranged and integrated with respect to x to give the following expression:

$$(1 - M_{ep}) \left(\frac{x_i}{L} \right)^2 + 2M_{ep} \left(\frac{x_i}{L} \right) - \frac{k_i}{k_1} (1 + M_{ep}) = 0 \dots\dots\dots(2.23)$$

Eq. 2.23 is a quadratic equation, therefore solving for $\frac{x_i}{L}$:

$$\frac{x_i}{L} = \frac{M_{ep} \pm \left(M_{ep}^2 + \frac{k_i}{k_1} (1 - M_{ep})^2 \right)^{0.5}}{(M_{ep} - 1)} \dots\dots\dots(2.24)$$

Generalizing Dykstra-Parsons **Eq. 2.24** for any two layers with $k_n > k_j$, and n is the layer, in which water just broke through:

$$\frac{x_j}{x_n} = \frac{M_{ep} - \left(M_{ep}^2 + \frac{k_j}{k_n} (1 - M_{ep})^2 \right)^{0.5}}{(M_{ep} - 1)} \dots\dots\dots(2.25)$$

Finally expression for the coverage can be obtained:

$$C_n = \frac{n + \sum_{n+1}^N \frac{x_j}{x_n}}{N} = n + \sum_{n+1}^N \left[\frac{M_{ep} - \left(M_{ep}^2 + \frac{k_j}{k_n} (1 - M_{ep})^2 \right)^{0.5}}{N(M_{ep} - 1)} \right] \dots\dots\dots(2.26)$$

And after rearrangement:

$$C_n = \frac{n + \frac{(N - n)M_{ep}}{M_{ep} - 1} - \frac{1}{M_{ep} - 1} \sum_{n+1}^N M_{ep} - \left(M_{ep}^2 + \frac{k_j}{k_n} (1 - M_{ep})^2 \right)^{0.5}}{N} \dots\dots\dots(2.27)$$

where N is the total number of layers.

Kufus and Lynch⁸ (1959): Kufus and Lynch in their paper presented work which can incorporate Buckley-Leverett theory in the Dykstra-Parsons calculations. Important assumptions Kufus and Lynch have made were that all layers have same relative permeability curves to oil and water and water injection rate in each layer is constant value and dependent only on the absolute permeability and on fraction of average water relative permeability to average fractional flow in the current layer, which is made

similar to Dykstra-Parsons model.. The data presented in the paper were valid only for viscosity ratio of unity. And as in Dykstra-Parsons it was assumed that relative permeabilities to oil and water were same for all layers.

Mobility ratio was represented by following equation:

$$M = \frac{\mu_o}{\mu_w k'_{ro}} \left(\frac{k_{rw}}{f_w} \right)_{av} \dots\dots\dots (2.28)$$

where k'_{ro} is the oil relative permeability ahead of the waterflood front. Using computation procedure the major parameters can be calculated.

Hiatt⁹ (1958): Hiatt presented a detailed prediction method concerned with the vertical coverage or vertical sweep efficiency attained by a waterflood in a stratified reservoir. Using a Buckley-Leverett type of displacement, he considered, for the first time, crossflow between layers. The method is applicable to any mobility ratio, but is difficult to apply.¹²

Warren and Cosgrove¹⁰ (1964): presented an extension of Hiatt's original work. They considered both mobility ratio and crossflow effects in a reservoir whose permeabilities were log-normally distributed. No initial gas saturation was allowed, and piston-like displacement of oil by water was assumed. The displacement process in each layer is represented by a sharp "pseudointerface" as in the Dykstra-Parsons model.

Reznik¹¹ *et al.* (1984): In this work the original Dykstra-Parsons discrete solution has been extended to continuous, real time basis. Work has been made considering two injection constraints: pressure and rate. This analytical model assumes piston-like displacement. The purpose of the paper was to extend the analytical, but discrete, stratification model of Dykstra-Parsons to analytically continuous space-time solutions. The Reznik *et al.* work retained the piston-like displacement assumption.

CHAPTER III

NEW ANALYTICAL METHOD

The main drawbacks of the Dykstra-Parsons method are that (1) oil displacement by water is piston-like, and (2) relative permeability end-point values are the same for all layers. Applying Buckley-Leverett theory to each layer is also not correct because it would mean that water injection rate is (1) constant for each layer, and (2) proportional to the kh of each layer.

Thus a new analytical model has been developed with the following simplifying main assumptions:

- (1) Pressure drop for all layers is the same.
- (2) Total water injection rate is constant.
- (3) Oil-water relative permeabilities may vary for each layer.
- (4) Water injection rate in each layer may vary.

3.1 Calculation procedure

The equations and steps used in the new analytical method are as follows. For simplicity, the method has been applied to a 2-layered system with no cross-flow.

Step 1-Calculate oil-water relative permeabilities

For relative permeability calculation Corey¹³ type relative permeability curves for oil and water have been used.

For oil
$$k_{ro} = k_{roe} \left(\frac{(S_o - S_{or})}{(1 - S_{wc} - S_{or})} \right)^{n_o} \dots\dots\dots(3.1)$$

where n_o is Corey exponent for oil

For water

$$k_{rw} = k_{rwe} \left(\frac{(S_w - S_{wc})}{(1 - S_{wc} - S_{or})} \right)^{n_w} \dots\dots\dots(3.2)$$

where n_w is Corey exponent for water

Using Corey equation the following relative permeability curves shown on **Fig. 3.1** were obtained:

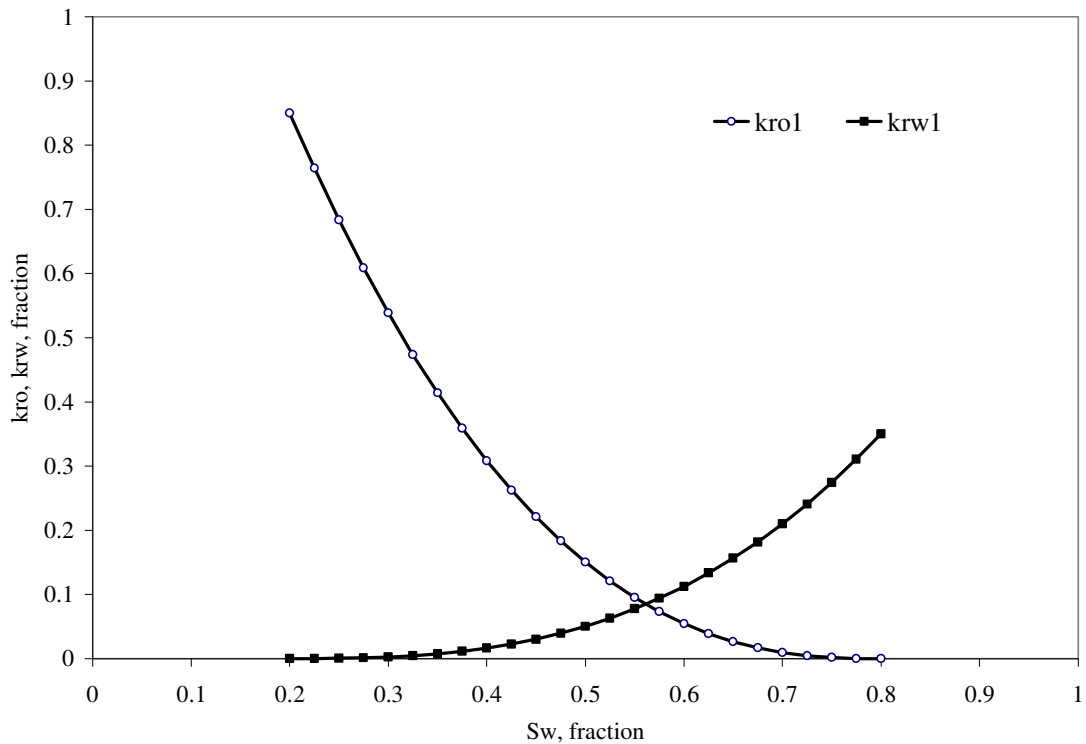


Figure 3.1 Corey type relative permeability curves for Case 1.

Step 2-Fractional flow calculations

After obtaining relative permeabilities for oil and water, the fractional flow curve is to be found. Using definition of fractional flow, f_w (**Eq. 2.2**), and substituting for k_{ro} and k_{rw} from **Eqs. 3.1** and **3.2**, we obtain:

$$f_w = \frac{1}{1 + \frac{\mu_w}{\mu_o} \frac{k_{roe} (S_o - S_{or})^{n_o} (1 - S_{wc} - S_{or})^{n_w}}{k_{rwe} (S_w - S_{wc})^{n_w} (1 - S_{wc} - S_{or})^{n_o}}}. \quad \dots\dots\dots(3.3)$$

Applying Welge technique: average saturation behind the waterflood front \bar{S}_w , fractional flow at the water breakthrough f_{wbt} , and water saturation at the breakthrough S_{wbt} are found. One necessary step is to calculate the fractional flow derivative $\frac{df_w}{dS_w}$. In order to perform this operation with the more precision; we must take derivative of **Eq. 3.3**. After necessary mathematical derivation the following equation should be used:

$$\frac{df_w}{dS_w} = (f_w - f_w^2) \left[\frac{n_o}{(1 - S_w - S_{or})} + \frac{n_w}{(S_w - S_{wc})} \right]. \quad \dots\dots\dots(3.4)$$

Fractional flow curve is shown on **Fig. 3.2**.

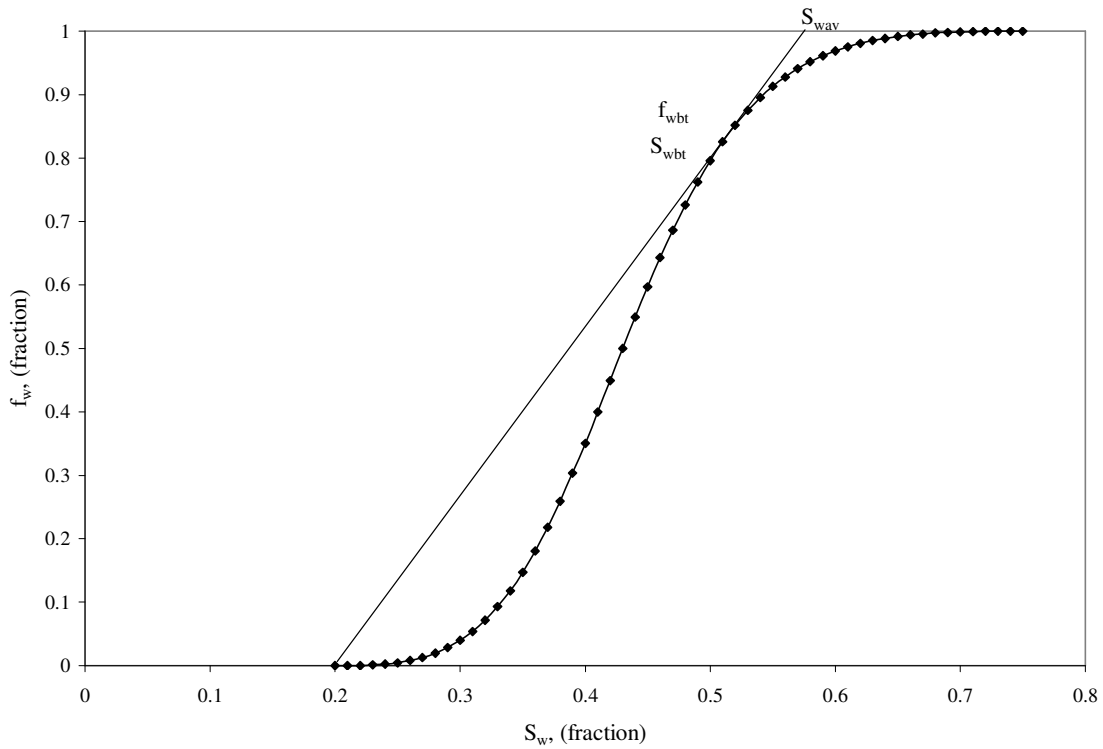


Figure 3.2 Fractional flow curve for Case 1.

Step 3-Estimate water injected in layer 1 at the moment of breakthrough

After obtaining the fractional flow, we calculate cumulative water injection in layer 1 at the moment of breakthrough. As we know the cumulative water injection in first layer at the moment of breakthrough W_{ilbr} can be calculated using Buckley-Leverett theory:

$$W_{ilbr} = PV \left(\overline{S_{wbt}} - S_{wc} \right) \dots\dots\dots(3.5)$$

where $PV = Lwh\phi/5.615$ is the pore volume of the first layer.

Step 4-Estimate water injection rate in layer 1

Although total injection rate is constant, water injection rate for each layer is going to change with time as the relative permeabilities of water and oil are going to change.

Because of that we can not use the following approach in calculating the water injection rate for layer 1:

$$i_{w1} = \frac{k_1 h}{\sum kh} i_{wt} \dots\dots\dots(3.6)$$

But **Eq. 3.6** can be used as an initial estimate or guess in the iterative procedure.

Step 5-Calculation of the time of breakthrough

After obtaining value of water injection rate in layer 1 using **Eq. 3.6**, the following steps should be taken: Using **Eq. 3.5** estimate water injection rate in layer 1, after which calculate time of breakthrough

$$t_{bt} = \frac{W_{i1bt}}{i_{w1}} \dots\dots\dots(3.7)$$

Step 6-Calculation of total cumulative water injected

In this step total cumulative water injected at the time of breakthrough is calculated,

$$W_{ibt} = i_{wt} t_{bt} \dots\dots\dots(3.8)$$

Step 7-Calculation of water injected in layer 2

Since the total cumulative water injection and cumulative water injection in layer 1 are available, from material balance the cumulative water injection in layer 2 can be obtained.

$$W_{i2} = W_{ibt} - W_{i1bt} \dots\dots\dots(3.9)$$

Step 8-Calculation of average water saturation in layer 2, pore volume displaced by water in layer 2 and location of waterflood in layer 2

Described process occurs at Buckley-Leverett frontal displacement, so the average water saturation of second layer behind the front before breakthrough is constant and equal to first layer average water saturation behind the front at the moment of breakthrough.

$$\overline{S}_{w2} = \frac{W_{i2}}{PV_x} + S_{wc2} = \frac{1}{f'_{w2}} + S_{wc2}, \dots \dots \dots (3.10)$$

where f'_{w2} is constant and equal to f'_{w1br} , PV_x is pore volume of layer 2 displaced by water. From **Eq. 3.10** we can obtain PV_x :

$$PV_x = W_{i2} f'_{w2}. \dots \dots \dots (3.11)$$

Main point of this calculation is to find x – the location of waterflood front in layer 2. It can be done using following expression

$$PV_x = xwh\phi/5.615. \dots \dots \dots (3.12)$$

The importance of x – value is crucial for the calculations after the layer 1 broke through as it is only controlling parameter specifying at which step after layer 1 broke through layer 2 is going to break through. **Fig. 3.3** shows waterflood process at the moment of water breakthrough in layer 1.

Step 9-Recalculation of water injection rate in layer 1

We need to develop different approach for calculating i_{w1} ; as it has been assumed the pressure gradient across all layers is the same

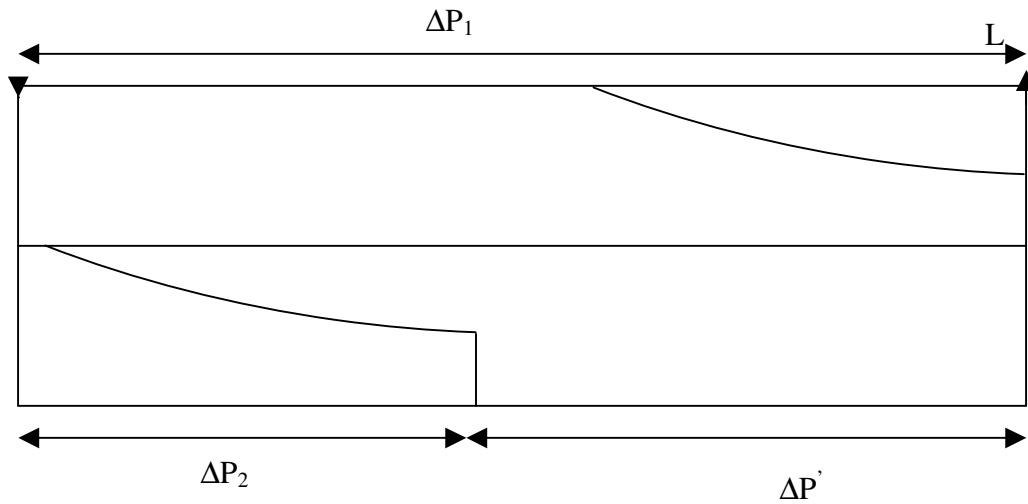


Figure 3.3 Schematic representation of the waterflood process at the moment of breakthrough in layer 1.

From this assumption the following expression can be derived:

$$\Delta P_1 = \Delta P_2 + \Delta P' \dots\dots\dots(3.13)$$

From Darcy’s law, water injection rate in layer 1 can be expressed as

$$i_{w1} = \frac{ck_1 \overline{k_{rw1}}}{\mu_w} \frac{\Delta P_1}{L} \dots\dots\dots(3.14)$$

where $\overline{k_{rw1}}$ is the average water relative permeability in layer 1.

Similarly for water injection rate in layer 2,

$$i_{w2} = \frac{ck_2 \overline{k_{rw2}}}{\mu_w} \frac{\Delta P_2}{x_2} \dots\dots\dots(3.15)$$

where $\frac{\Delta P_2}{x}$ is pressure gradient of the region in layer 2, which has been displaced by water.

Using Darcy's law again for oil flow in layer 2

$$q_{o2} = \frac{ck_2k_{ro2}}{\mu_o} \frac{\Delta P'}{(L-x_2)} \dots\dots\dots(3.16)$$

For incompressible flow $i_{w2}B_w = q_{o2}B_o$; applying **Eq. 3.13** to **Eqs. 3.14-3.16** we obtain the following expression:

$$\frac{i_{w1}L\mu_w}{k_1k_{rw1}} = \frac{i_{w2}x_2\mu_w}{k_2k_{rw2}} + \frac{i_{w2}(L-x_2)\mu_o}{k_2k_{ro2}} \dots\dots\dots(3.17)$$

Knowing that total water injection rate is constant, simple material balance expression follows:

$$i_{w2} = i_{wt} - i_{w1} \dots\dots\dots(3.18)$$

Substituting **Eq. 3.18** in **Eq. 3.17** gives the following:

$$\frac{i_{w1}L\mu_w}{k_1k_{rw1}} = (i_{wt} - i_{w1}) \left(\frac{x_2\mu_w}{k_2k_{rw2}} + \frac{(L-x_2)\mu_o}{k_2k_{ro2}} \right) \dots\dots\dots(3.19)$$

And solving for i_{w1} :

$$i_{w1} = \frac{i_{wt} \left[\frac{x_2\mu_w}{k_2k_{rw2}} + \frac{(L-x_2)\mu_o}{k_2k_{ro2}} \right]}{\frac{L\mu_w}{k_1k_{rw1}} + \left[\frac{x_2\mu_w}{k_2k_{rw2}} + \frac{(L-x_2)\mu_o}{k_2k_{ro2}} \right]} \dots\dots\dots(3.20)$$

Eq. 3.20 may be rearranged to give:

$$i_{w1} = \frac{i_{wt}}{1 + \frac{Lk_2k_{ro2}\mu_w}{k_1k_{rw1}} \frac{k_{rw2}}{(x_2\mu_wk_{ro2} + (L-x_2)\mu_o k_{rw2})}} \dots\dots\dots (3.21)$$

Step 10-Repeat Steps 5-9 until iterated water injection rate in layer 1 is obtained.

At this point of calculation we use the estimated value of water injection rate in layer 1. Using **Eq. 3.21**, where relative permeabilities calculated using the Corey type curves, we can obtain a value of water injection rate in layer 1, and compare it to the estimated value. In case of inconsistency, iterate until the true value of i_{w1} is reached.

Step 11-Calculation of cumulative oil produced

The N_p value at the time of breakthrough can be calculated using Buckley-Leverett approach

$$N_p = \frac{W_{itbt}}{B_o} \dots\dots\dots(3.22)$$

Also there is slightly different method to calculate N_p value, using Dykstra-Parsons method using the vertical sweep efficiency or so-called coverage factor C_n

$$N_p = \frac{Lwh\phi}{B_o} (S_{oi} - S_{wc}) C_n \dots\dots\dots(3.23)$$

Substituting **Eq. 3.23** in **Eq. 3.22** the following expression for C_n could be obtained

$$C_n = \frac{PV}{PV} \frac{(S_w - S_{wc})}{(1 - S_{wc} - S_{or})} \dots\dots\dots(3.24)$$

where **Eq. 3.24** is a general expression for coverage factor after breakthrough. However in current case second layer haven't reached the producer yet, in which case coverage factor must be divided in two parts C_1 and C_2 , where

$$C_1 = \frac{PV_1}{PV_t} \frac{(\overline{S_{w1}} - S_{wc1})}{(1 - S_{wc1} - S_{or1})}, \dots\dots\dots(3.25)$$

and

$$C_2 = \frac{PV_x}{PV_t} \frac{(\overline{S_{w2}} - S_{wc2})}{(1 - S_{wc2} - S_{or2})}. \dots\dots\dots(3.26)$$

And finally N_p calculation:

$$N_p = \frac{MOV_t}{B_o} (C_1 + C_2), \dots\dots\dots(3.27)$$

where MOV_t is total moveable oil in the reservoir.

Step 12-Calculation after the breakthrough in layer 1 and subsequently in layer 2

Second part of procedure starts after the 1st layer breakthrough but before the 2nd layer breakthrough. It is necessary to specify the saturation change step in the first layer, for which the following expression can be used:

$$\Delta S_w = \frac{(1 - S_{or} - \overline{S_{wbt}})}{N}, \dots\dots\dots(3.28)$$

where N is the number of steps to be defined.

During the course of the calculation procedure $\overline{S_w}$ is going to be calculated using **Eq. 2.10** where $S_{we} = S_w + \Delta S_w$. Basically all calculation steps will remain unchanged except

the several equations such as: calculation of cumulative water injected in layer 1, after breakthrough

$$W_{i1} = \frac{1}{\frac{df_w}{dS_w}|_{S_{we}}} \dots\dots\dots(3.29)$$

Another difference between the 1st stage of procedure and the 2nd stage is N_p calculation, as the equation has to account for produced water from layer 1. In order to calculate produced water at each saturation change, the cumulative oil production from the first layer N_{p1} has to be calculated:

$$N_{p1} = \frac{PV(S_{oi} - (1 - \overline{S_w}))}{B_o} \dots\dots\dots(3.30)$$

After N_{p1} and W_{i1} are calculated, water produced can be calculated as follows:

$$W_{p1} = W_{i1}B_w - N_{p1}B_o \dots\dots\dots(3.31)$$

In the procedure the ΔN_{p1} , ΔW_{i1} and ΔW_{p1} are used to calculate their corresponding cumulative amounts.

Finally last part of the calculation procedure interprets behavior of the reservoir when the second layer breaks through and beyond. Because of change in process, calculation steps must contain the ΔN_{p2} calculation, which is analogical to ΔN_{p1} and mass balance must account for the produced water from 2nd layer ΔW_{p2} .

The method presented here differs from Buckley-Leverett original solution by calculating water injection rate in specific layer on each saturation change, whereas for Buckley-Leverett method applied by Craig¹⁴, water injection rate in each layer is constant and depends only on the kh of each layer.

In order to plot changing water injection rates in layer 1 and layer 2 before breakthrough, cumulative water injected in layer 1 at the moment of breakthrough $W_{i_{bt}}$ must be calculated using **Eq. 3.5**. Then divide $W_{i_{bt}}$ by the number of steps needed. As the upper limit is known there are no further complications: considering **Eqs. 3.7-3.12** waterflood performance can be obtained. Only change will include deriving the water injection rate in layer 1 before the breakthrough i_{w1} , and it can be found by following expression:

$$i_{w1} = \frac{i_{wt}}{1 + \frac{Lk_2k_{roe2}k_{rw2}\mu_w}{k_1k_{rw1}k_{roe1}} \frac{x_1\mu_wk_{roe1} + (L-x_1)\mu_o k_{rw1}}{x_2\mu_wk_{roe2} + (L-x_2)\mu_o k_{rw2}}}, \dots\dots\dots(3.32)$$

where x_1 is the distance of the front in layer 1.

All programming work has been done in Microsoft VBA and Excel and can be found in **APPENDIX B**.

Nine cases have been studied in which injection rate and reservoir parameters are varied. Results based on the new analytical model are compared against simulation results to verify the validity of the new model. Brief descriptions of each of the nine cases follow.

3.2 Case 1

Current research based on the implementing Buckley-Leverett theory to the two phase homogeneous, horizontal reservoir consisting of the two non-communicating layers with the different absolute permeabilities. Major assumptions are the constant total injection rate i_{wt} , constant pressure gradient across all layers $\frac{\Delta P}{L}$, incompressible and immiscible displacement and no capillary or gravity forces. Parameters for case 1 are shown in **Table 3.1**.

TABLE 3.1 RESERVOIR PROPERTIES FOR CASE 1

Reservoir properties	Value
Reservoir length, L	1200, ft
Reservoir width, w	400, ft
Reservoir height, h	70, ft
Reservoir porosity, ϕ	25 %
First layer permeability, k_1	500, md
Second layer permeability, k_2	350, md
End point relative permeability of oil, k_{roe}	0.85
End point relative permeability of water, k_{rwe}	0.35
Initial oil saturation, S_{oi}	80%
Connate water saturation, S_{wc}	20%
Residual oil saturation, S_{or}	20%
Oil viscosity, μ_o	8, cp
water viscosity, μ_w	0.9, cp
Total water injection rate, i_{wt}	800, STB/D
Oil formation volume factor, B_o	1.25, RB/STB
Water formation volume factor, B_w	1, RB/STB

The height of layer 1 is equal to the height of layer 2 in case 1.

Below are oil production results of new analytical model compared to simulation model:

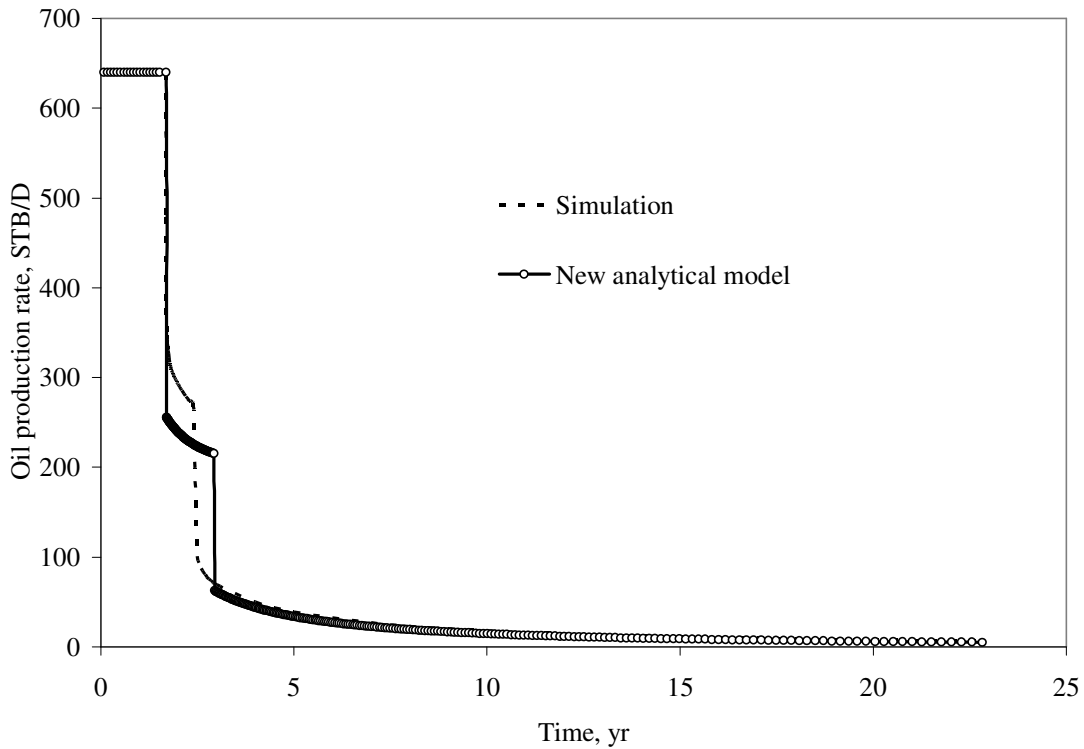


Figure 3.4 Comparison of oil production rate of new analytical model vs. simulation (Case 1).

From **Fig. 3.4**, it can be seen that oil production rates based on the new model and simulation are practically identical. However after breakthrough in layer 1, oil production rate is about 50 STB/D higher based on simulation. Breakthrough time for layer 1 is almost identical based on the new model and simulation. However, there is significant difference in the second layer breakthrough times. This difference is probably caused by the method used in calculating water injection rate in each layer.

Fig. 3.5 presents the water injection rate by layer based on the new model and compared against simulation results. It can be seen that layer injection rate before breakthrough in layer – based on the new model and simulation – is in very good agreement. However,

after breakthrough in layer 2, layer injection rate is about 25 STB/D higher in layer 1 and about 25 STB/D lower in layer 2 based on the new model compared to simulation.

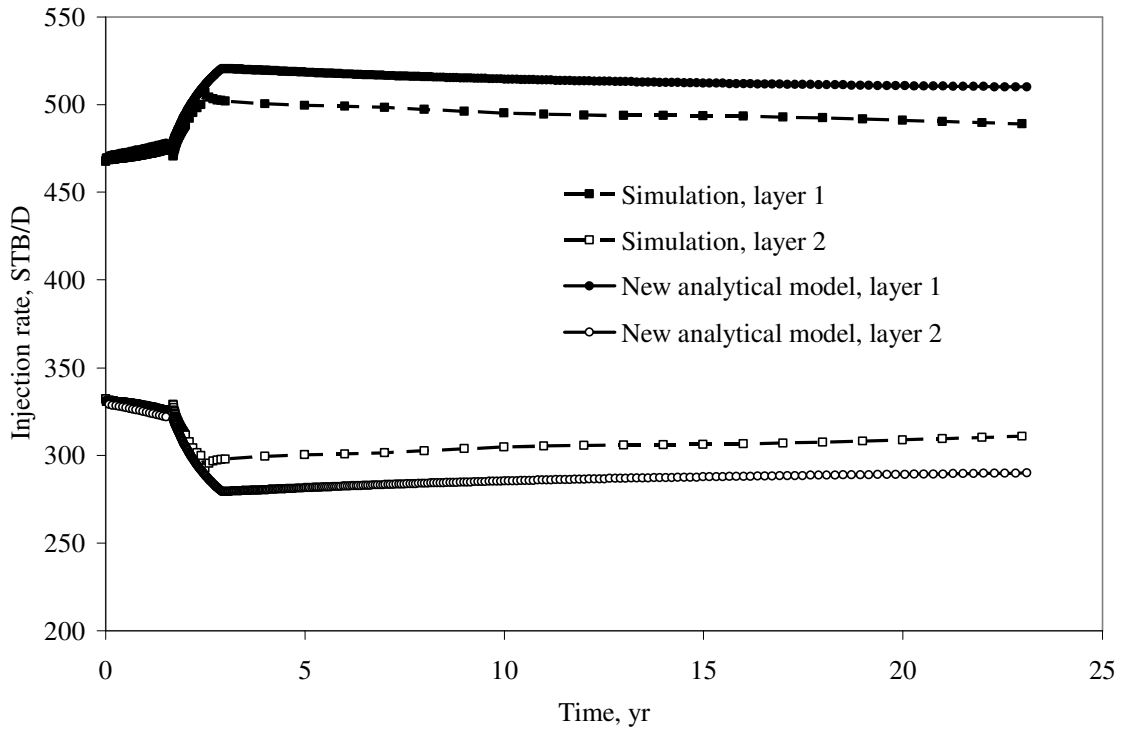


Figure 3.5 Comparison of water injection rate of new analytical model vs. simulation by layers (Case 1).

Fig. 3.6 shows cumulative oil production versus time. It can be seen that cumulative oil production based on the new model and simulation is in close agreement.

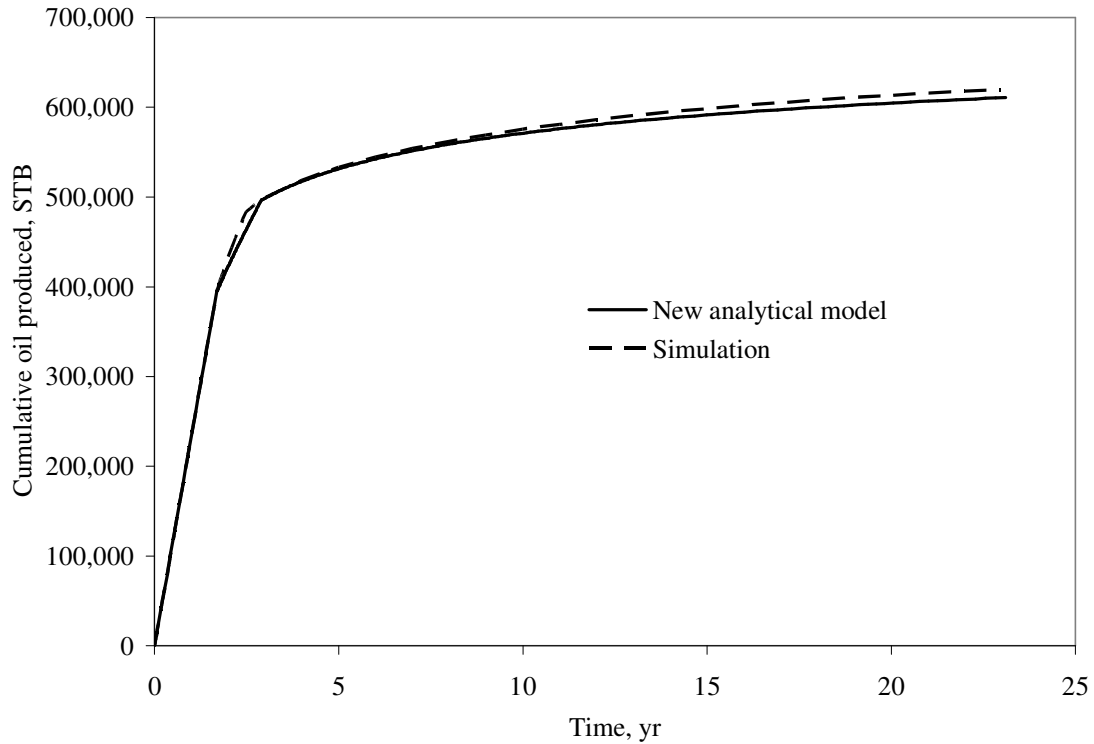


Figure 3.6 Comparison of cumulative oil produced calculated with new analytical model vs. simulation (Case 1).

Fig. 3.7 shows oil production rate by layer. It can be seen that oil production rates for both layers before breakthrough in layer 1 based on the new model is very similar to that based on simulation. However after breakthrough in layer 1, oil production rate in layer 2 is higher based on simulation. Nevertheless, after breakthrough in layer 2, oil production rate for both layers based on the new model are in close agreement with simulation results.

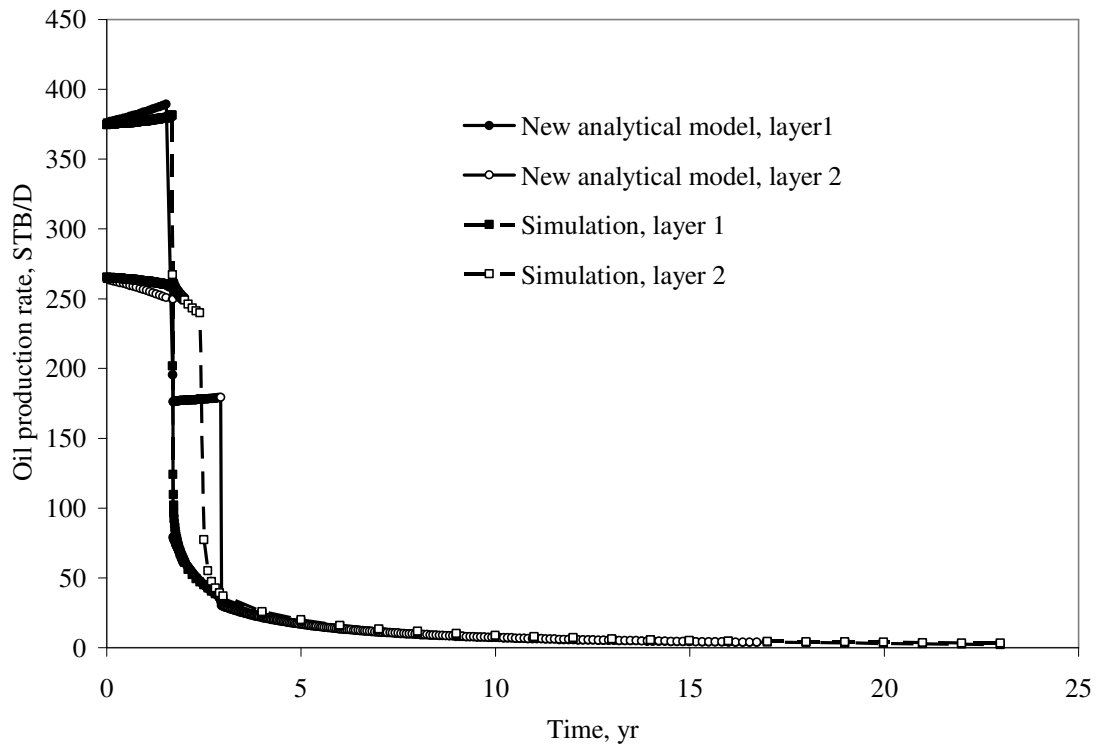


Figure 3.7 Oil production rates by layers, new analytical model vs. simulation (Case 1).

Fig. 3.8 presents water production rate by layer. Because of higher water injection rate in layer 1 based on the new model, it can be seen that water production rate in layer 1 is also higher, and vice-versa for layer 2.

However, as can be noted from **Fig. 3.9**, the total water production rate based on the new model is in good agreement with simulation results after breakthrough in layer 2.

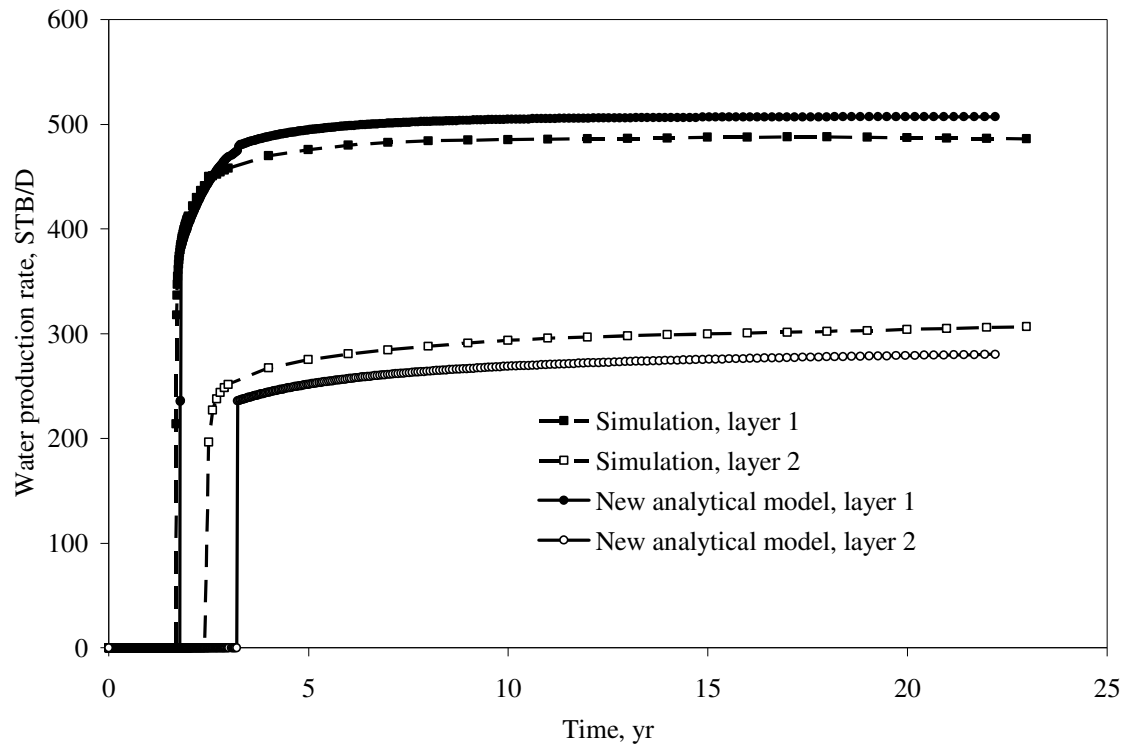


Figure 3.8 Water production rate by layers, new analytical model vs. simulation (Case 1).

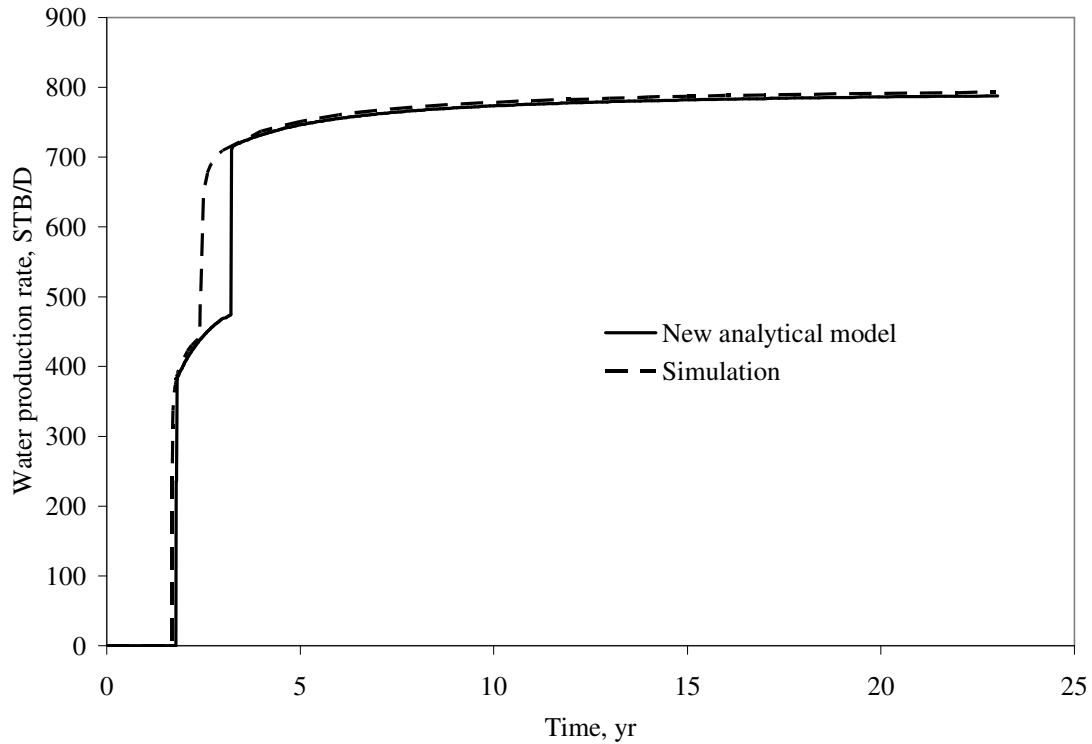


Figure 3.9 Total water production rate comparison of new analytical model vs. simulation (Case 1).

3.3 Case 2

One of the goals of this study was to apply different sets of relative permeability to different layers and compare calculated results to that of simulation. Case 2 is identical to Case 1 except the oil-water relative permeability set for layer 2 has been changed as follows: k_{roe2} is 0.9 and k_{rwe2} is 0.5 fraction, residual oil saturation S_{or2} is 35 %, and S_{wc2} is 20 %. Parameters for Case 2 are shown in **Tables 3.2-3.3**.

TABLE 3.2 RESERVOIR PROPERTIES OF LAYER 1 FOR CASE 2.

Layer 1 Characteristics	Value
Layer 1 length, L	1200, ft
Layer 1 width, w	400, ft
Layer 1 height, h	35, ft
Layer 1 porosity, ϕ	25 %
Layer 1 permeability, k_1	500, md
End point relative permeability of oil, k_{roe}	0.85
End point relative permeability of water, k_{rwe}	0.35
Initial oil saturation, S_{oi}	80%
Connate water saturation, S_{wc}	20%
Residual oil saturation, S_{or}	20%
Oil viscosity, μ_o	8, cp
water viscosity, μ_w	0.9, cp
water injection rate in layer 1, i_{w1}	variable, STB/D
Oil formation volume factor, B_o	1.25, RB/STB
Water formation volume factor, B_w	1, RB/STB

TABLE 3.3 RESERVOIR PROPERTIES OF LAYER 2 FOR CASE 2.

Layer 2 Characteristics	Value
Layer 2 length, L	1200, ft
Layer 2 width, w	400, ft
Layer 2 height, h	35, ft
Layer 2 porosity, ϕ	25 %
Layer 2 permeability, k_2	350, md
End point relative permeability of oil, k_{roe}	0.9
End point relative permeability of water, k_{rwe}	0.5
Initial oil saturation, S_{oi}	70%
Connate water saturation, S_{wc}	30%
Residual oil saturation, S_{or}	35%
Oil viscosity, μ_o	8, cp
water viscosity, μ_w	0.9, cp
water injection rate in layer 2, i_{w2}	variable, STB/D
Oil formation volume factor, B_o	1.25, RB/STB
Water formation volume factor, B_w	1, RB/STB

Two sets of oil-water relative permeability are shown in **Fig. 3.10**.

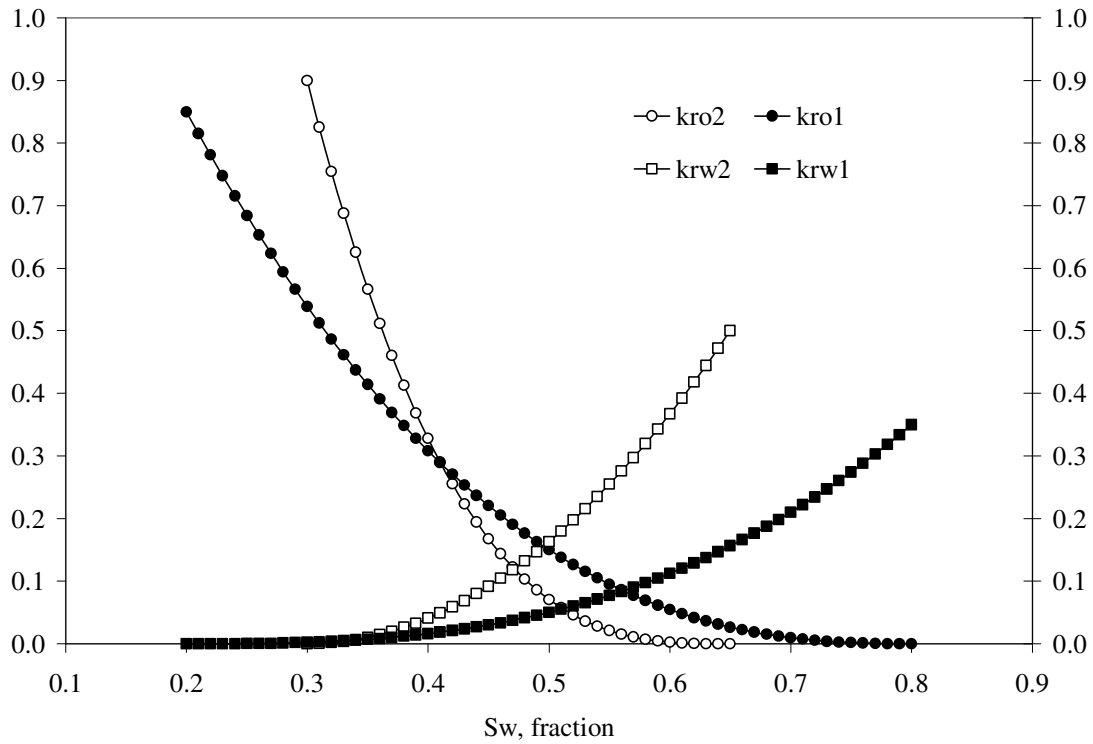


Figure 3.10 Sets of relative permeabilities for layers 1 and 2 (Case 2).

Based on the relative permeability data two fractional flow curves have to be created, as shown in **Fig. 3.11**.

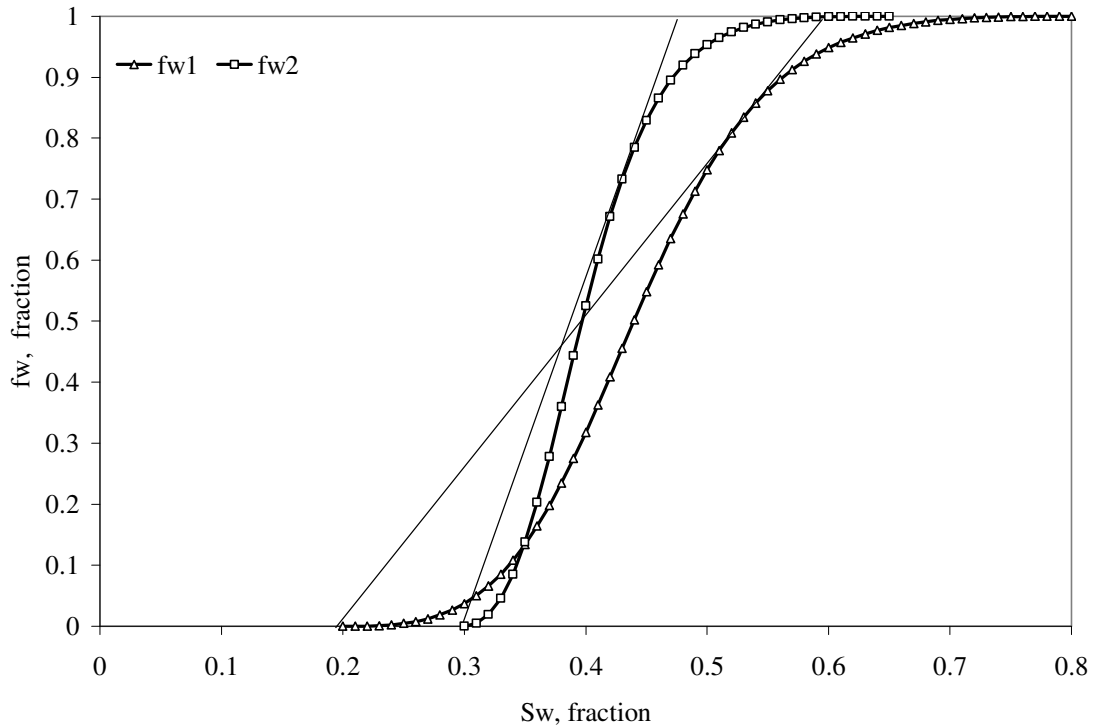


Figure 3.11 Fractional flow curves for layers 1 and 2 respectively (Case 2).

From **Fig. 3.12**, it can be seen that oil production rates based on the new model and simulation are in very good agreement. However after breakthrough in layer 1, oil production rate is about 70 STB/D higher based on simulation. Breakthrough time for layer 1 is almost identical based on the new model and simulation. Note that there is significant difference in the second layer breakthrough times. This difference might be caused by the method used in calculating water injection rate in each layer.

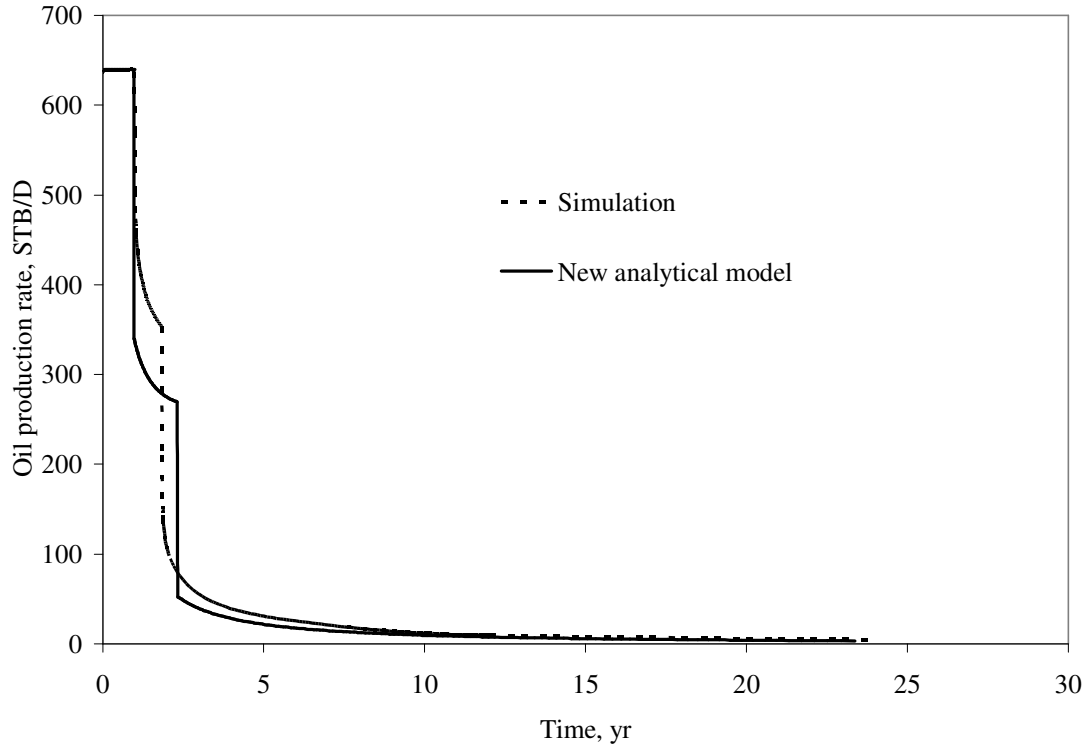


Figure 3.12 Oil production rate of new analytical model vs. simulation, different sets of relative permeabilities are applied (Case 2).

Fig. 3.13 presents the water injection rate by layer based on the new model and simulation results. It can be noted, that layer injection rate before breakthrough is in very good agreement. Nevertheless, after breakthrough in layer 2, layer injection rate is about 60 STB/D higher in layer 1, and about 60 STB/D lower in layer 2 according to the new model compared against simulation.

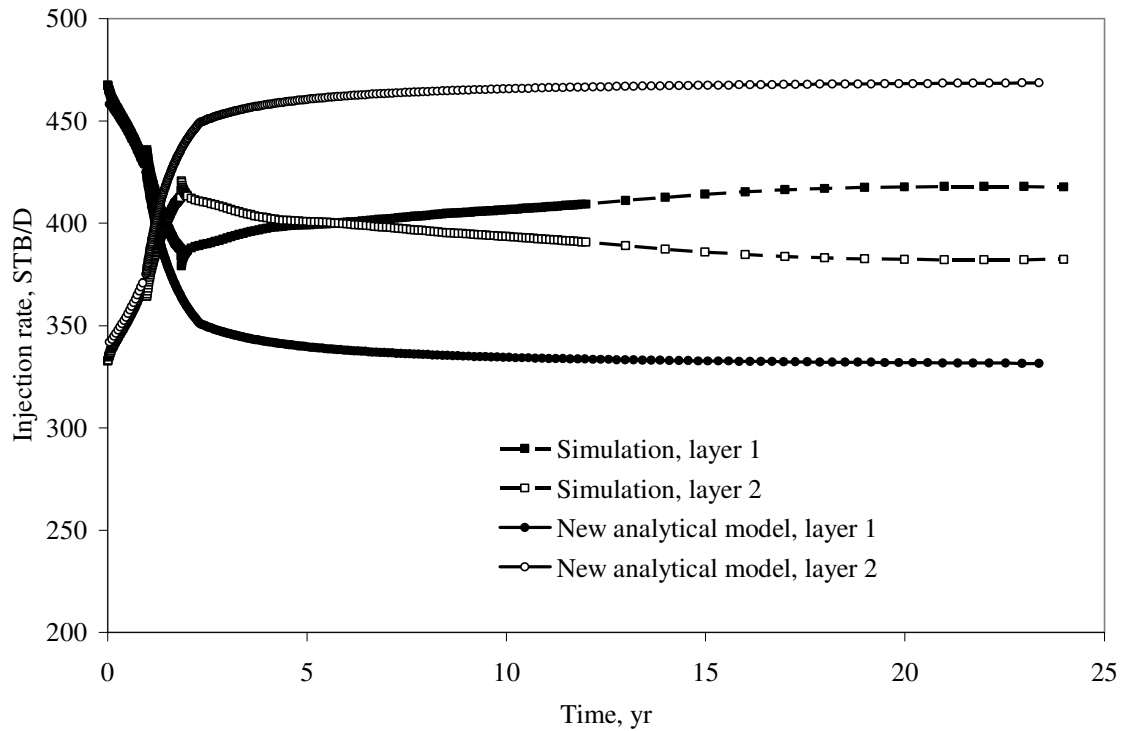


Figure 3.13 Water injection rates by layers of new analytical model vs. simulation, different sets of relative permeabilities are applied (Case 2).

Fig. 3.14 shows cumulative oil production versus time. We can see that for the first four years of production cumulative oil produced is in good agreement for new model versus simulation. However for the next 20 years of production new model shows quite significant difference against that of simulation.

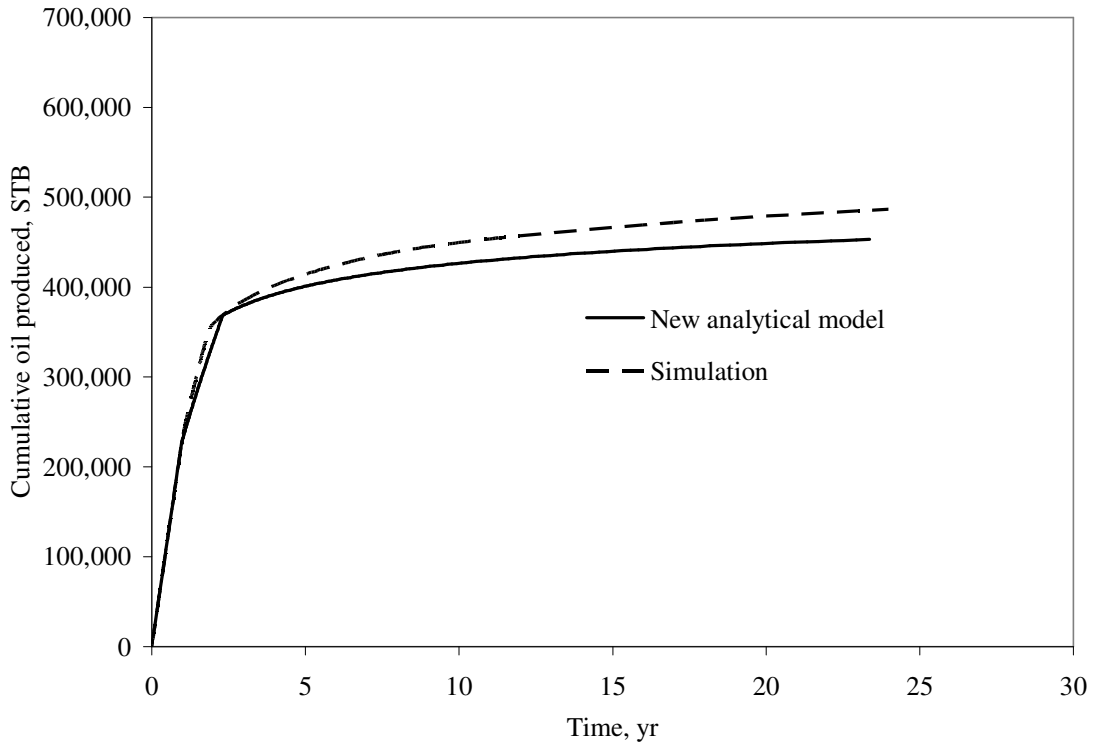


Figure 3.14 Cumulative oil produced comparison of new analytical model vs. simulation, two sets of relative permeability are provided for each layer (Case 2).

Fig. 3.15 shows oil production rate by layer. It can be seen that oil production rates for both layers before breakthrough in layer 2 (as due to difference in oil-water relative permeability layer 2 breaks through first) based on the new model is very similar to that based on simulation. However after breakthrough in layer 2, oil production rate in layer 1 is higher based on simulation. Nevertheless, after breakthrough in layer 1, oil production rate for both layers based on the new model are in close agreement with simulation results.

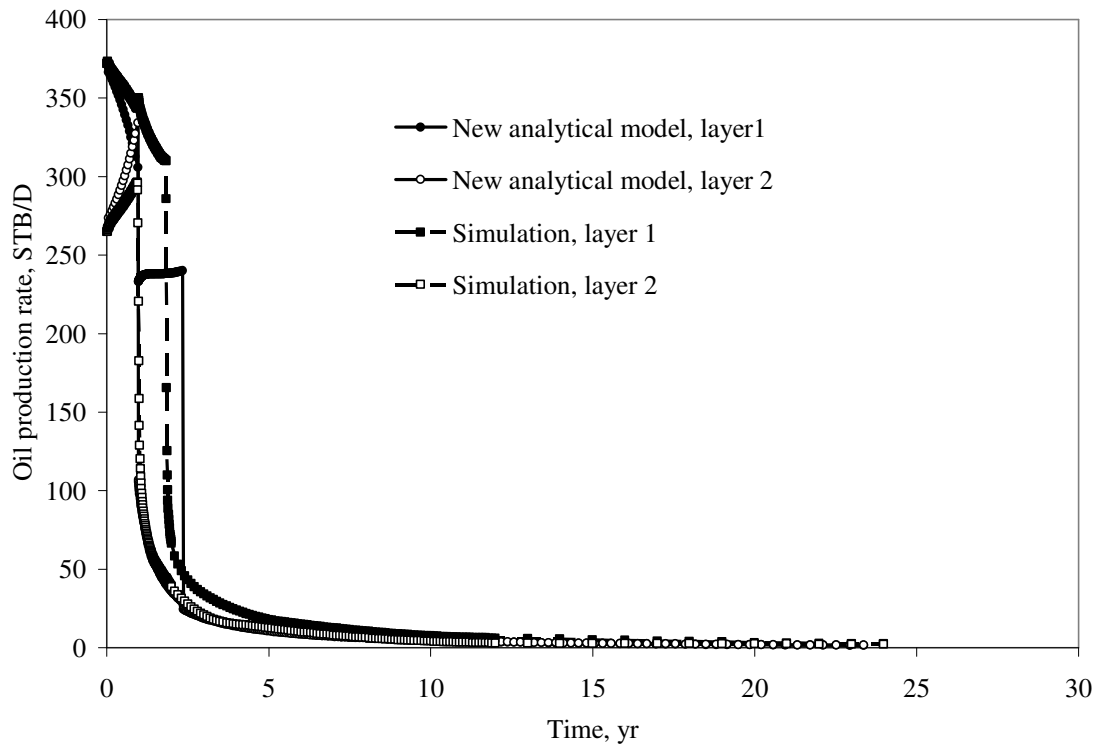


Figure 3.15 Oil production rate by layers comparison of new analytical model vs. simulation, two sets of relative permeability are provided for each layer (Case 2).

Fig. 3.16 presents water production rate by layer. Because of higher water injection rate in layer 2 based on the new model, it can be seen that water production rate in layer 2 is also higher, and vice-versa for layer 1.

However, as can be noted from **Fig. 3.17**, the total water production rate based on the new model is in good agreement with simulation results after breakthrough in layer 1.

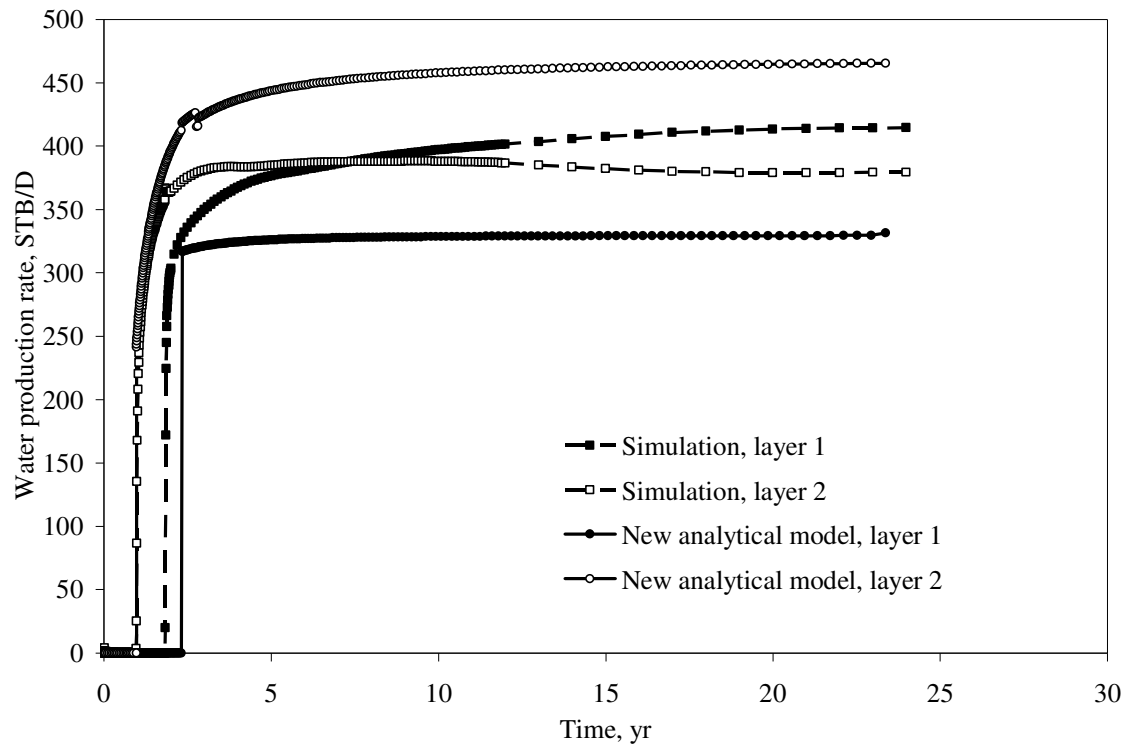


Figure 3.16 Water production rate by layers, comparison of new analytical model vs. simulation, two sets of relative permeability are provided for each layer (Case2).

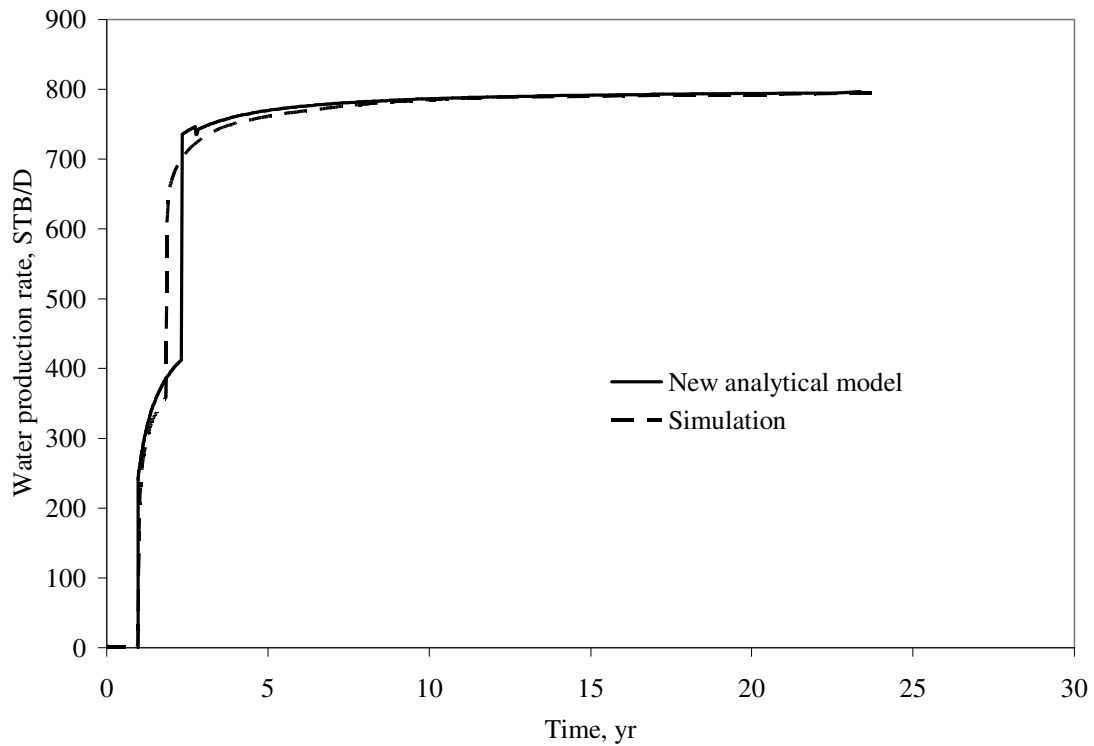


Figure 3.17 Total water production rate, comparison of new analytical model vs. simulation, two sets of relative permeability are provided for each layer (Case 2).

3.4 Case 3

Next case represents the variation of the case 1 with different set of kh . **Table 3.4** contains the changes made to the model:

TABLE 3.4 HEIGHT AND PERMEABILITY VARIATION IN LAYERS 1 AND 2.

Characteristics	Value
Absolute permeability of layer 1, k_1	500, md
Height of layer 1, h_1	50, ft
Absolute permeability of layer 2, k_2	100, md
Height of layer 2, h_2	25, ft

From **Fig. 3.18**, it can be seen that oil production rates based on the new model and simulation are in good agreement. However after breakthrough in layer 1, oil production rate is about 30 STB/D lower based on simulation. Breakthrough time for layer 1 is very close based on the new model and simulation. Note that there is significant difference of 2.5 years in the second layer breakthrough times. This difference is probably caused by the method used in calculating water injection rate in each layer.

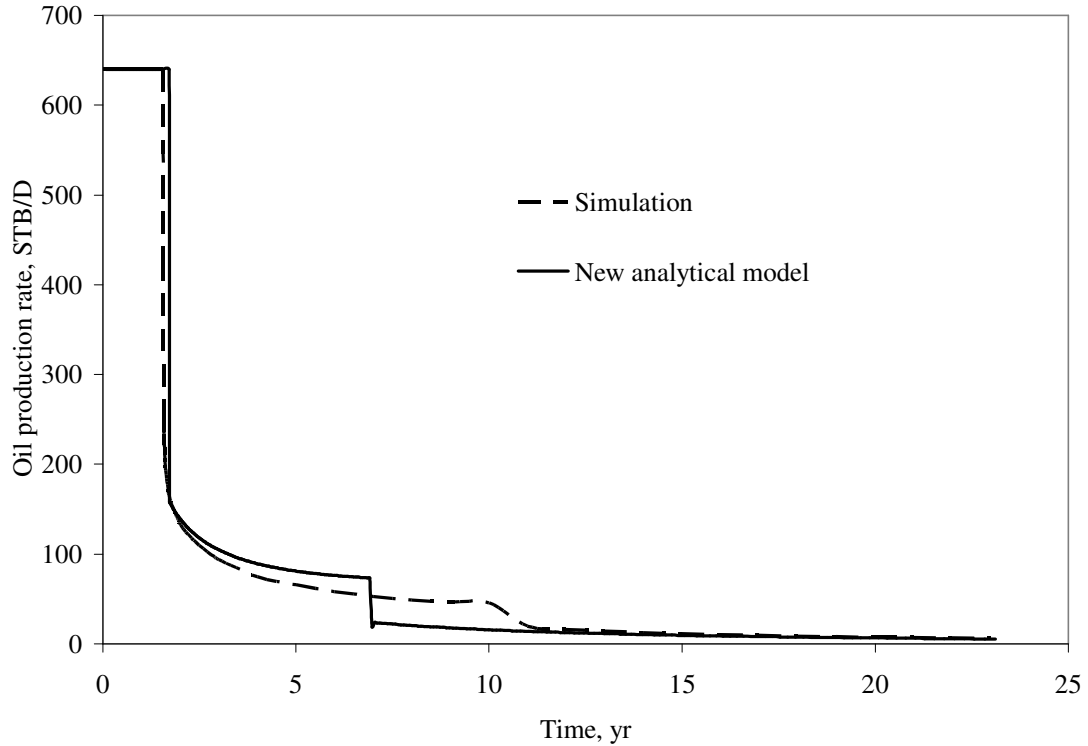


Figure 3.18 Oil production comparison of new analytical model to the simulation, variable kh is applied (Case 3).

Fig. 3.19 presents the water injection rate by layer based on the new model and simulation results. It can be noted, that there is constant difference of 30 STB/D in layer injection rate before and after breakthrough.

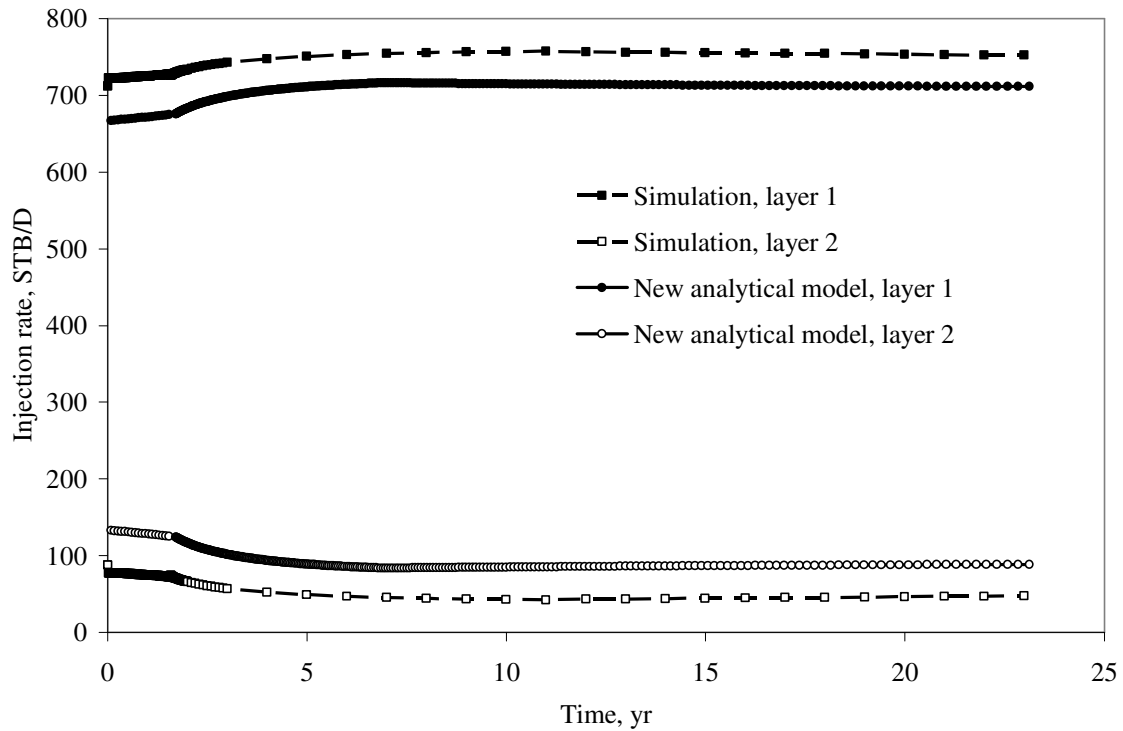


Figure 3.19 Water injection rate comparison of new analytical model versus simulation, variable kh is applied (Case 3).

Fig. 3.20 shows cumulative oil production versus time. We can see that overall cumulative oil production is in good agreement for new model versus simulation. However for period of time from 2nd year of production to 10th year there is significant difference of new model against that of simulation.

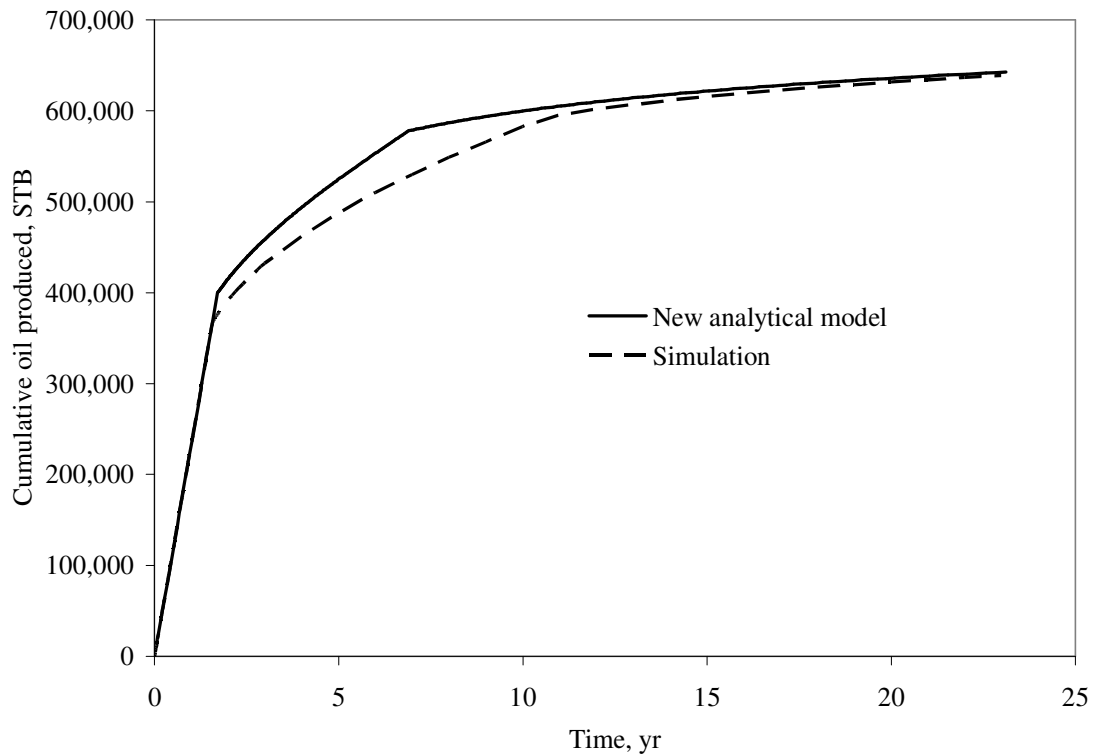


Figure 3.20 Cumulative oil produced comparison of new analytical model to the simulation, variable kh is applied (Case 3).

Fig. 3.21 shows oil production rate by layer. It can be seen that oil production rate for both layers before breakthrough in layer 1 based on the new model gives a difference of 30 STB/D to that based on simulation, where simulation production rate is higher. However after breakthrough in layer 2, oil production rate in layer 2 is higher based on new model. Nevertheless, after breakthrough in layer 1, oil production rate for both layers based on the new model are in close agreement with simulation results.

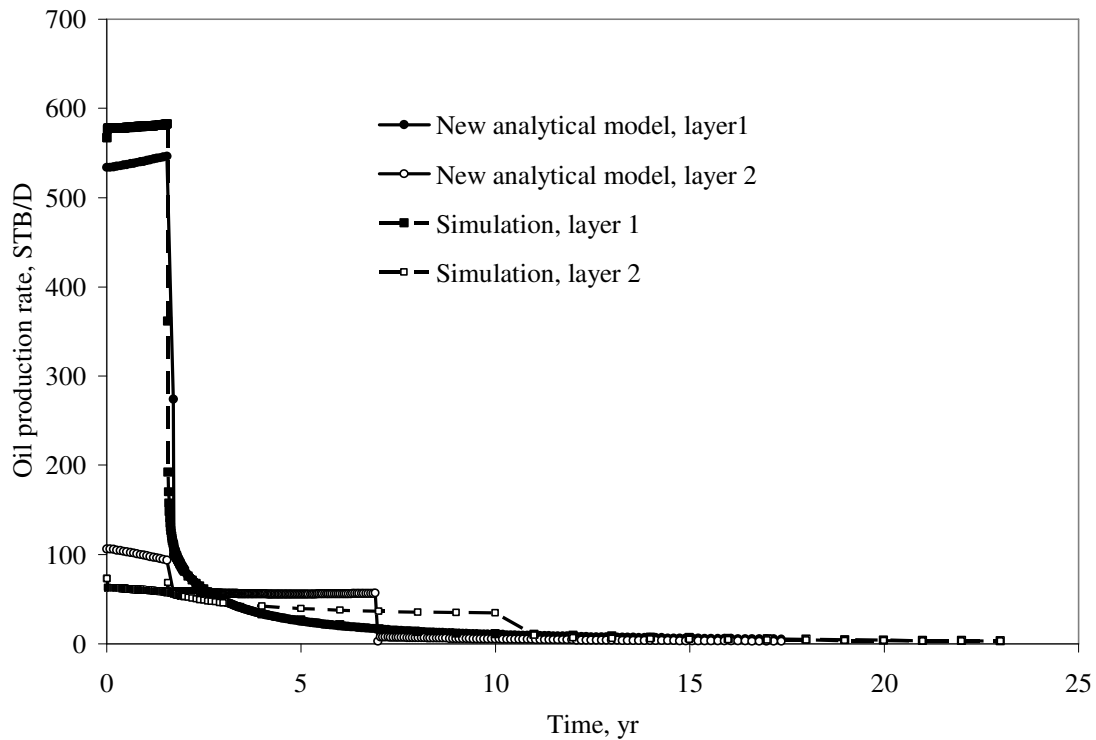


Figure 3.21 Oil production layer by layer comparison of new analytical model to the simulation, variable kh is applied (Case 3).

Fig. 3.22 presents water production rate by layer. Because of higher water injection rate in layer 1 based on the simulation, it can be seen that water production rate in layer 1 is also higher, and vice-versa for layer 2.

However, as can be noted from **Fig. 3.23**, the total water production rate based on the new model is in close agreement with simulation results after breakthrough in layer 2 based on the simulation.

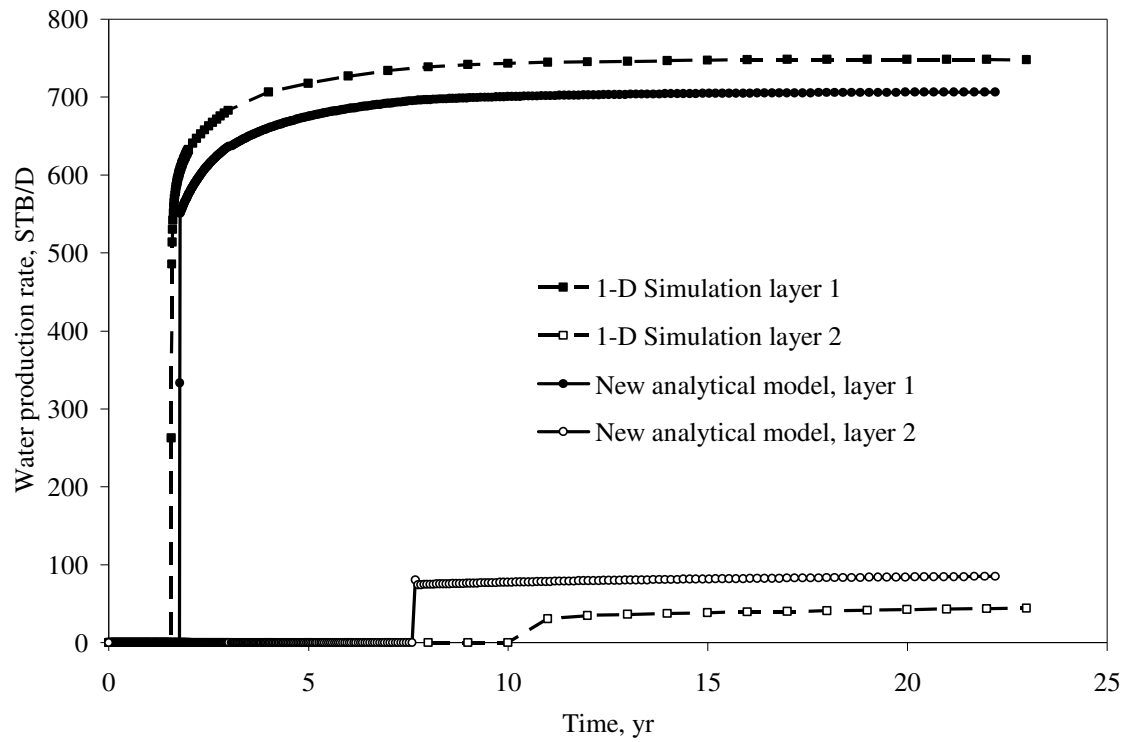


Figure 3.22 Water production layer by layer comparison of new analytical model to the simulation, variable kh is applied (Case 3).

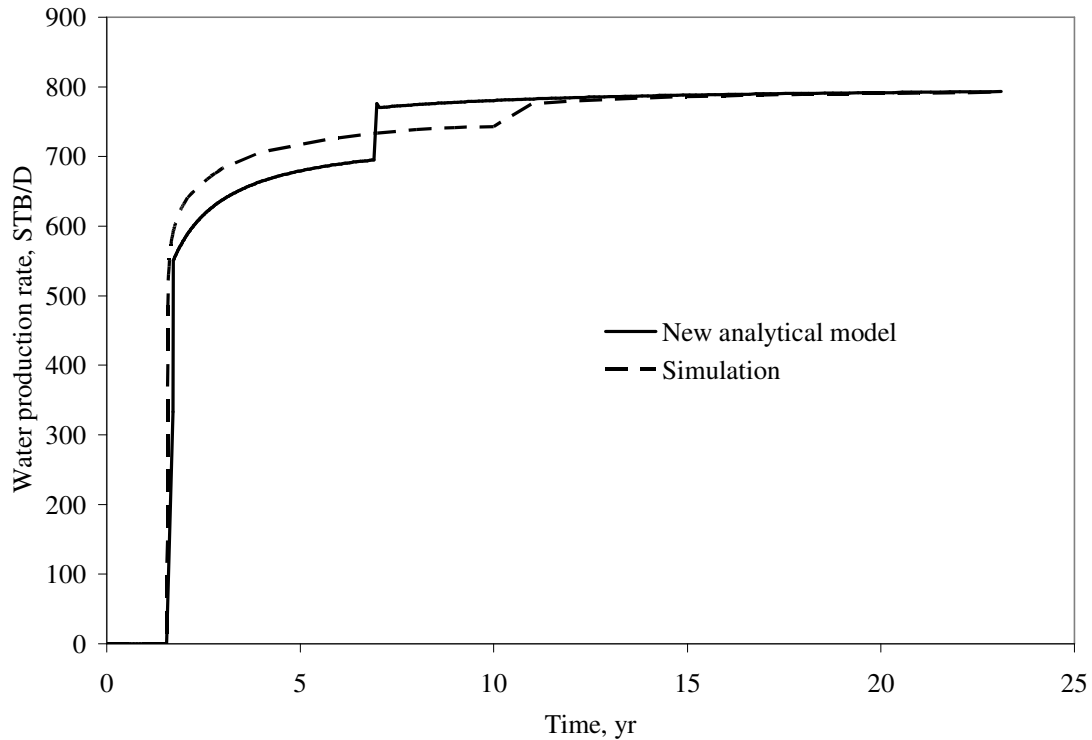


Figure 3.23 Total water production comparison of new analytical model to the simulation, variable kh is applied.

3.5 Case 4

Case 4 is obtained by using kh parameters of Case 3 applied to the different oil-water relative permeability set of Case 2.

From **Fig. 3.24**, it can be noted that oil production rates based on the new model and simulation are in good agreement. However after breakthrough in layer 1, oil production rate is about 50 STB/D higher based on simulation. Breakthrough time for layer 1 is very close based on the new model and simulation. Note that there is significant difference in

the second layer breakthrough times. This difference is probably caused by the method used in calculating water injection rate in each layer.

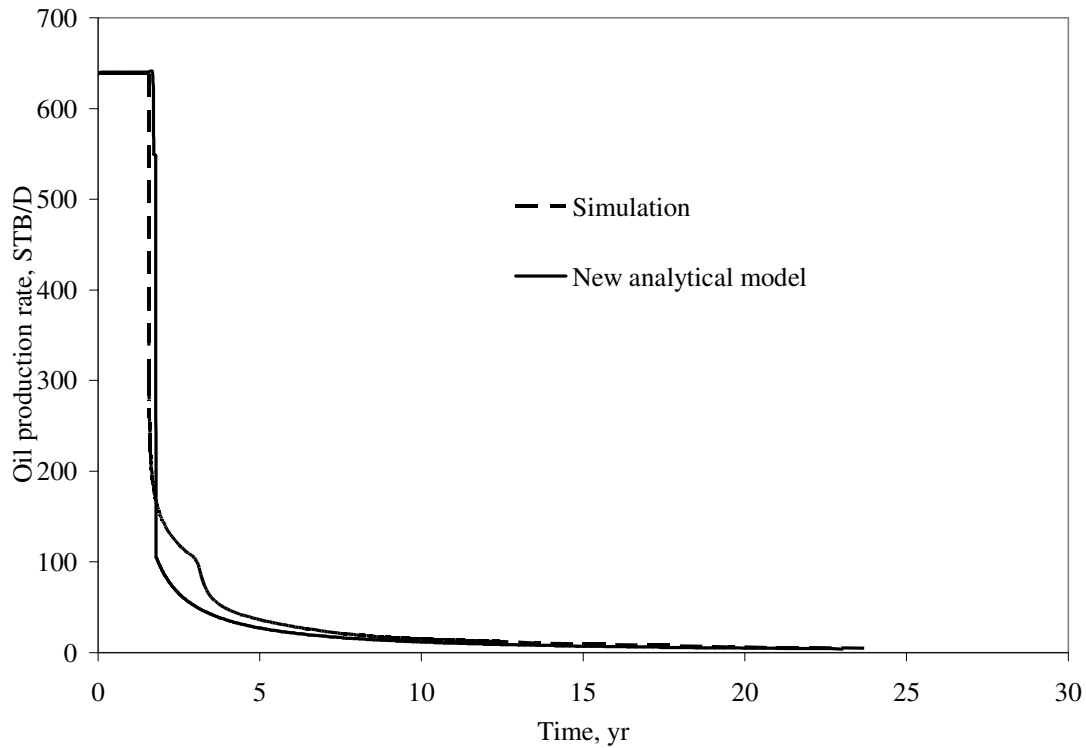


Figure 3.24 Total oil production comparison of new analytical model versus simulation, variable kh and relative permeability sets are applied (Case 4).

Fig. 3.25 presents the water injection rate by layer based on the new model and simulation results. In this case the most significant difference of 100 STB/D among all cases can be seen. We might note that simulation results for layer 1 show higher values than that of the new model.

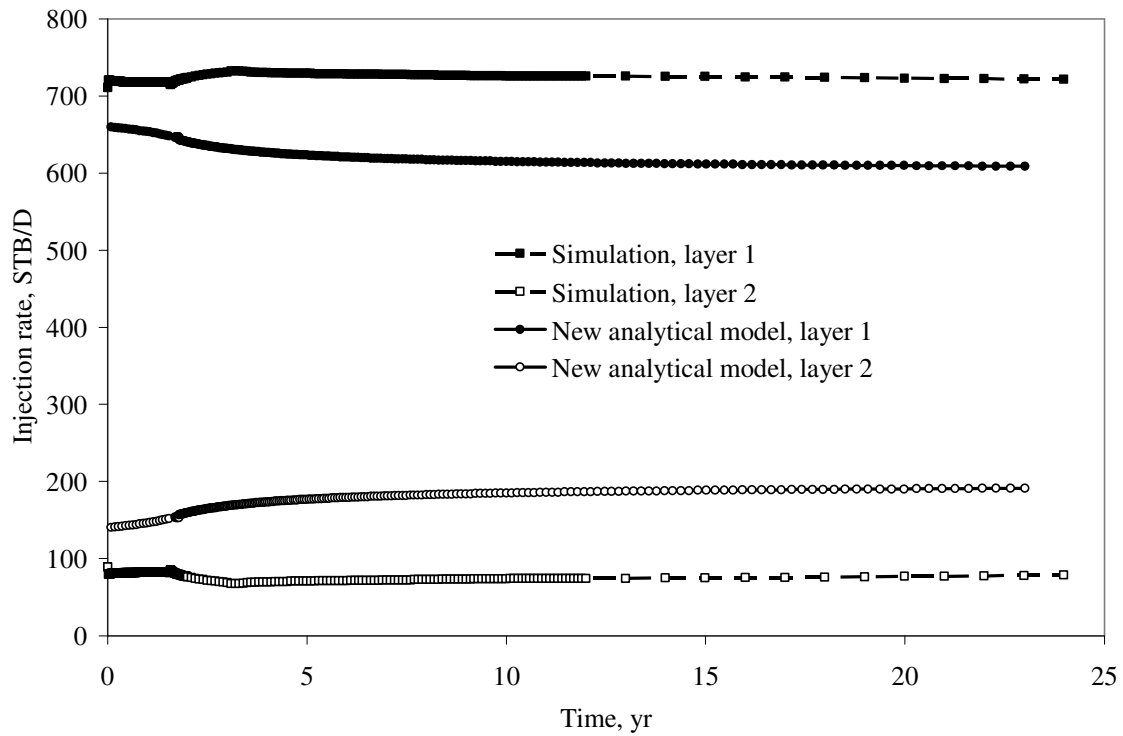


Figure 3.25 Water injection layer by layer comparison of new analytical model to the simulation, variable kh and relative permeability sets are applied (Case 4).

In spite of the difference in **Fig. 3.25**, in **Fig. 3.26**, which shows cumulative oil production versus time, it can be seen that cumulative oil production based on the new model and simulation is in close agreement.

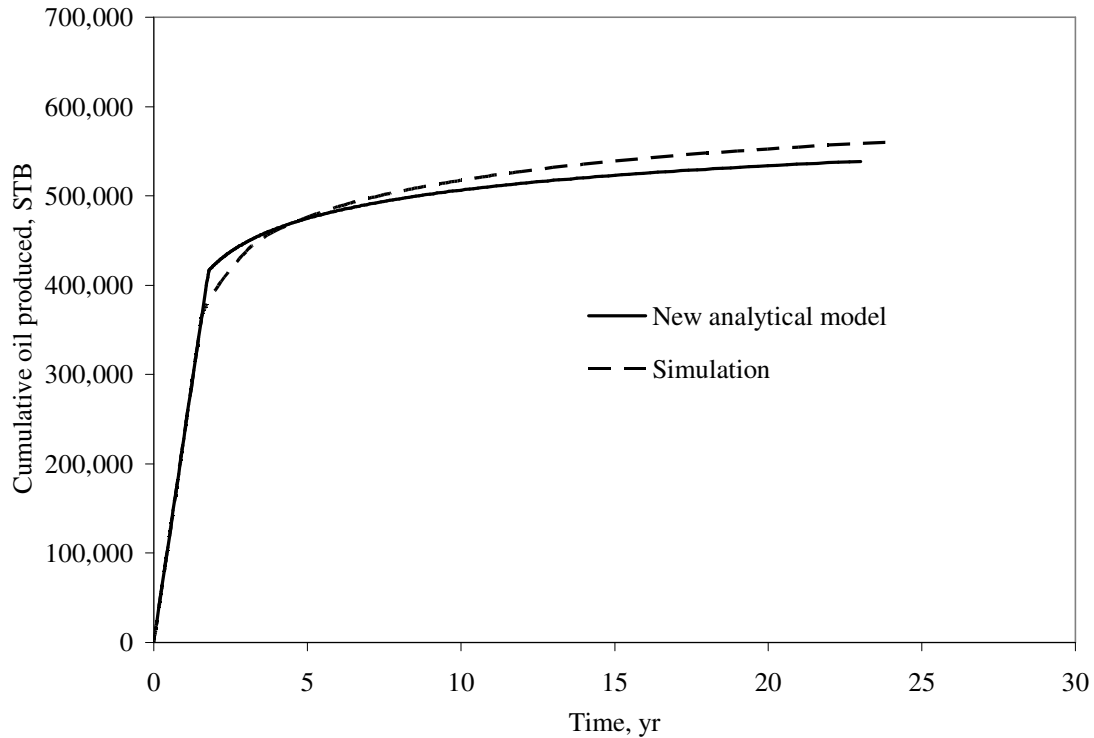


Figure 3.26 Cumulative oil produced, comparison of new analytical model to simulation, variable kh and relative permeability sets are applied (Case 4).

Fig. 3.27 shows oil production rate by layer. It can be seen that oil production rate for both layers before breakthrough in layer 1 based on the new model gives a significant difference of 70 STB/D to that based on simulation, where simulation production rate is higher for layer 1. However after breakthrough in layer 2, oil production rate in layer 2 is higher based on new model. However, after breakthrough in layer 1, oil production rate for both layers based on the new model are in close agreement with simulation results.

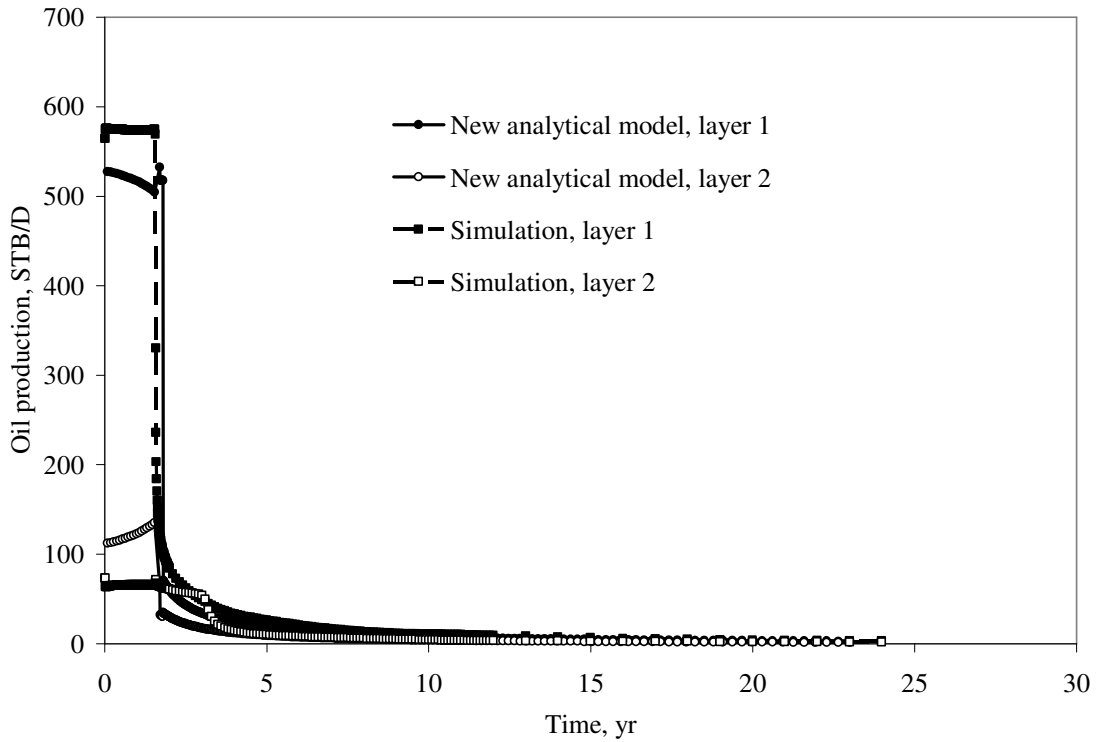


Figure 3.27 Oil production layer by layer, comparison of new analytical model to simulation, variable kh and relative permeability sets are applied (Case 4).

Fig. 3.28 presents water production rate by layer. Because of higher water injection rate in layer 1 based on the simulation, it can be seen that water production rate in layer 1 is also higher, and vice-versa for layer 2. The difference is about 110 STB/D.

However, as can be noted from **Fig. 3.29**, the total water production rate based on the new model is in close agreement with simulation results.

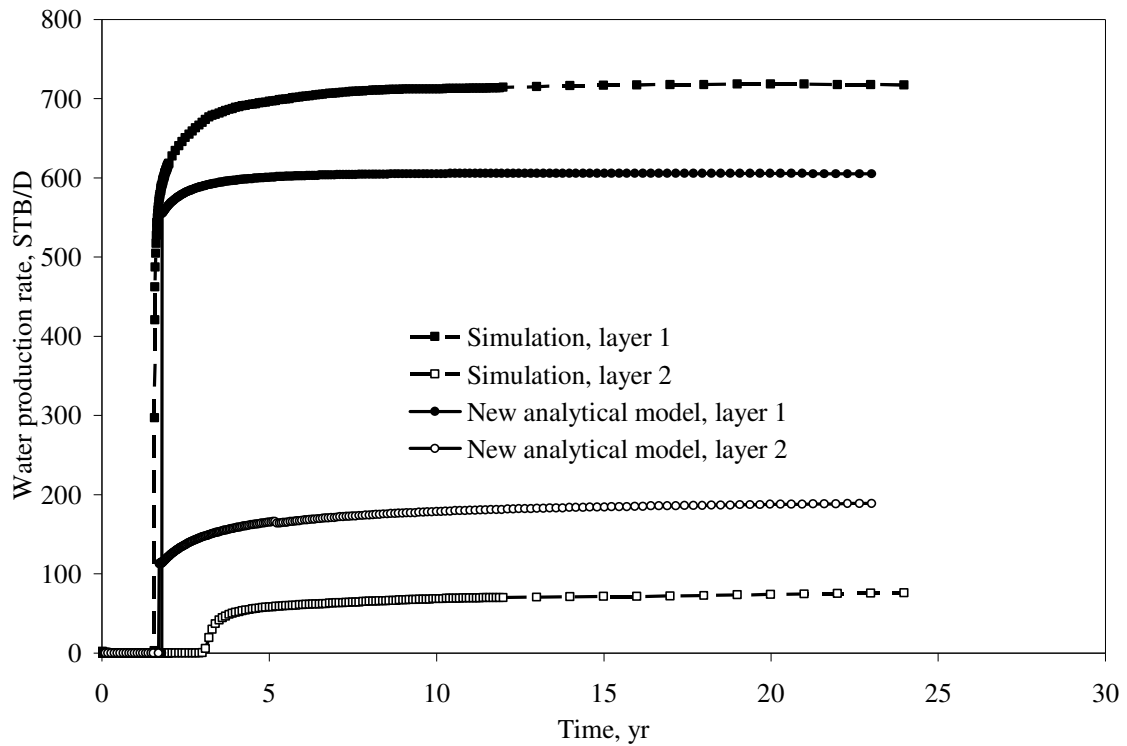


Figure 3.28 Water production layer by layer, comparison of new analytical model to simulation, variable kh and relative permeability sets are applied (Case 4).

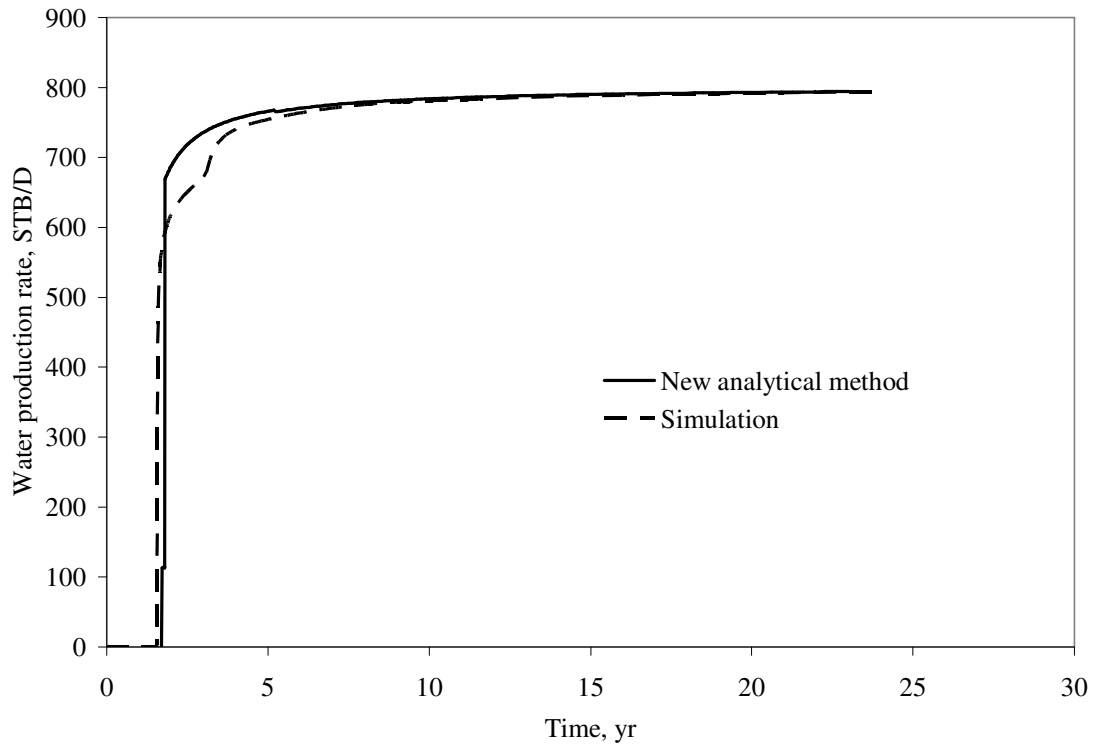


Figure 3.29 Water production rate, comparison of new analytical model to the simulation, variable kh and relative permeability sets are applied (Case 4).

3.6 Case 5

In following case I kept all parameters of Case 1 unchanged except total injection rate, which I increased twice to a value of 1600 STB/D.

Fig. 3.30 shows the oil production rate based on the new model versus simulation results. As it can be seen from **Fig. 3.30** it shows exactly the same behavior as in **Fig. 3.4** but with doubled production rate and halved time of breakthrough.

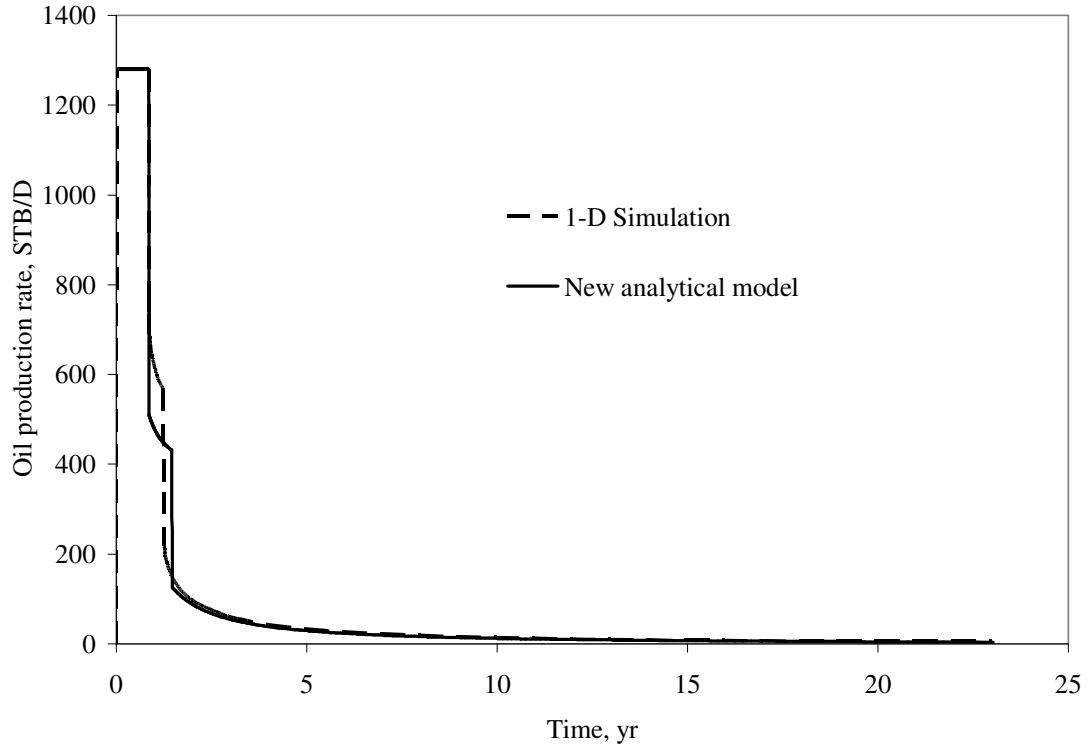


Figure 3.30 Oil production rate, comparison of new analytical model to the simulation, injection rate of 1600 STB/D is applied (Case 5).

Fig. 3.31 presents the water injection rate by layer comparison of the new model against that of simulation. Similarly it can be seen from **Fig. 3.31** that it shows exactly the same behavior as in **Fig. 3.5** but with doubled injection rate and halved time of breakthrough.

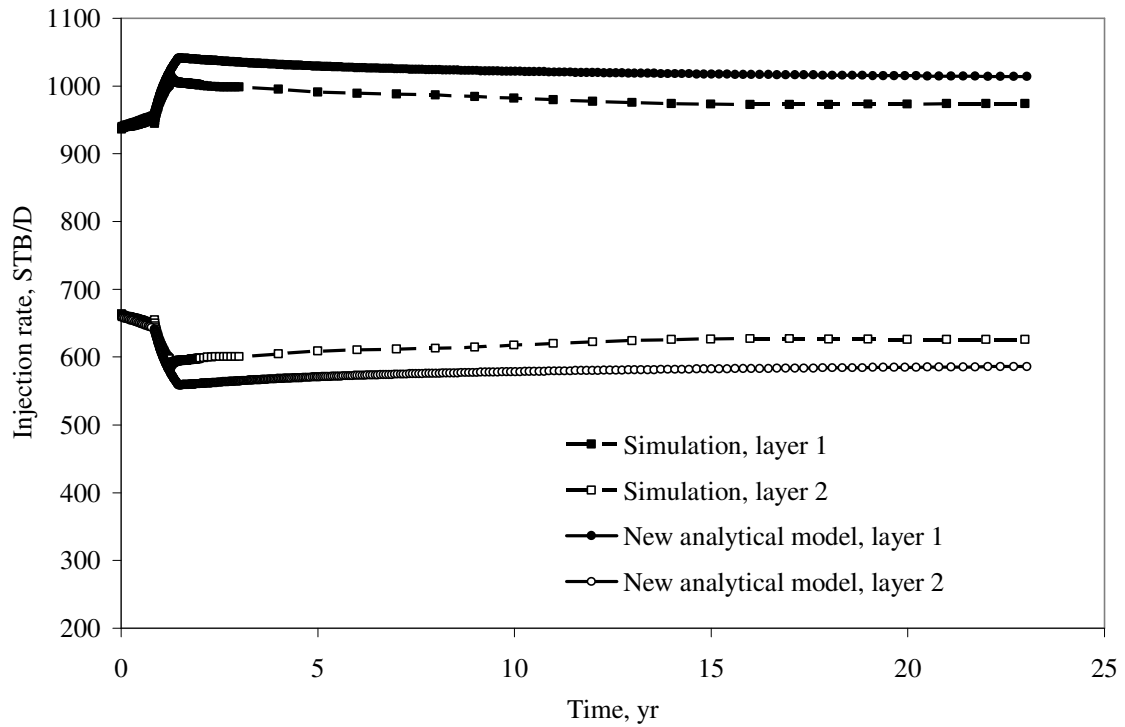


Figure 3.31 Water injection rate by layers, comparison of new analytical model to simulation, injection rate of 1600 STB/D is applied (Case 5).

Fig. 3.32 presents the cumulative oil production comparison of the new model against that of simulation. Similarly it can be seen from **Fig. 3.32** that it shows exactly the same behavior as in **Fig. 3.6**.

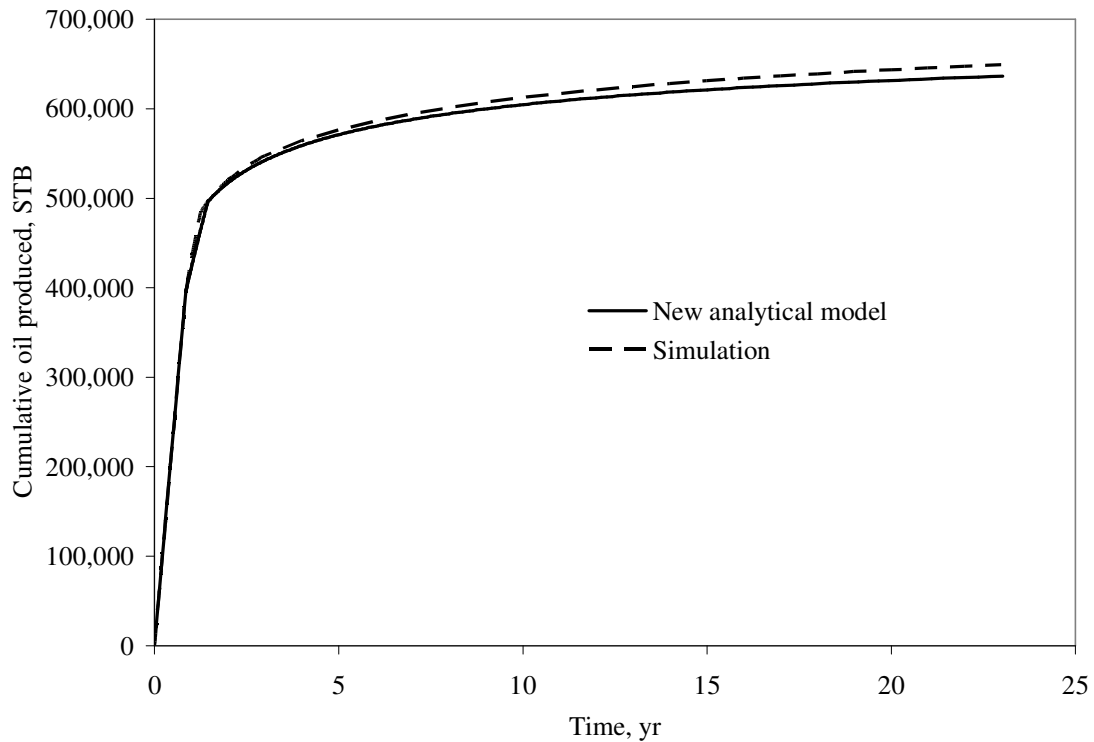


Figure 3.32 Cumulative oil production, comparison of new analytical model to simulation, injection rate of 1600 STB/D is applied (Case 5).

Fig. 3.33 shows oil production rate by layer. It can be seen that oil production rates for both layers before breakthrough in layer 1 based on the new model is very similar to that based on simulation. However after breakthrough in layer 1, oil production rate in layer 2 is higher based on simulation. Nevertheless, after breakthrough in layer 2, oil production rate for both layers based on the new model are in close agreement with simulation results. **Fig. 3.33** is similar to **Fig. 3.7**.

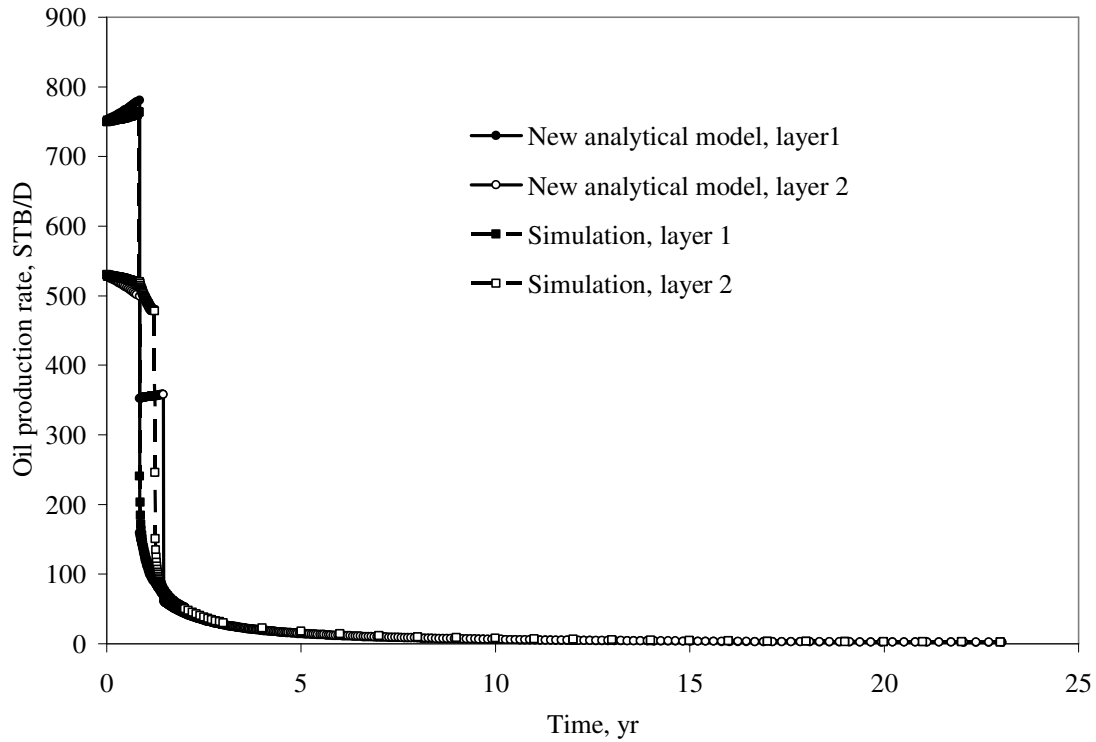


Figure 3.33 Oil production rate on layer basis, comparison of new analytical model to simulation, injection rate of 1600 STB/D is applied (Case 5).

Fig. 3.34 presents water production rate by layer. The results are similar to **Fig. 3.8** results of Case 1.

However, as can be noted from **Fig. 3.35**, the total water production rate based on the new model has significant difference in breakthrough time comparing to **Fig. 3.9**.

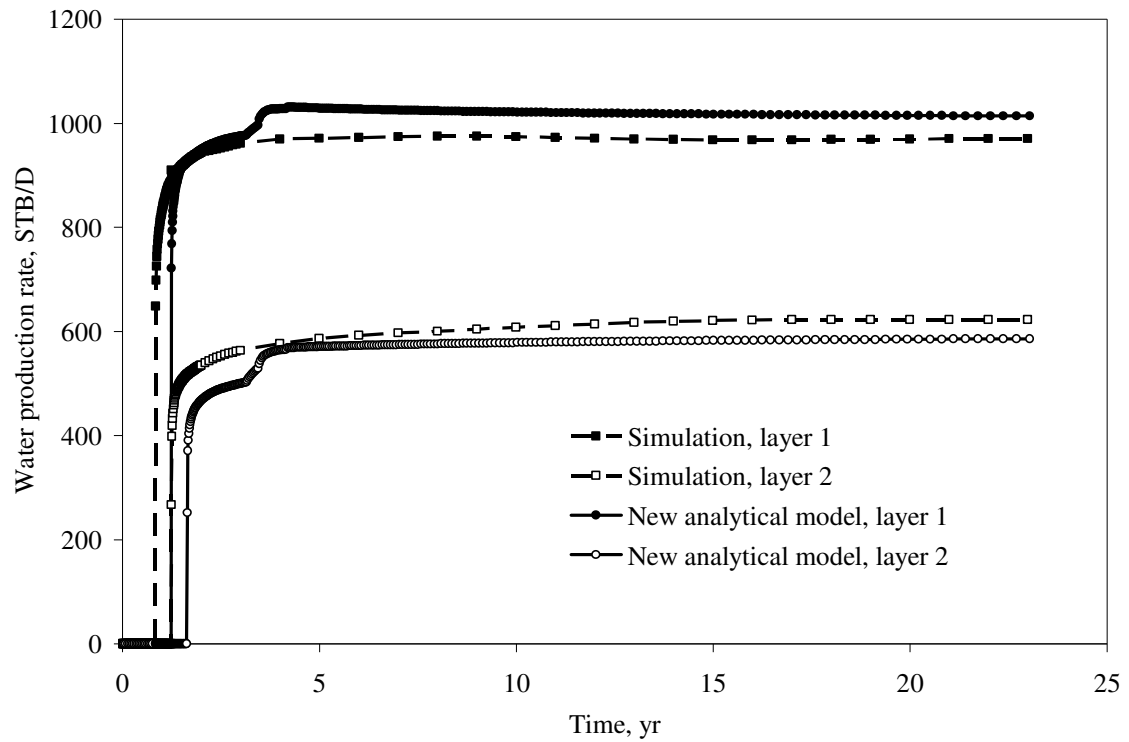


Figure 3.34 Water production on layer basis, comparison of new analytical model to simulation, injection rate of 1600 STB/D is applied (Case 5).

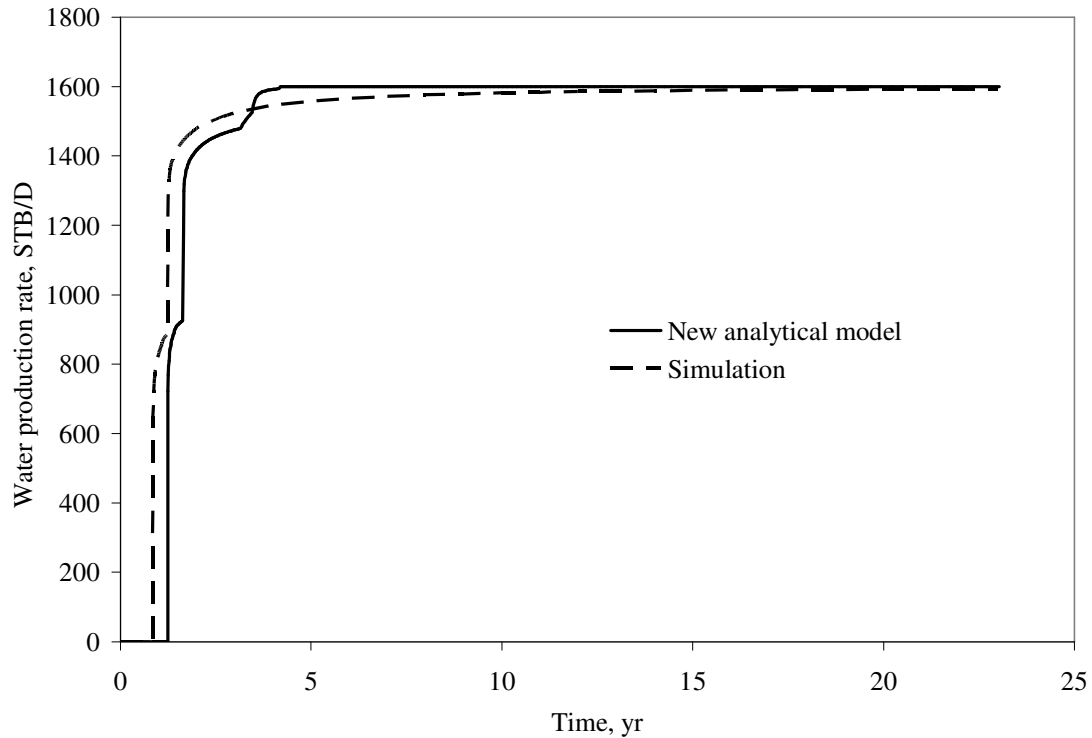


Figure 3.35 Water production rate, comparison of new analytical model to simulation, injection rate of 1600 STB/D is applied (Case 5).

3.7 Case 6

Case 6 represents the variation of Case 2 where injection rate value has been increased to the 1600 STB/D of water.

Fig. 3.36 shows the oil production rate based on the new model versus simulation results. As can be seen from **Fig. 3.36** it shows exactly the same behavior as in **Fig. 3.12** from Case 2 but with doubled production rate and halved time of breakthrough.

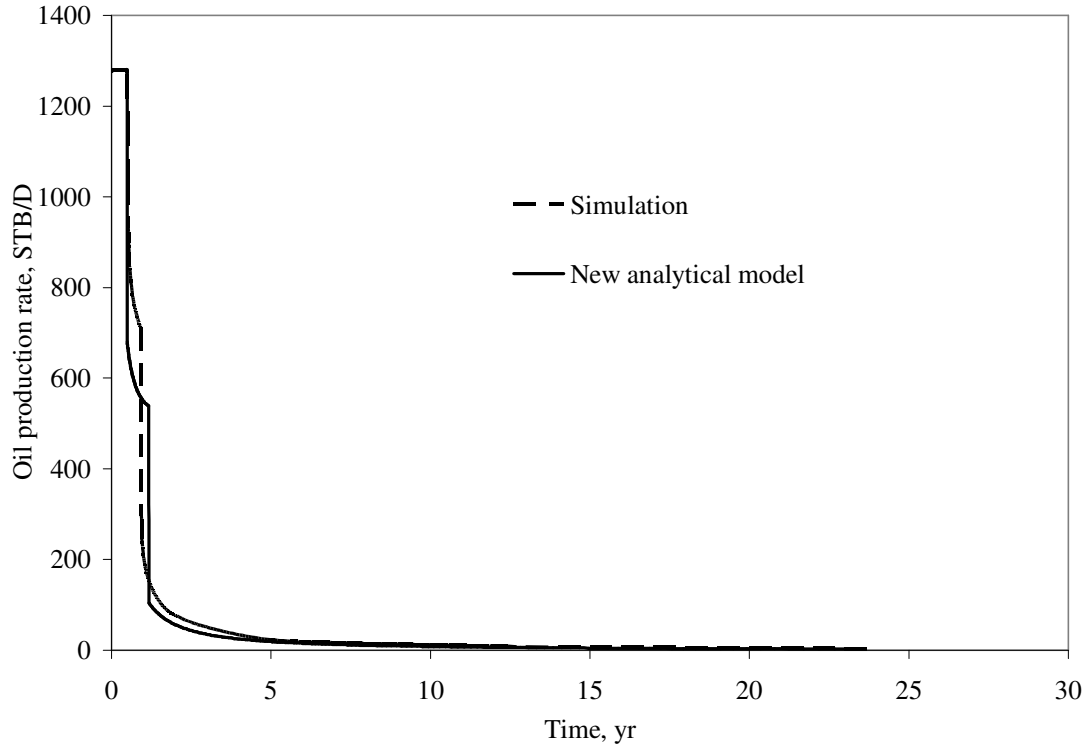


Figure 3.36 Oil production rate, comparison of new analytical model to simulation, 2 relative permeability sets and injection rate of 1600 STB/D are applied (Case 6).

Fig. 3.37 presents the water injection rate by layer comparison of the new model against that of simulation. Similarly it can be seen from **Fig. 3.37** that it shows exactly the same behavior as in **Fig. 3.13** of Case 2, but with doubled injection rate.

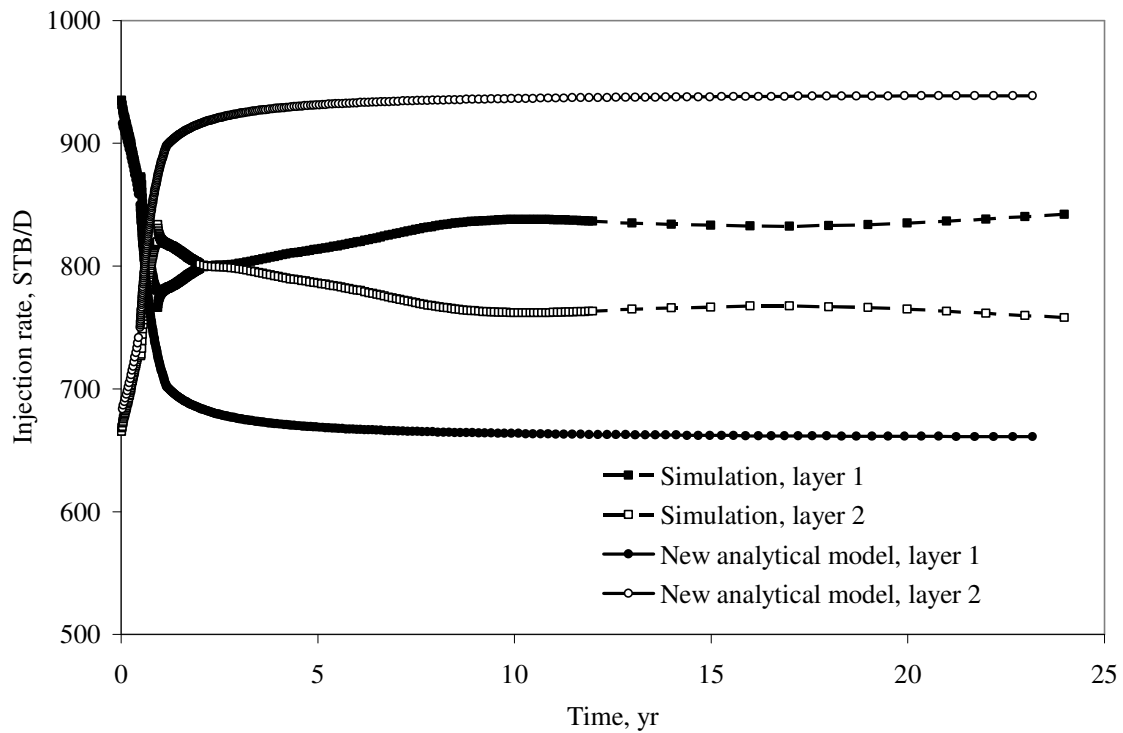


Figure 3.37 Water injection rate by layers, comparison of new analytical model to simulation, 2 relative permeability sets and injection rate of 1600 STB/D are applied (Case 6).

Fig. 3.38 presents the cumulative oil production comparison of the new model against that of simulation. Similarly it can be seen from **Fig. 3.38** that it shows exactly the same behavior as in **Fig. 3.14**.

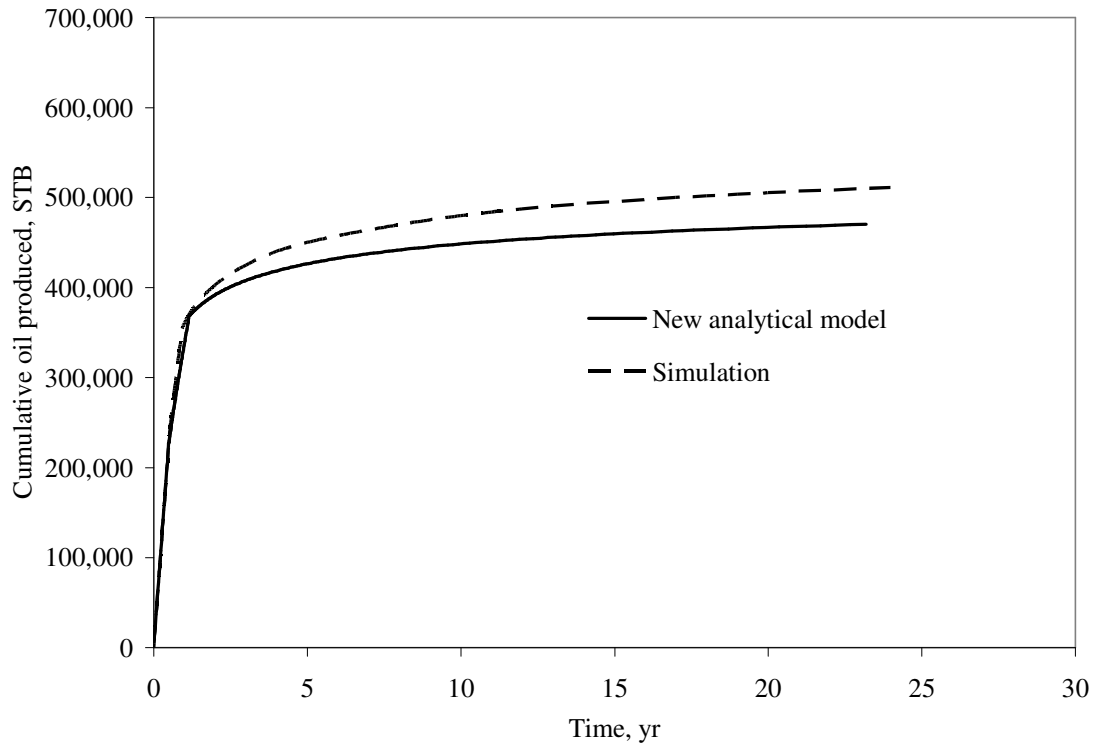


Figure 3.38 Cumulative oil produced, comparison of new analytical model to simulation, 2 relative permeability sets and injection rate of 1600 STB/D are applied (Case 6).

Fig. 3.39 shows oil production rate by layer. It can be seen that **Fig. 3.39** oil production rates are similar to **Fig. 3.15** oil production rates.

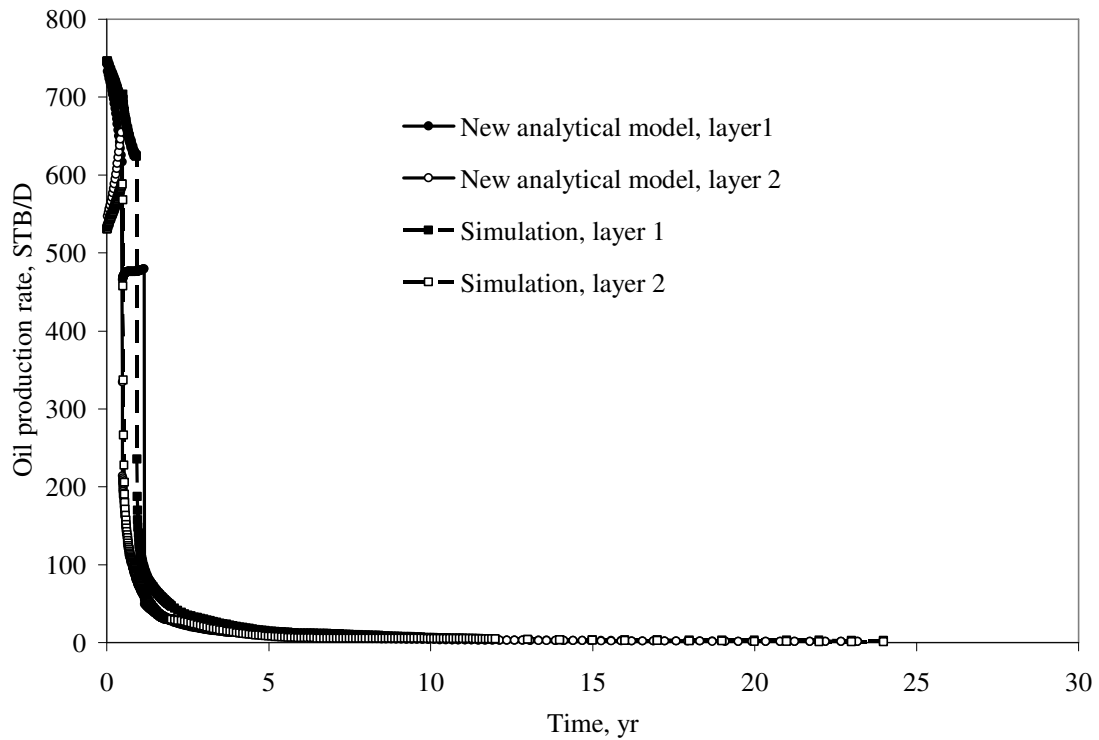


Figure 3.39 Oil production rate by layers, comparison of new analytical model to simulation, 2 relative permeability sets and injection rate of 1600 STB/D are applied (Case 6).

Fig. 3.40 presents water production rate by layer. The results are similar to **Fig. 3.16** results of Case 2.

However, as can be noted from **Fig. 3.41**, the total water production rate based on the new model is in good agreement to that of simulation.

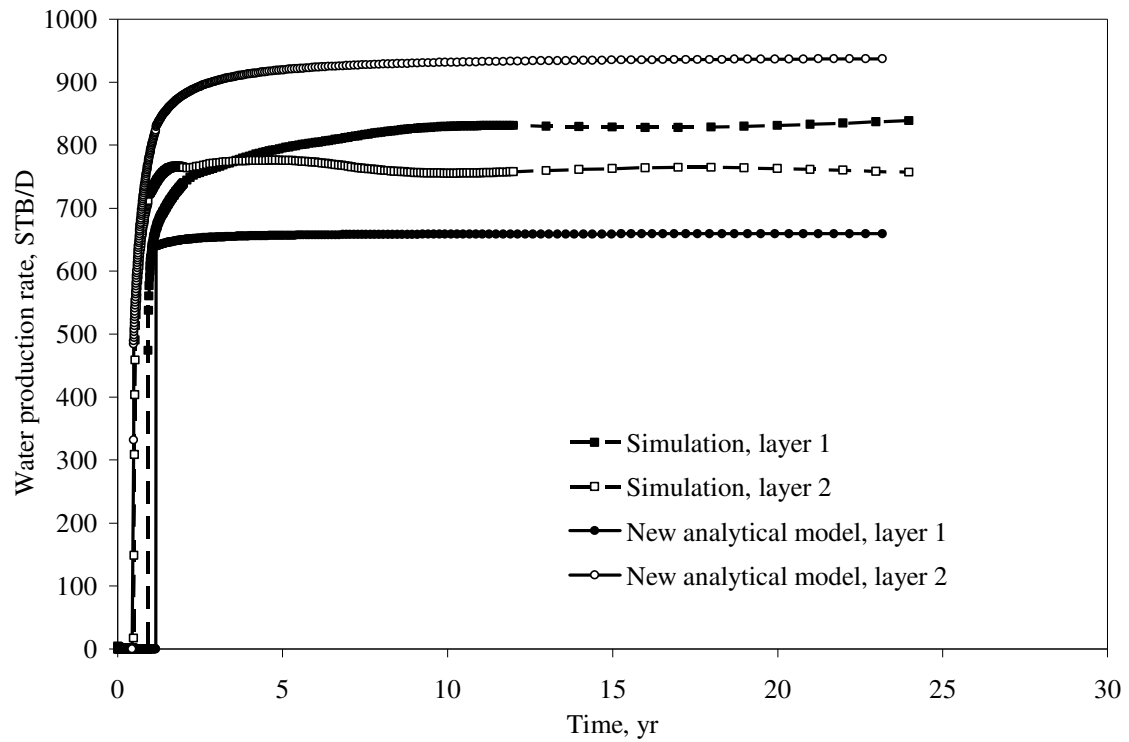


Figure 3.40 Water production rate by layers, comparison of new analytical model to simulation, 2 relative permeability sets and injection rate of 1600 STB/D are applied (Case 6).

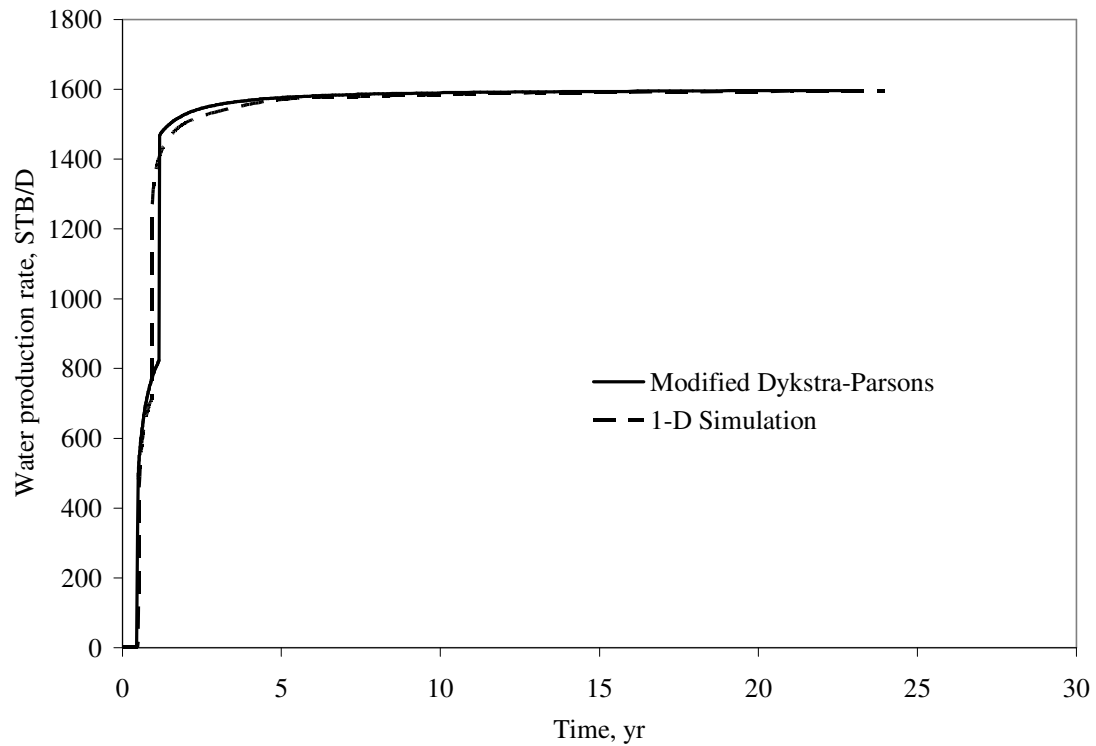


Figure 3.41 Total water production rate, comparison of new analytical model to simulation, 2 relative permeability sets and injection rate of 1600 STB/D are applied (Case 6).

3.8 Case 7

In this case it was decided to use increased injection rate of 1600 STB/D on the Case 3, model with single relative permeability set and with substantial difference in kh .

Fig. 3.42 shows the oil production rate based on the new model versus simulation results. As it can be seen from **Fig. 3.42** it shows exactly the same behavior as in **Fig. 3.18** from Case 3, but with doubled production rate and halved time of breakthrough.

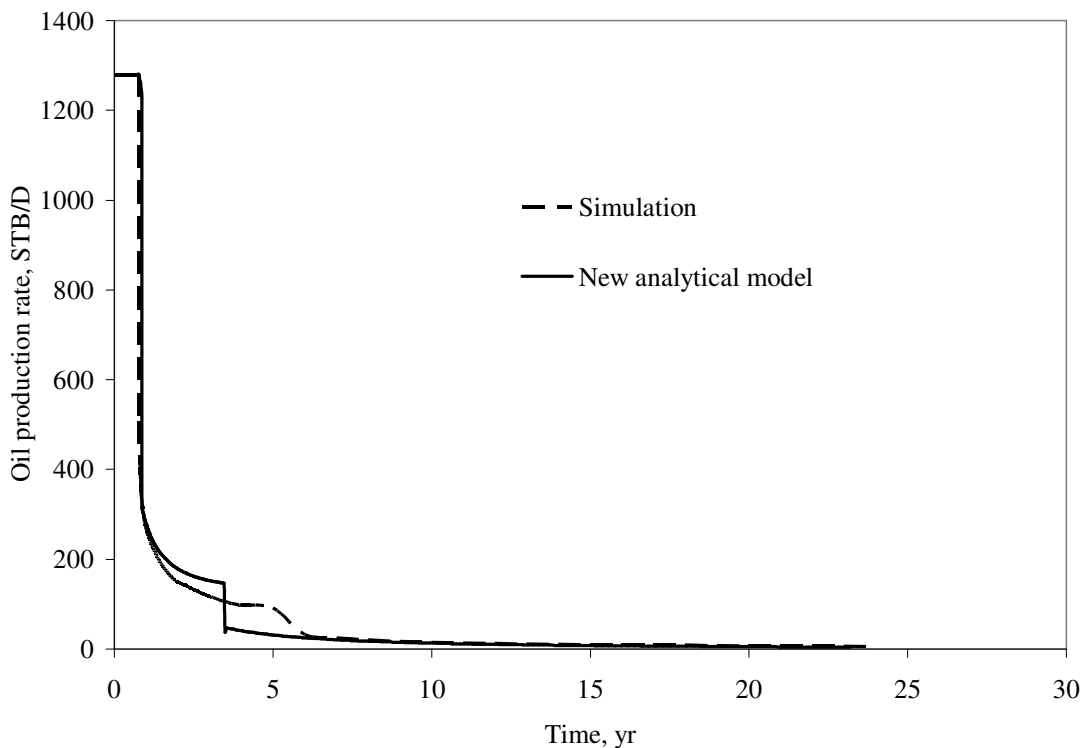


Figure 3.42 Oil production rate, comparison of new analytical model to simulation, different kh and injection rate of 1600 STB/D are applied (Case 7).

Fig. 3.43 presents the water injection rate by layer comparison of the new model against that of simulation. Similarly it can be seen from **Fig. 3.43** that it shows exactly the same behavior as in **Fig. 3.19** of Case 3, but with doubled injection rate.

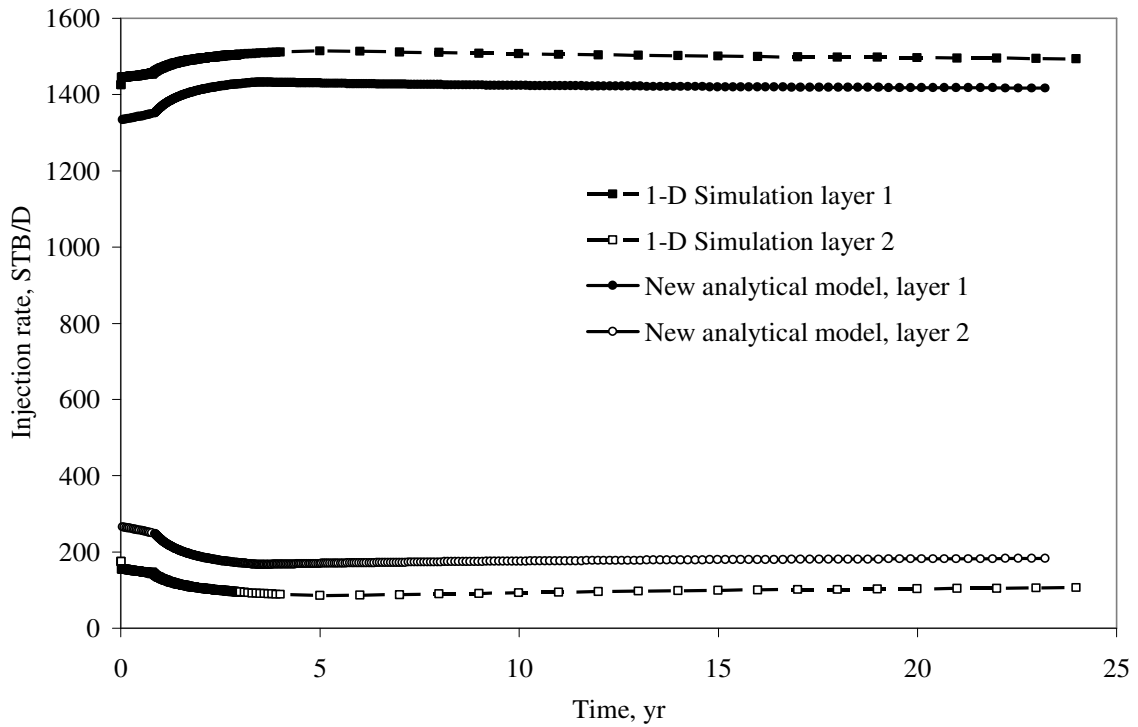


Figure 3-43 Water injection rate by layers, comparison of new analytical model to simulation, different kh and injection rate of 1600 STB/D are applied (Case 7).

Fig. 3.44 presents the cumulative oil production comparison of the new model against that of simulation. Similarly it can be seen from **Fig. 3.44** that it shows exactly the same behavior as in **Fig. 3.20**.

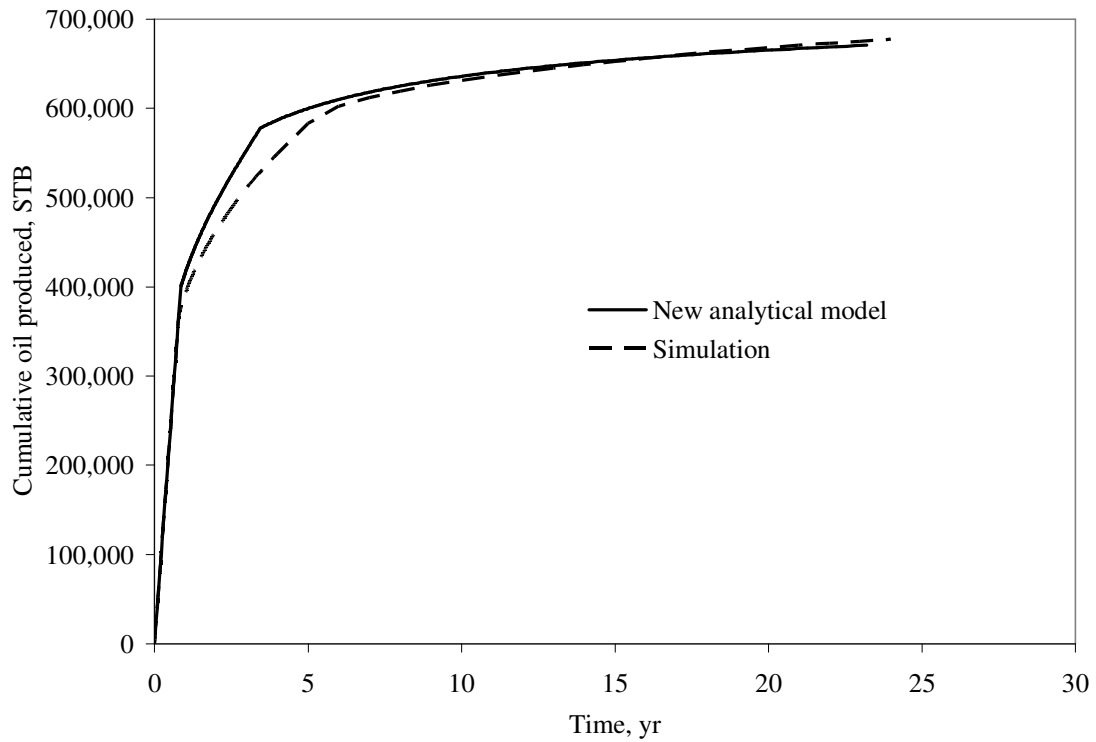


Figure 3.44 Cumulative oil produced, comparison of new analytical model to simulation, different kh and injection rate of 1600 STB/D are applied (Case 7).

Fig. 3.45 shows oil production rate by layer. It can be seen that **Fig. 3.45** oil production rates are similar to **Fig. 3.21** oil production rates of Case 3.

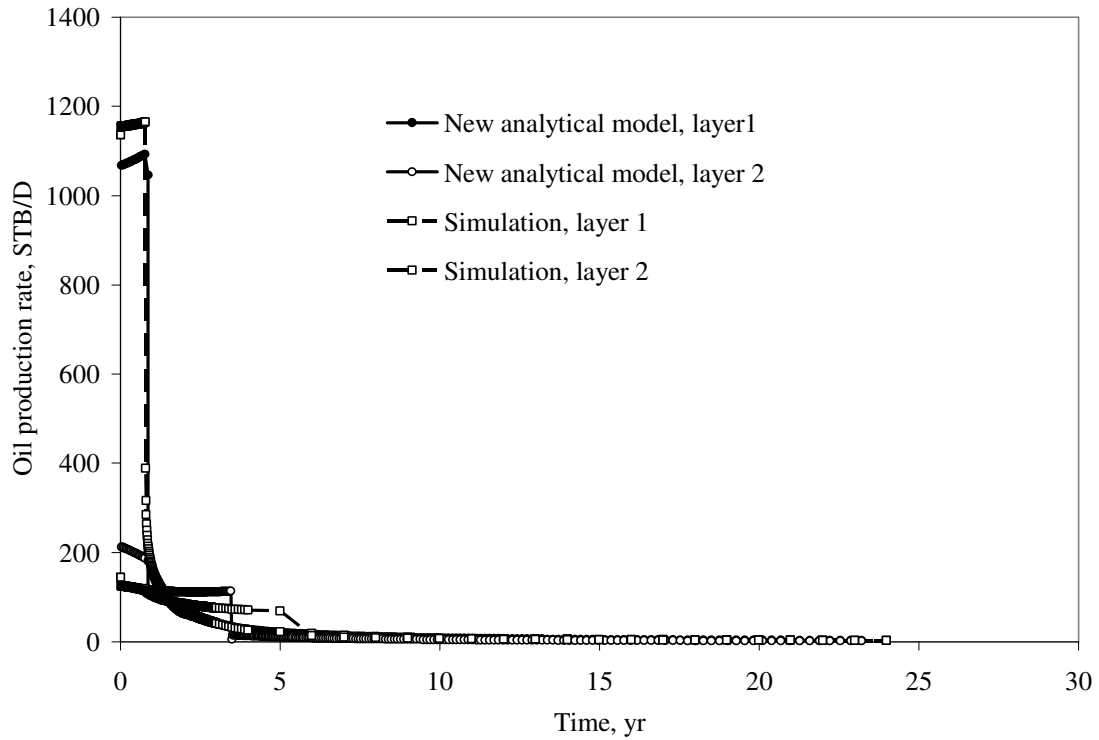


Figure 3.45 Oil production by layers, comparison of new analytical model to simulation, different kh and injection rate of 1600 STB/D are applied (Case 7).

Fig. 3.46 presents water production rate by layer. The results are similar to **Fig. 3.22** results of Case 3.

However, as can be noted from **Fig. 3.47**, the total water production rate based on the new model is in good agreement to that of simulation after breakthrough in layer 2.

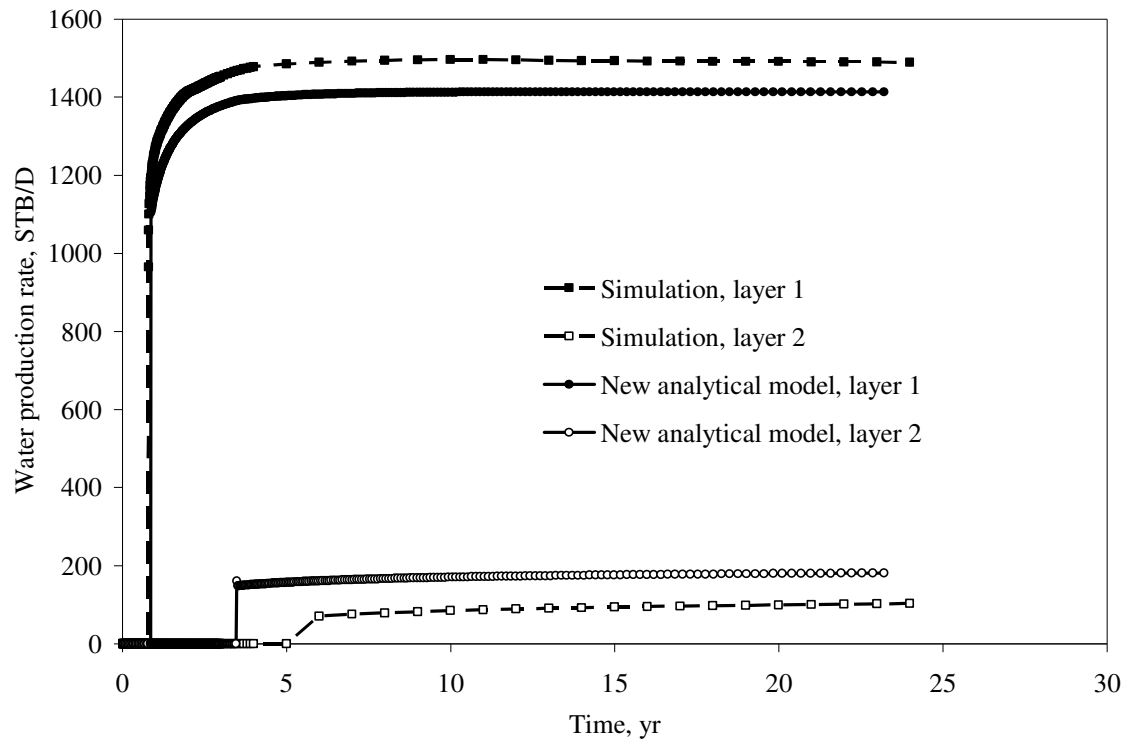


Figure 3.46 Water production by layers, comparison of new analytical model to simulation, different kh and injection rate of 1600 STB/D are applied (Case 7).

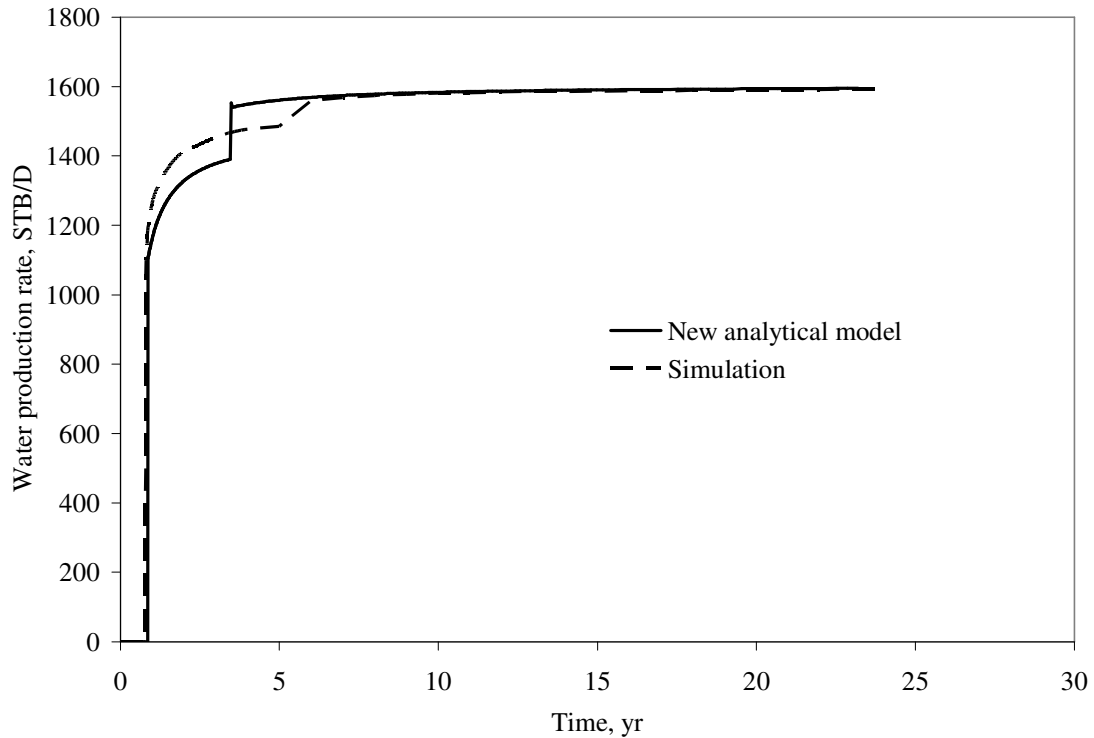


Figure 3.47 Total water production, comparison of new analytical model to simulation, different kh and injection rate of 1600 STB/D are applied (Case 7).

3.9 Case 8

Current case is the same as Case 4 except total injection rate will be changed to 1600 STB/D.

Fig. 3.48 shows the oil production rate based on the new model versus simulation results. As can be seen from **Fig. 3.48**, it shows exactly the same behavior as in **Fig. 3.24** from Case 4, but with doubled production rate and halved time of breakthrough.

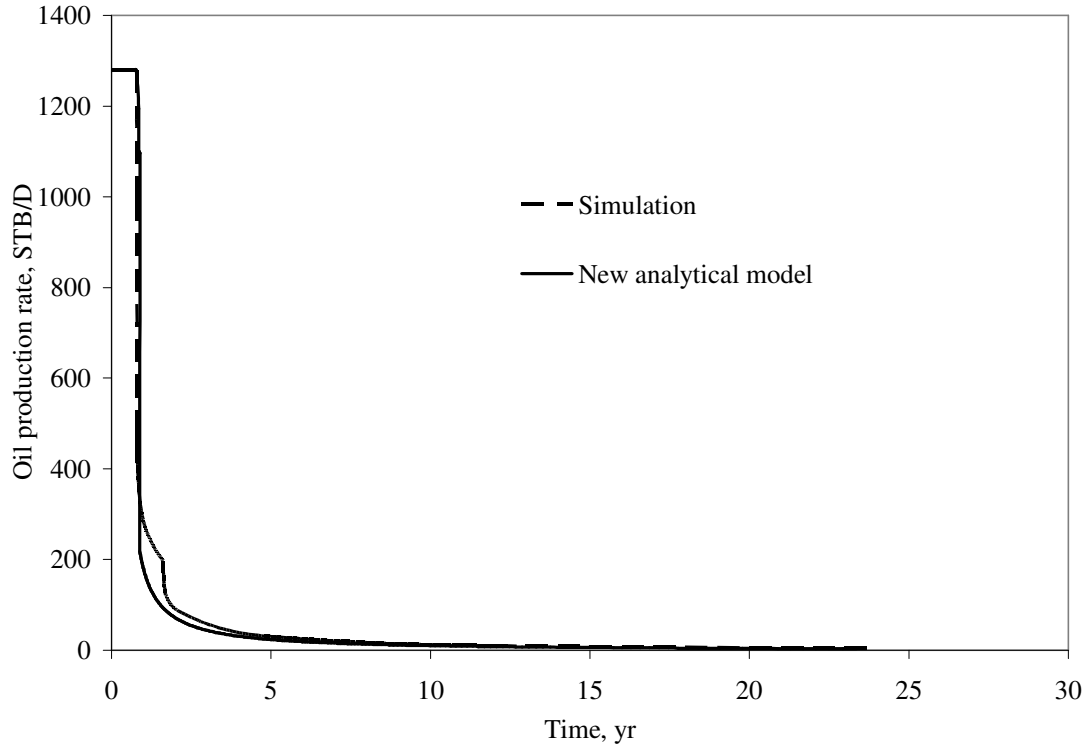


Figure 3.48 Total oil production rate, comparison of new analytical model to simulation, 2 relative permeability sets and injection rate of 1600 STB/D are applied (Case 8).

Fig. 3.49 presents the water injection rate by layer comparison of the new model against that of simulation. Similarly it can be seen from **Fig. 3.49** that it shows exactly the same behavior as in **Fig. 3.25**.

As can be seen from **Fig.3.49**, water injection rate comparison of analytical versus numerical models shows the most significant difference by analogy to Case 4.

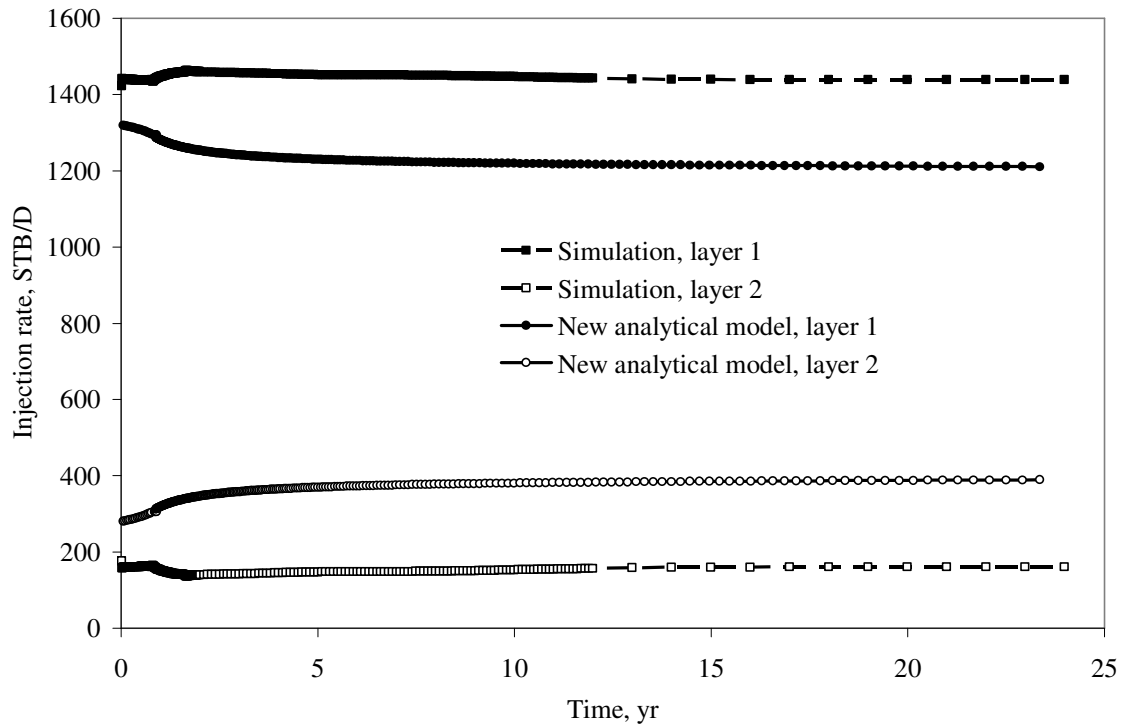


Figure 3.49 Water injection rate by layers, comparison of new analytical model to simulation, 2 relative permeability sets and injection rate of 1600 STB/D are applied (Case 8).

Fig. 3.50 presents the cumulative oil production comparison of the new model against that of simulation. Similarly it can be seen from **Fig. 3.50** that it shows exactly the same behavior as in **Fig. 3.26**.

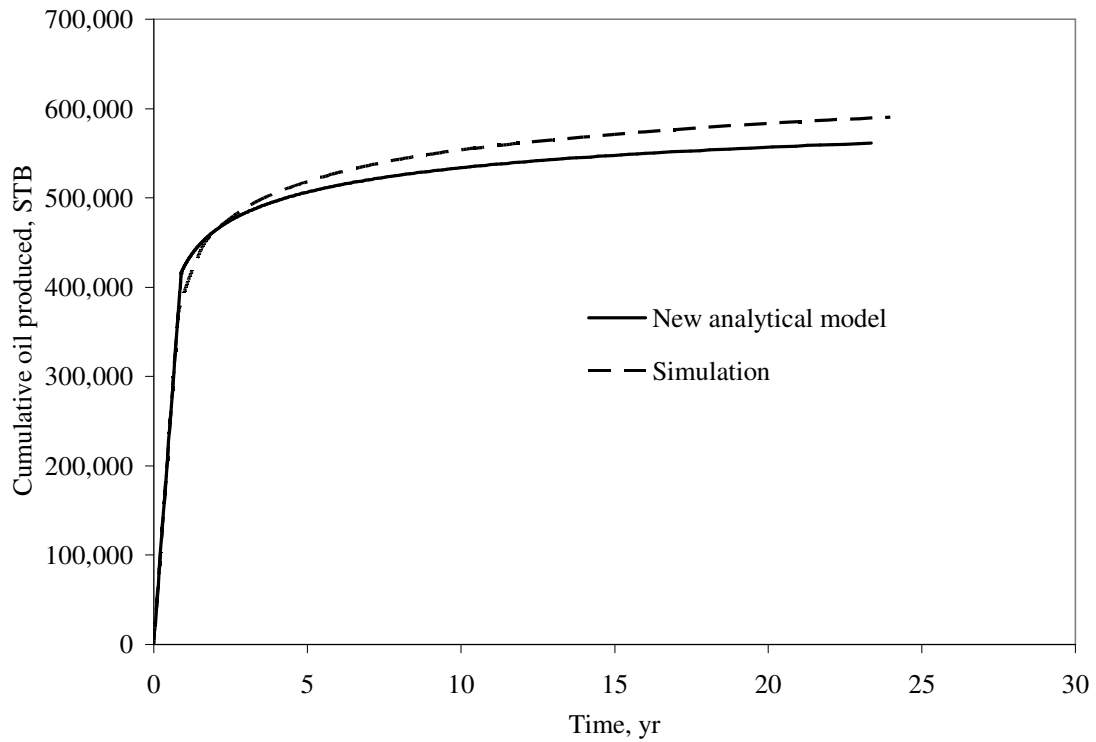


Figure 3.50 Cumulative oil, comparison of new analytical model to simulation, 2 relative permeability sets and injection rate of 1600 STB/D are applied (Case 8).

Fig. 3.51 shows oil production rate by layer. It can be seen that **Fig. 3.51** oil production rates are similar to **Fig. 3.27** oil production rates of Case 4.

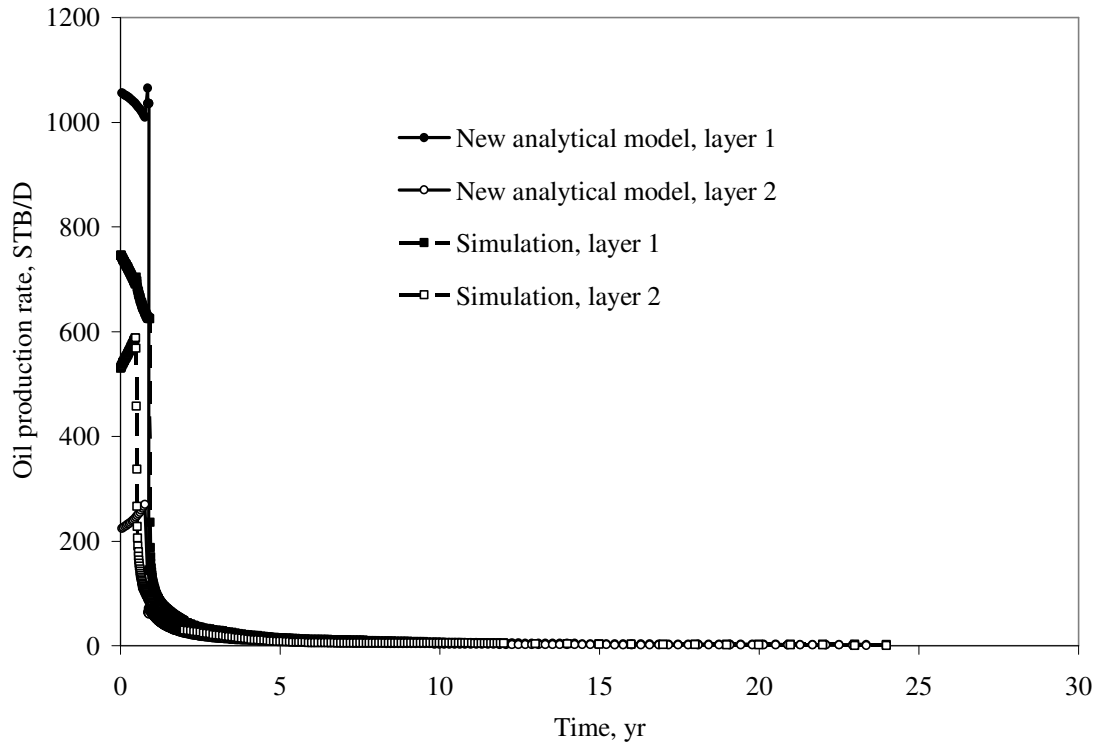


Figure 3.51 Oil production by layers, comparison of new analytical model to simulation, 2 relative permeability sets and injection rate of 1600 STB/D are applied (Case 8).

Fig. 3.52 presents water production rate by layer. The results are similar to **Fig. 3.28** results of Case 4.

However, as can be noted from **Fig. 3.53**, the total water production rate based on the new model is in good agreement to that of simulation after breakthrough in layer 2.

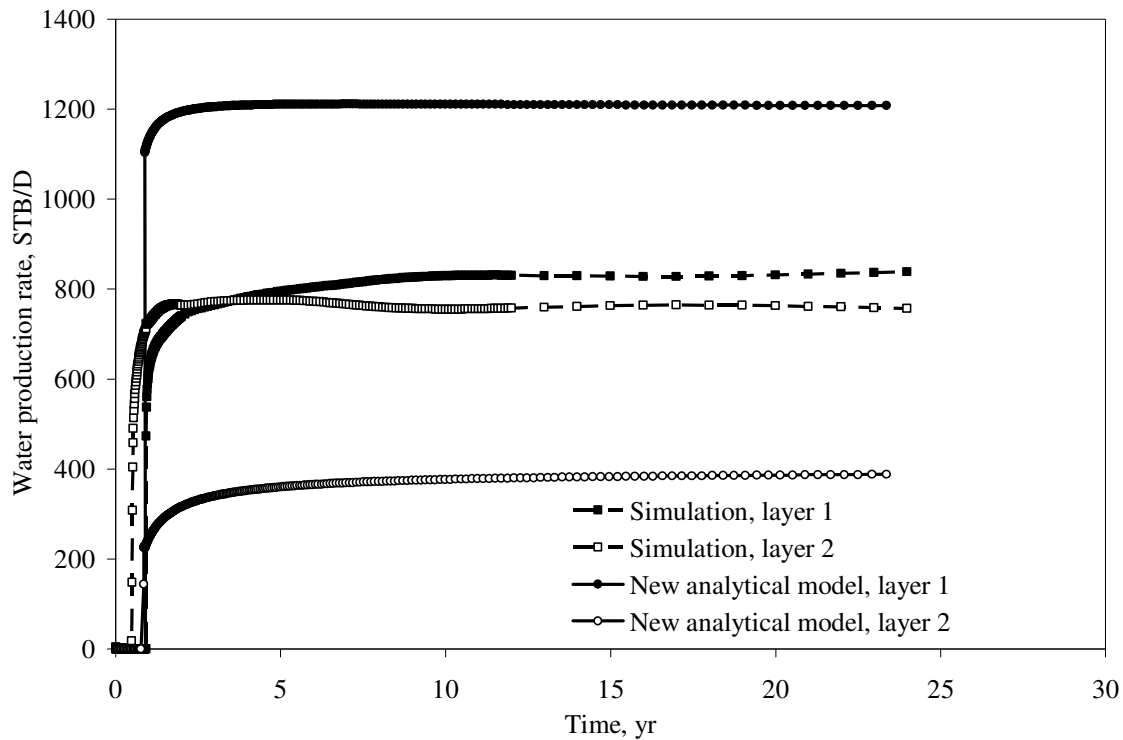


Figure 3.52 Water production by layers, comparison of new analytical model to simulation, 2 relative permeability sets and injection rate of 1600 STB/D are applied (Case 8).

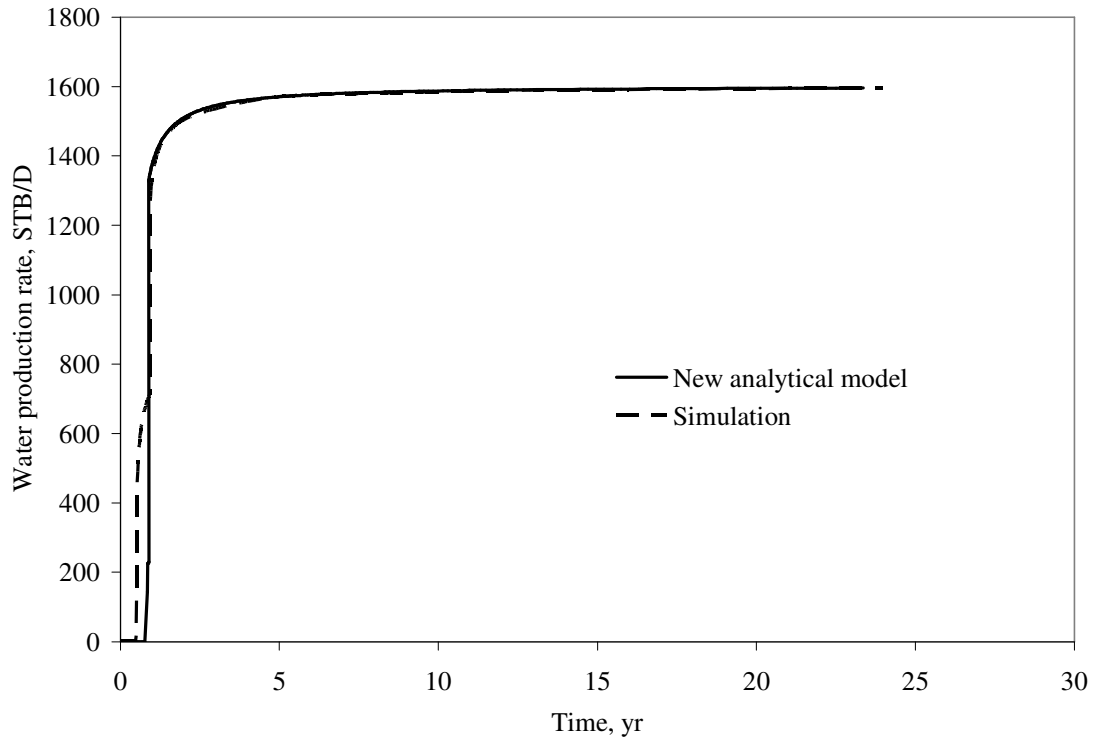


Figure 3.53 Water production rate, comparison of new analytical model to simulation, 2 relative permeability sets and injection rate of 1600 STB/D are applied (Case 8).

3.10 Case 9

In the Case 9, the reservoir parameters are identical for both layers. This case was run basically for validation of the analytical model program.

Fig. 3.54 presents oil production rate of the new model compared to simulation, as it can be seen from the **Fig. 3. 54** the results are practically identical.

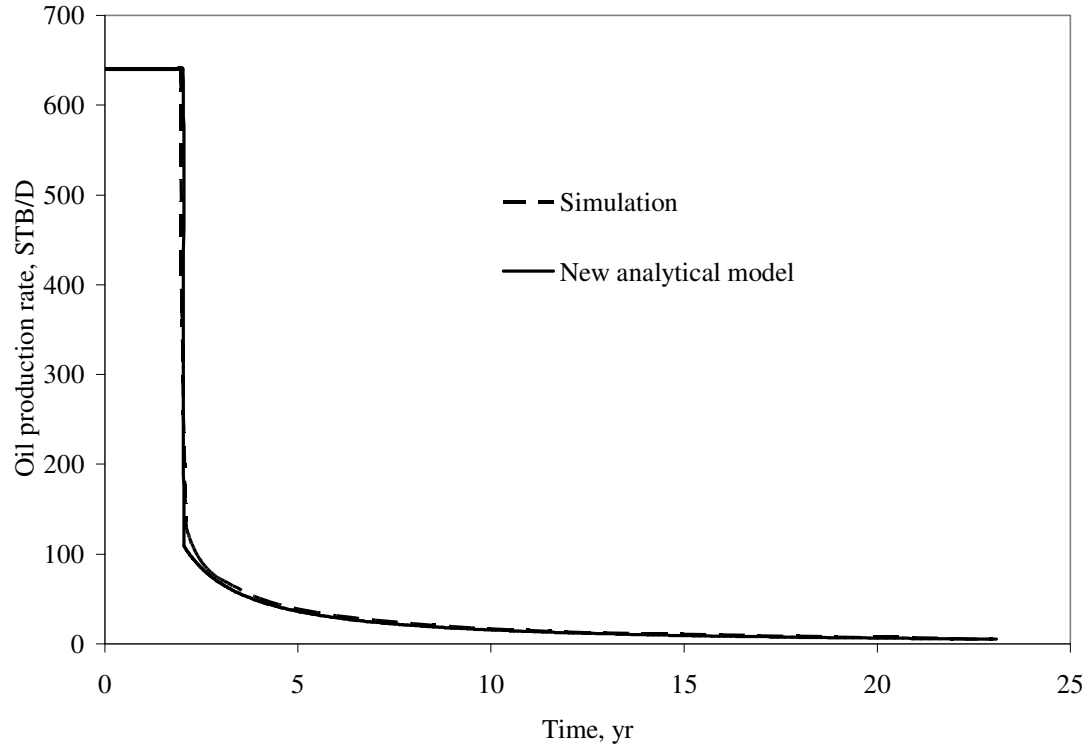


Figure 3.54 Oil production rate, comparison of new analytical model to simulation, for 2 identical layers (Case 9).

Fig. 3.55 presents the water injection rate by layer comparison of the new model against that of simulation. Water injection rate for each layer shows the good match.

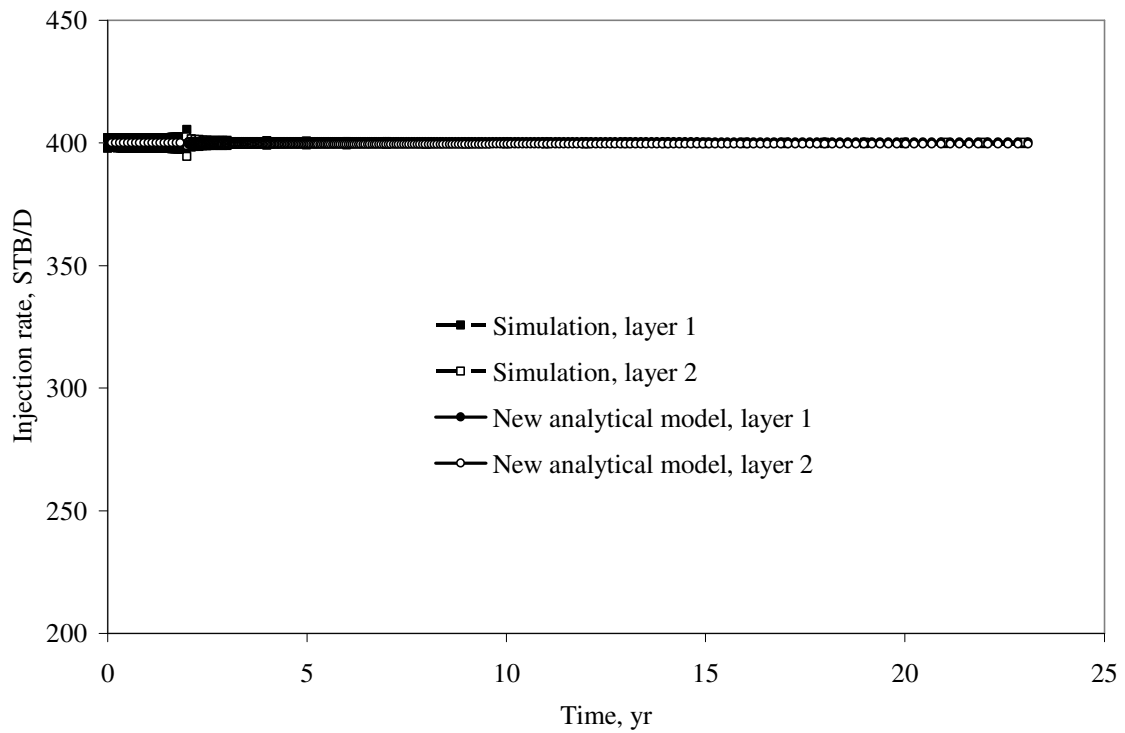


Figure 3.55 Water injection rate by layers, comparison of new analytical model to simulation, for 2 identical layers (Case 9).

Fig. 3.56 presents the cumulative oil production comparison of the new model against that of simulation, showing a very good agreement.

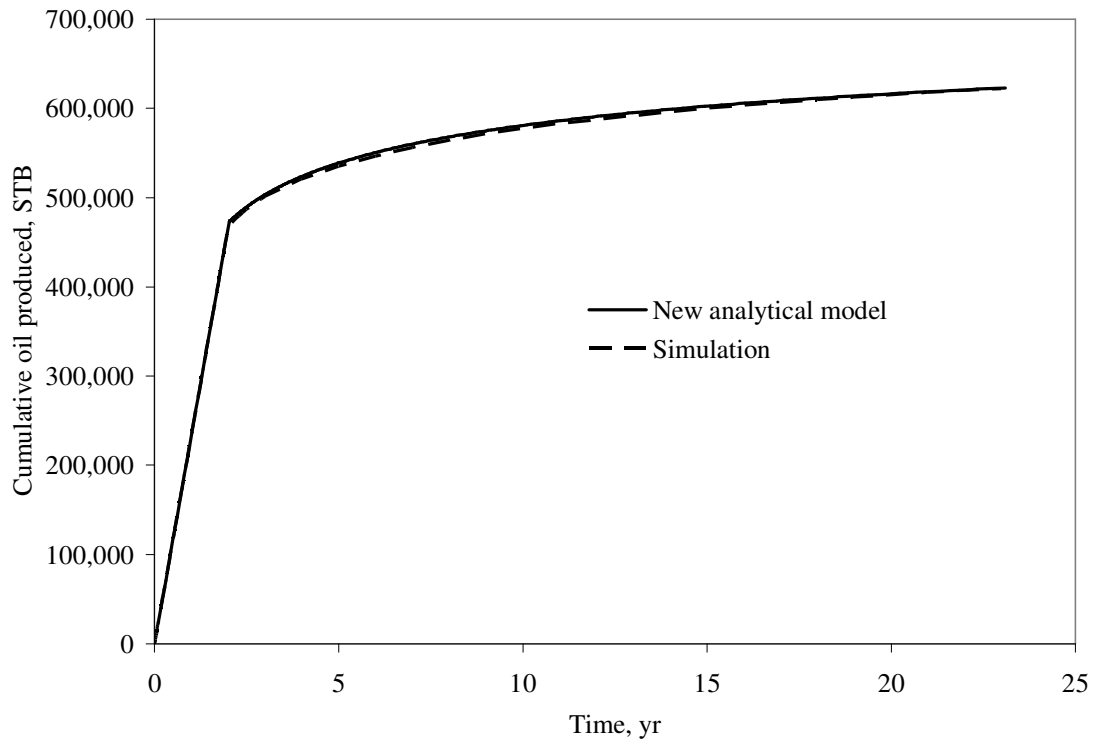


Figure 3.56 Cumulative oil produced, comparison of new analytical model to simulation, for 2 identical layers (Case 9).

Fig. 3.57 is comparison of the oil production rate by layer of the new model versus simulation. Very close agreement achieved on the **Fig. 3.57** as well.

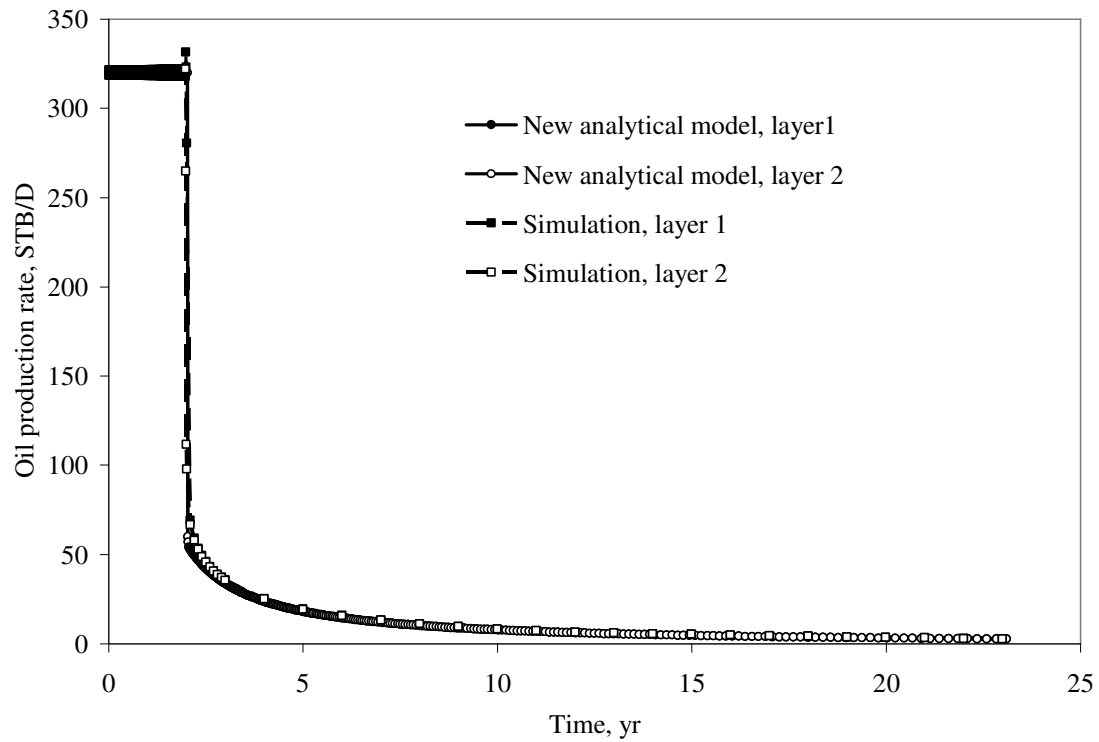


Figure 3.57 Oil production by layers, comparison of new analytical model to simulation, for 2 identical layers (Case 9).

So far analytical model showed very close results compared with numerical simulation model. **Fig. 3.58** shows water production rate by layer.

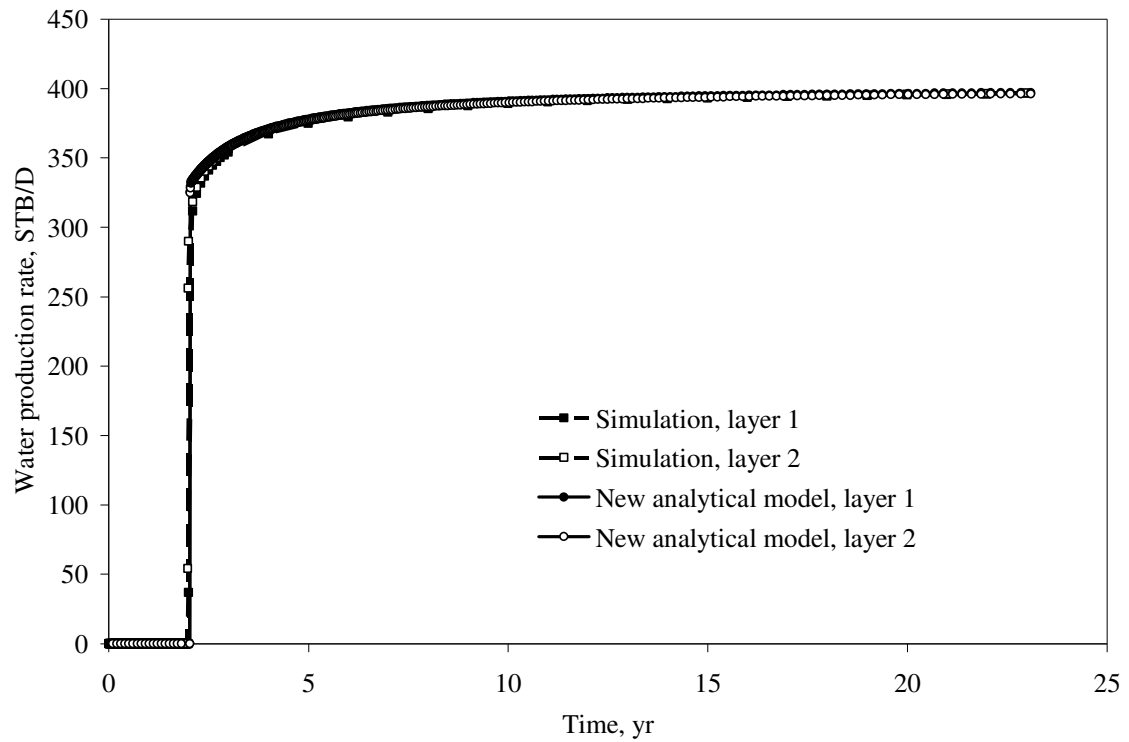


Figure 3.58 Water production by layers, comparison of new analytical model to simulation, for 2 identical layers (Case 9).

Fig. 3.59 shows total water production rate of the new model compared to that of simulation.

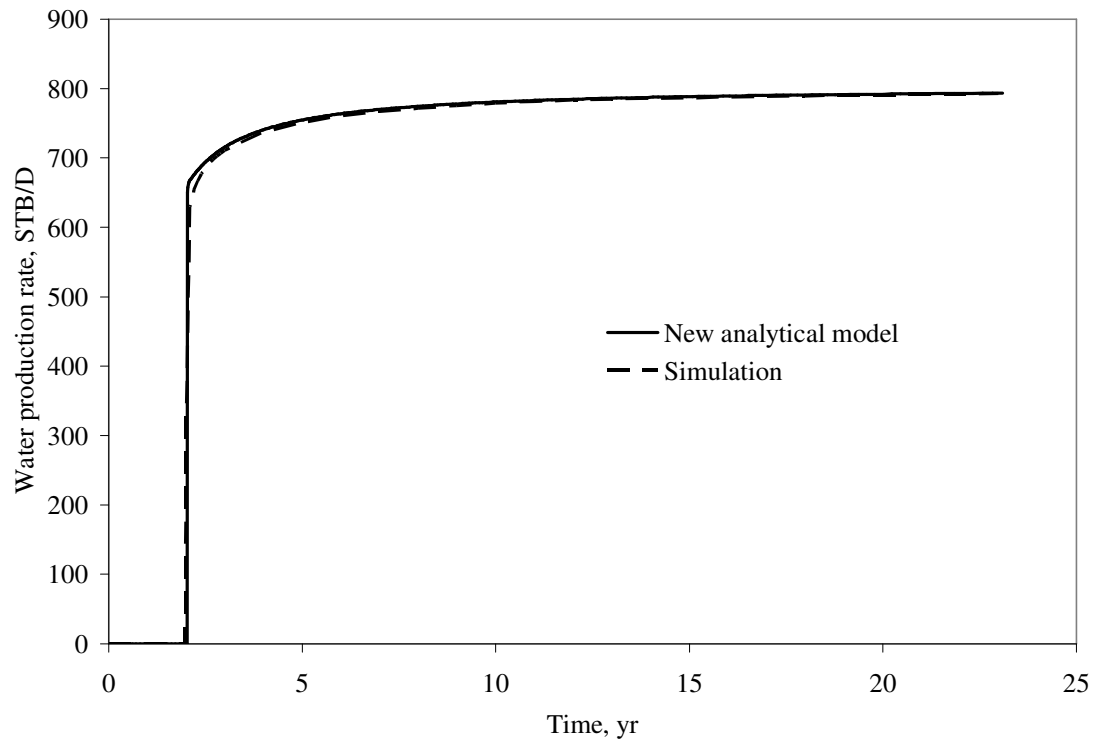


Figure 3.59 Water production rate, comparison of new analytical model to simulation, for 2 identical layers (Case 9).

CHAPTER IV

SIMULATION MODEL OVERVIEW

For comparison of the new analytical model to numerical simulation, I used GeoQuest Eclipse 100 software as the simulator. A 2-layer simulation grid model was used, with no crossflow between the layers, and 1-D displacement in each layer. By constructing simulation model in this manner, both gravity and capillary pressure effects are ignored. Using data provided for each of the nine cases in chapter 3, modifications to the reservoir properties were made. However for all nine cases, the grid dimensions were kept the same.

As an initial step, a simple 2-layer numerical simulation model was created. The model had 1x100x2 grid blocks, with variable grid in the y-direction. Initial time step Δt was 36.5 days. For sensitivity purposes the grid in the y-direction was varied from 200 grid blocks to 400 grid blocks or from 1x100x2 to 1x200x2. The initial time step Δt was reduced to 3.65 days. The result of the refinement is shown in **Fig. 4.1**, indicating practically identical results. Thus, since each simulation run takes only about two minutes, the finer grid 1x200x2 model was used for the study.

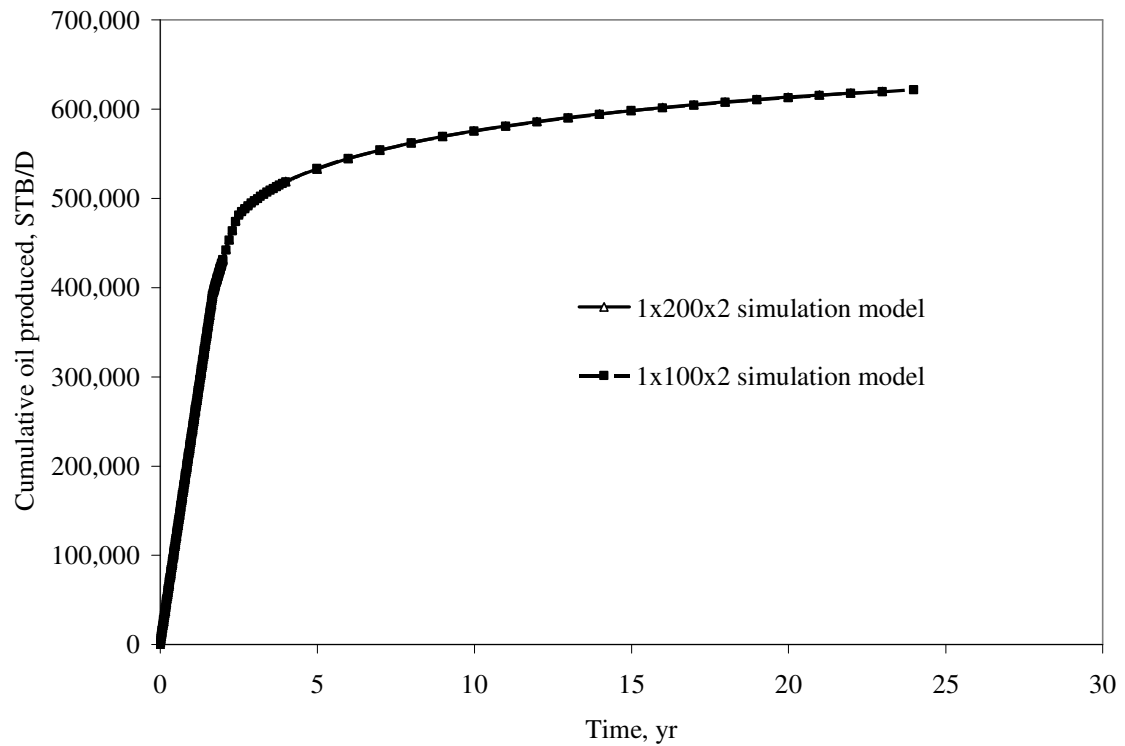


Figure 4.1 Simulation results indicate cumulative oil production with and without grid refinement is practically identical.

The nine cases studied represent different reservoir parameters for the 2-layered reservoir, as summarized in **Tables 4.1** and **4.2**.

TABLE 4.1 SUMMARY OF RESERVOIR PROPERTIES FOR EACH CASE.

Case	i_{wt} , STB/D	h_1 , ft*	h_2 , ft	k_1 , md*	k_2 , md	Relative permeability set**
1	800	35	35	500	350	1
2	800	35	35	500	350	2
3	800	50	25	500	100	1
4	800	50	25	500	100	2
5	1600	35	35	500	350	1
6	1600	35	35	500	350	2
7	1600	50	25	500	100	1
8	1600	50	25	500	100	2
9	800	35	35	500	500	1

* Subscripts 1 and 2 denote layer number (1 = upper, 2 = lower)

** Relative permeability set data listed in **Table 4.2**.

TABLE 4.2 OIL-WATER RELATIVE PERMEABILITY SET PARAMETERS.

Parameters	Set 1	Set 2
S_{wc} , fraction	0.2	0.3
S_{or} , fraction	0.2	0.35
k_{roe} , fraction	0.85	0.9
k_{rwe} , fraction	0.35	0.5
n_o	2.5	3
n_w	2.8	2

The effect of varying the parameters for each of the nine cases is significant, as shown in **Figs. 4.2 – 4.10**. These figures show the oil saturation profile in each layer at 274 days since injection, from which we can see the different waterflood advancement. The fact that these advancements differ significantly for each case is desired to fully test the validity of the new analytical model.

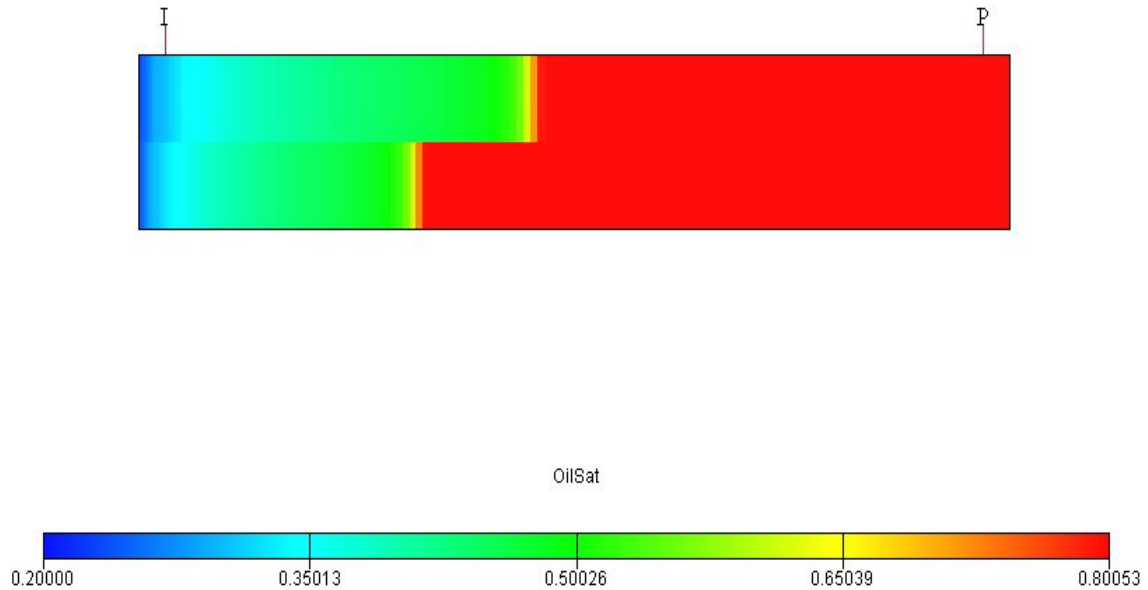


Figure 4.2 Simulation results for Case 1 at 274 days, showing earlier water breakthrough in layer that has a higher kh .

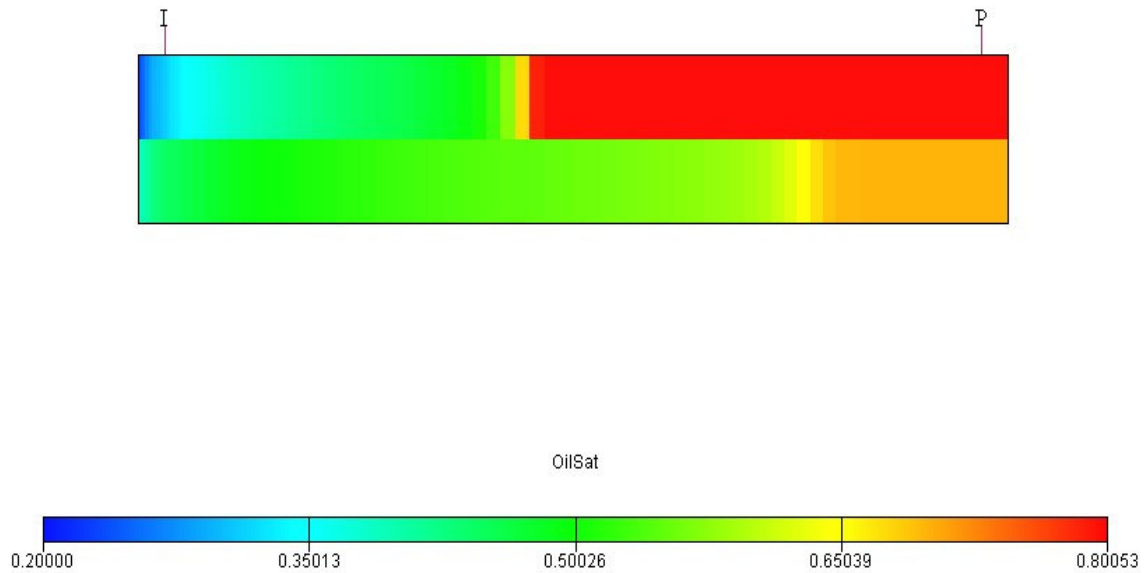


Figure 4.3 Simulation results for Case 2 at 274 days, showing faster waterflood displacement in lower layer, which has different oil-water relative permeability.

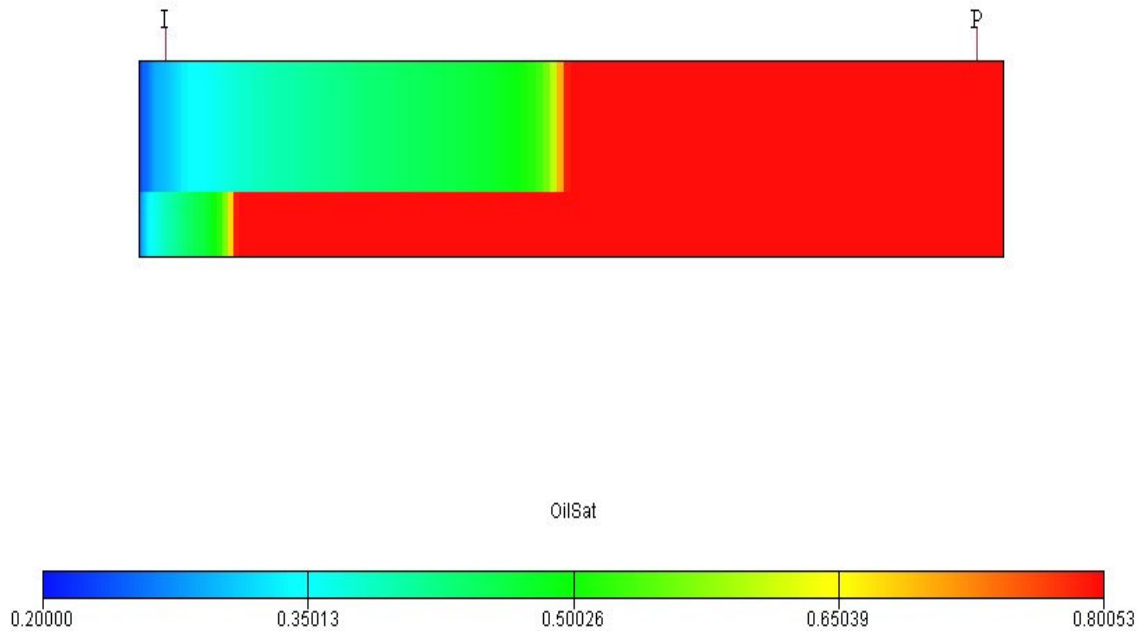


Figure 4.4 Simulation results for Case 3 at 274 days, showing faster water front propagation in upper layer that has a higher kh value.

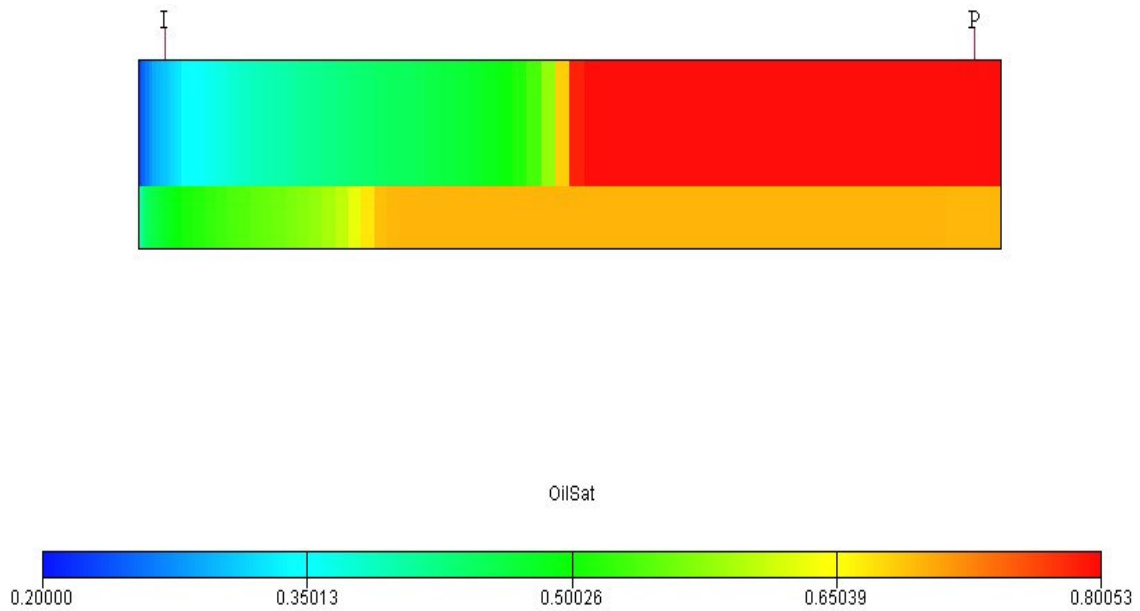


Figure 4.5 Simulation results for Case 4 at 274 days, showing faster oil displacement in upper layer that has a higher kh value.

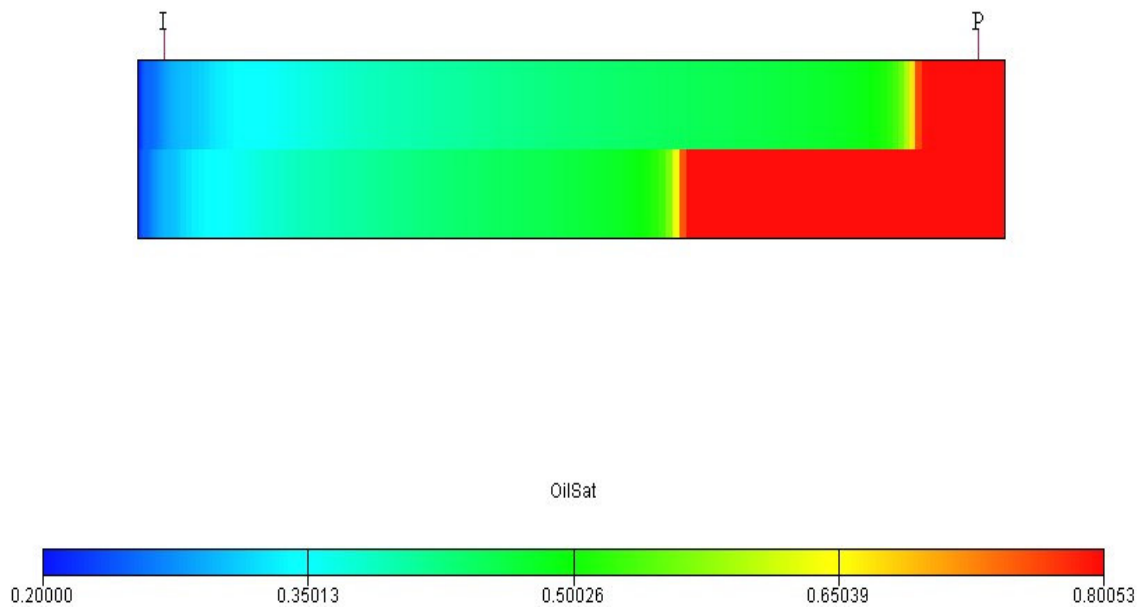


Figure 4.6 Simulation results for Case 5 at 274 days, showing that flood front advanced more than that in Case 1, as water injection rate was doubled.

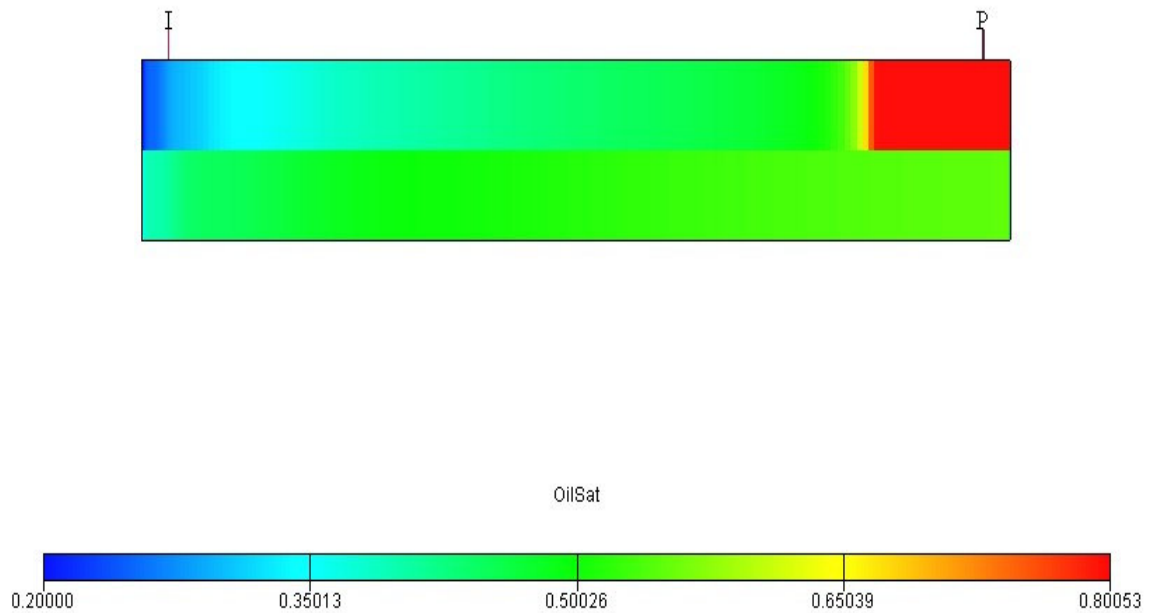


Figure 4.7 Simulation results for Case 6 at 274 days, showing similarity to Case 2 except that lower layer broke through.

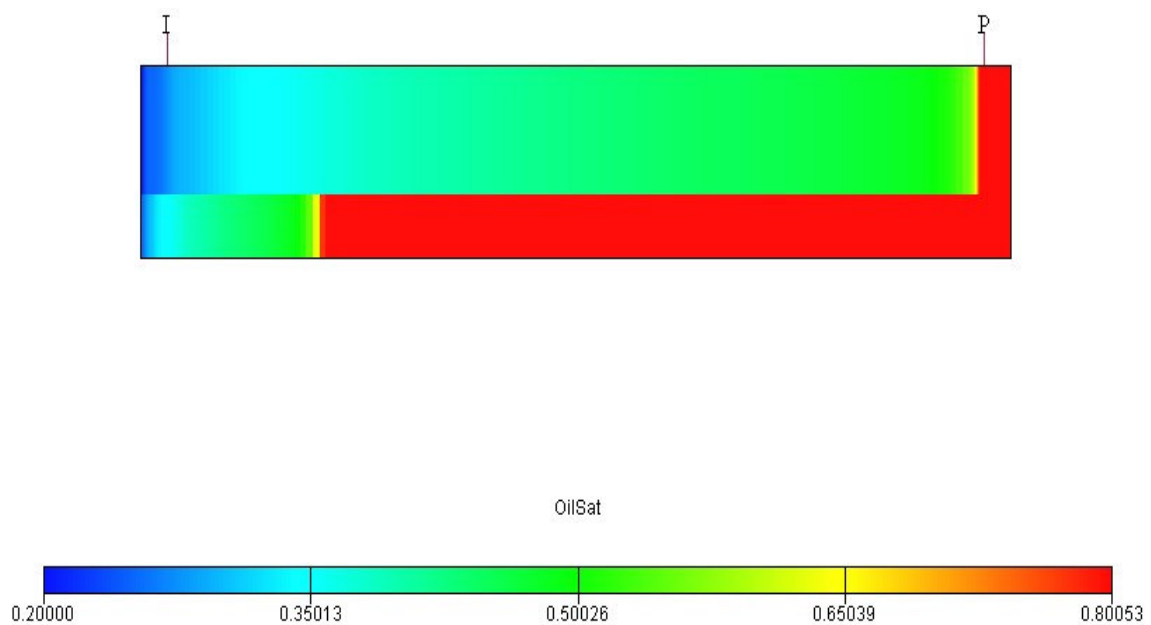


Figure 4.8 Simulation results for Case 7 at 274 days, showing faster front propagation than that in Case 3 due to increased injection rate.

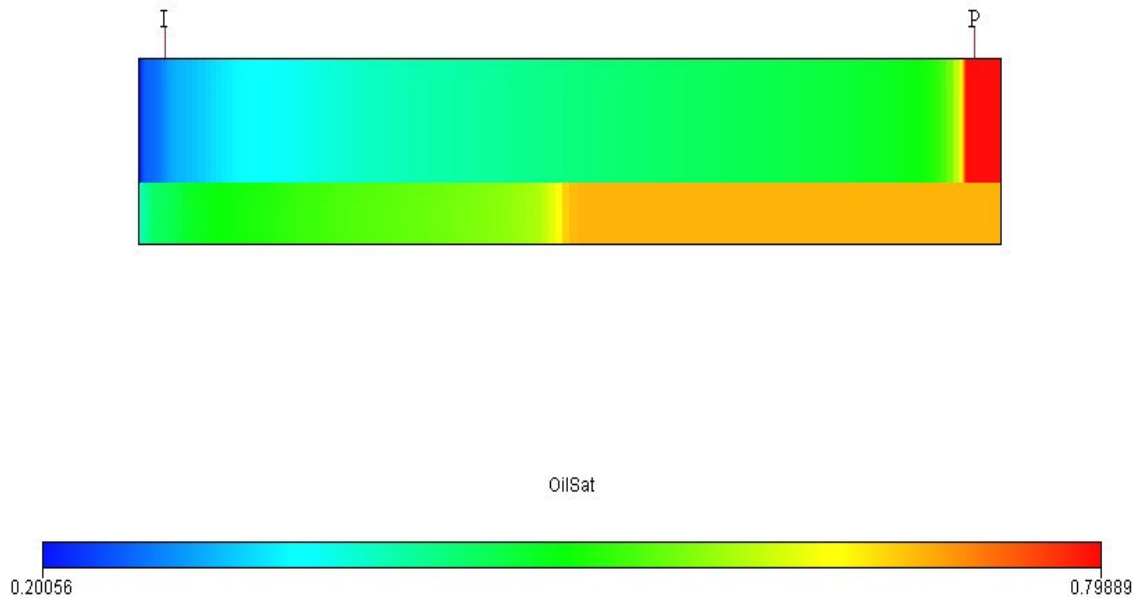


Figure 4.9 Simulation results for Case 8 at 274 days, showing faster front propagation than that in Case 4 due to increased injection rate.

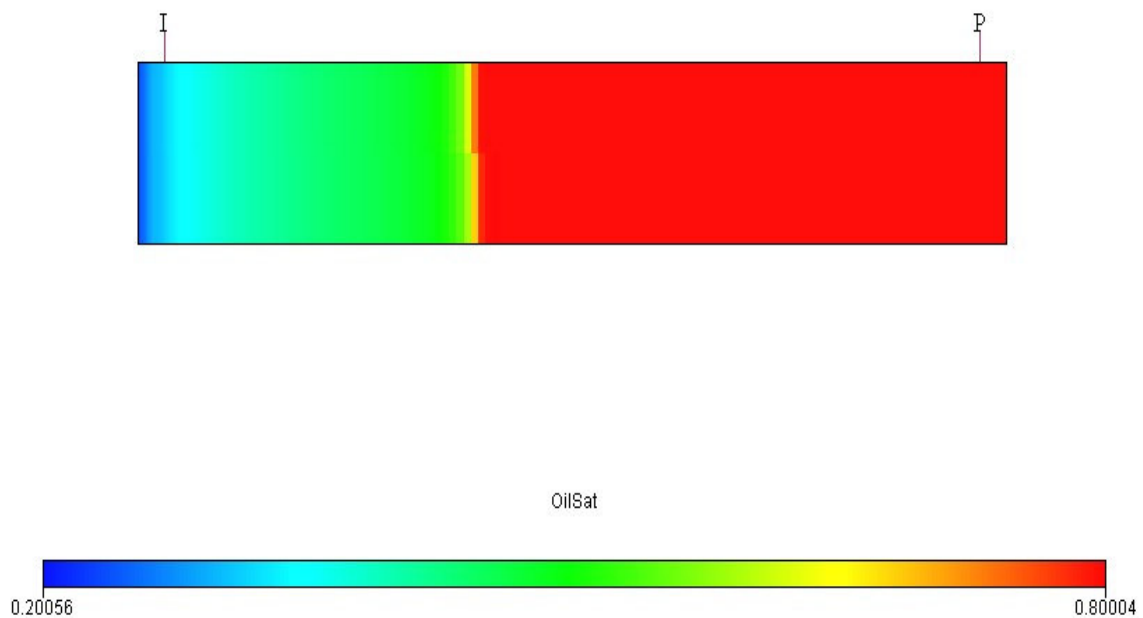


Figure 4.10 Simulation results for Case 9 at 274 days, showing identical displacement in both layers, as both layers have identical reservoir properties.

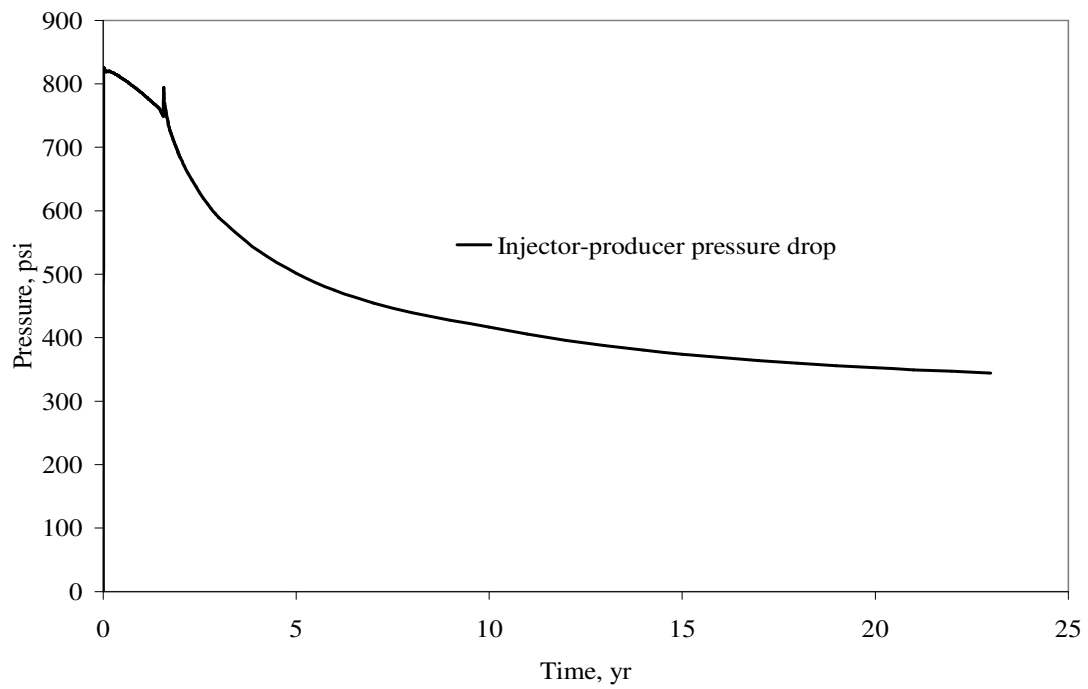


Figure 4.11 Injector-producer pressure drop for simulation model on example of Case 3.

CHAPTER V

SUMMARY, CONCLUSIONS AND RECOMMENDATIONS

5.1 Summary

The Dykstra-Parsons model has been modified to incorporate Buckley-Leverett displacement and the possibility of applying different oil-water relative permeability for each layer of a multi-layered reservoir. To verify the new model, calculated results have been compared against that of numerical simulation for a two-layered reservoir. A computer program in Microsoft Visual Basic was written to enable solving the extensive iterative procedure used in the new analytical method. The simulation model used was a 1x200x2 Cartesian model with no cross flow between the layers and with the constraint of total water injection rate and total liquid production rate (in RB/D) being equal. GeoQuest's Eclipse 100 simulation was used in the study.

Nine cases were studied in which the following parameters were varied: total water injection rate (800 and 1600 STB/D), layer thickness (25', 35', and 50'), permeability (100, 350, and 500 md), and oil-water relative permeability (two sets of Corey type curves).

5.2 Conclusions

Main conclusions based on the cases studied are as follows:

- (1) Based on the new model, cumulative oil production (N_p) up to 20 years are in good agreement with simulation results. In the worst case studied, N_p based on the new model is 468 MSTB compared to 507 MSTB from simulation, that is a difference of 39 MSTB or 8 %.

- (2) Water breakthrough times for the layer with the highest permeability-thickness product (kh) based on the new model are in good agreement with numerical simulation results. For the worst case studied, in which the kh product difference is maximum between the layers and each layer has a different oil-water relative permeability, breakthrough time based on the new model is 625 days compared to 573 days based on simulation. This is a difference of 52 days or 9 %.
- (3) However, breakthrough times for the layer with the lower kh product based on the new model are generally shorter than that based on simulation. In the worst case studied – in which the layers have the maximum kh product contrast and the same oil-water relative permeability set – the breakthrough time based on the new model is 1273 days compared to 2188 days based on simulation. This is an error of 915 days or 42 %. This difference in breakthrough is due to the inaccuracy in layer injection rate based on the new model, probably resulting from the assumption that pressure gradient is uniform behind the front, ahead of the front and throughout a layer after breakthrough in that layer. Nevertheless, the layer injection rate does not appear to affect the accuracy of the total cumulative oil production after breakthrough compared to simulation results.
- (4) The initial objective of my research was to improve the vertical sweep efficiency value in the Dykstra-Parsons model. However, a completely different approach was subsequently developed. The main attractive capability of the new model is that it can handle different oil-water relative permeability for each layer.

5.3 Recommendations

For future research, it is recommended to avoid the assumption of a uniform pressure gradient behind the front, ahead of the front and throughout a layer after breakthrough in that layer. Instead find a method to more accurately estimate pressure gradients (and thus injector-producer pressure drop) as a function of time for each layer. By doing so, it

would be possible to arrive at a more accurate estimate of layer water injection and oil production rates, and layer water breakthrough time.

NOMENCLATURE

A = area of reservoir, ft²
 B_o = oil formation volume factor, RB/STB
 B_w = water formation volume factor, RB/STB
 C = coverage or vertical sweep efficiency of layer 1, fraction
 C_2 = coverage or vertical sweep efficiency of layer 2, fraction
 C_n = total reservoir coverage or vertical sweep efficiency, fraction
 c = unit conversion constant,
 f_w = fractional flow, fraction
 f_{we} = fractional flow at saturation S_{we} , fraction
 h_1 = height of layer 1, ft
 h_2 = height of layer 2, ft
 i_{wt} = total water injection rate, STB/D
 i_{w1} = water injection rate in layer 1, STB/D
 i_{w2} = water injection rate in layer 2, STB/D
 k_1 = absolute permeability of layer 1, md
 k_2 = absolute permeability of layer 2, md
 k_{roe} = end point relative permeability to oil of layer 1, fraction
 k_{rwe} = end point relative permeability to water of layer 2, fraction
 $\overline{k_{rw1}}$ = average water relative permeability of layer 1, fraction
 $\overline{k_{rw2}}$ = average water relative permeability of layer 2, fraction
 L = reservoir length, ft
 M_{ep} = end-point mobility ratio, dimensionless
 M = mobility ratio based on water relative permeability at average water saturation behind the front, dimensionless
 MOV = total movable oil, RB
 MOV_1 = layer 1 movable oil, RB
 MOV_2 = layer 2 movable oil, RB
 N_p = cumulative oil produced, STB
 N_{p1} = cumulative oil produced from layer 1, STB
 N_{pD} = cumulative oil produced as a fraction of total pore volume, dimensionless
 n_o = Corey exponent for oil, dimensionless
 n_w = Corey exponent for water, dimensionless
 P = pressure, psi
 PV = total pore volume, RB
 PV_1 = pore volume of layer 1, RB
 PV_2 = pore volume of layer 2, RB
 PV_x = pore volume in layer 2 occupied by injected water, RB
 q_o = oil flow rate, STB/D
 q_w = water flow rate, STB/D

$\underline{S_{wbt}}$ = water saturation at the breakthrough, fraction

S_w = average water saturation behind the waterflood front, fraction

S_{oi} = initial oil saturation, fraction

S_{wc} = connate water saturation, fraction

S_{or} = residual oil saturation

t = time, days

W_{it} = total cumulative water injected, STB

W_{i1} = cumulative water injected in layer 1, STB

W_p = cumulative water produced, STB

x_1 = water distance of flood front from injector in layer 1, ft

x_2 = water distance of flood front from injector in layer 2, ft

μ_o = oil viscosity, cp

μ_w = water viscosity, cp

ϕ = porosity, fraction

Subscripts

1 = as for layer 1

2 = as for layer 2

bt = at breakthrough

D = dimensionless

i = initial

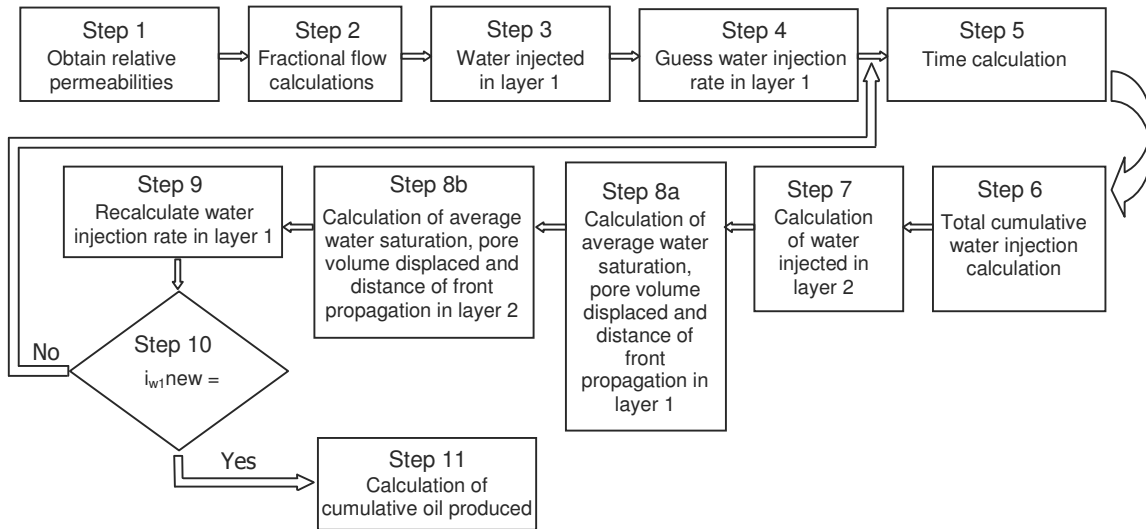
REFERENCES

1. Leverett, M. C.: "Capillary Behavior in Porous Solids," *Trans.*, AIME (1941) **142**, 152.
2. Buckley, S.E. and Leverett, M. C.: "Mechanism of Fluid Displacement in Sands," *Trans.*, AIME, (1946) **146**, 107.
3. Dykstra, H. and Parsons, R.L.: "The Prediction of Oil Recovery by Waterflooding," *Secondary Recovery of Oil in the United States*, Smith, J., Second edition, API, New York, (1950), 160.
4. Welge, H. J.: "A Simplified Method for Computing Oil Recovery by Gas or Water Drive," *Trans.*, AIME, (1952) **195**, 91.
5. Dake, L.P.: *Fundamentals of Reservoir Engineering*, Elsevier Scientific Publishing Co., New York City (1978) 365.
6. Stiles, W.E.: "Use of Permeability Distribution in Waterflood Calculations," *Trans.*, AIME (1949) **186**, 9.
7. Johnson, J. P.: "Predicting Waterflood Performance by the Graphical Representation of Porosity and Permeability Distribution," *JPT* (November 1965) 1285.
8. Kufus, H.B., and Lynch, E.J.: "Linear Frontal Displacement in Multi-Layer Sands," *Prod. Monthly* (December, 1959) **24**, No. 12, 32.
9. Hiatt, W. N.: "Injected-Fluid Coverage of Multi-Well Reservoirs with Permeability Stratification," *Drilling and Production Practices*, Johnston, K., API, San Antonio, (1958), 165.

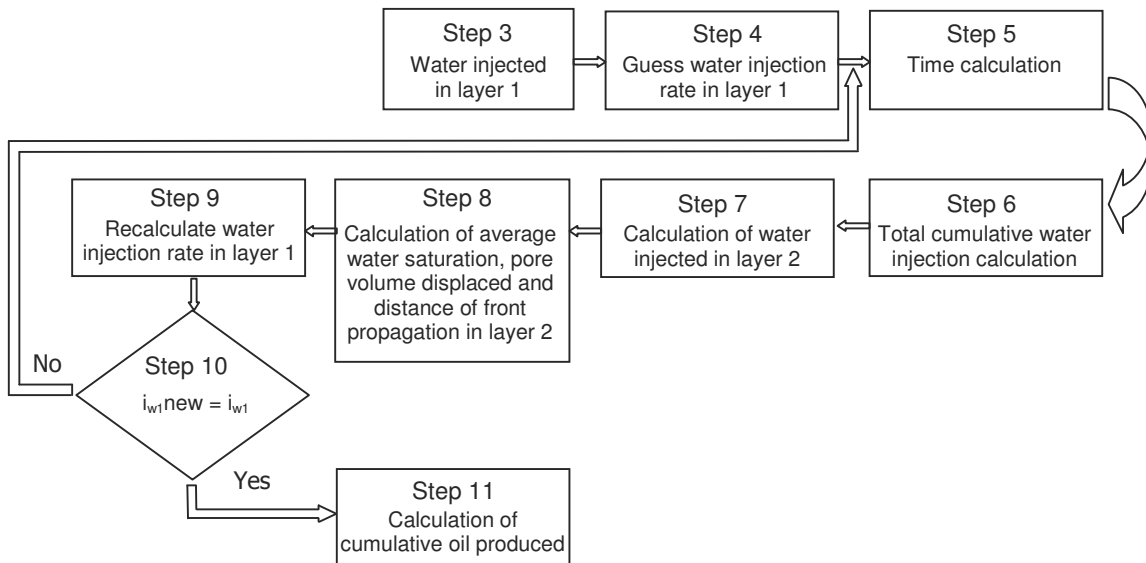
10. Warren, J.E., and Cosgrove, J.J.: "Prediction of Waterflood Behavior in a Stratified System," *SPE Journal*, (June, 1964), 149.
11. Reznik, A. A., Enick, R. M., Panvelker, S. B.: "An Analytical Extension of the Dykstra-Parsons Vertical Stratification Discrete Solution to a Continuous, Real-Time Basis," *SPE Journal*, (December, 1984), 643.
12. Craig, F. F., Jr.: *The Reservoir Engineering Aspects of Waterflooding*, Monograph Series, Richardson, Texas, *SPE*, (1993), **3**.
13. Corey, A. T.: "The Interrelation between Gas and Oil Relative Permeabilities," *Prod. Monthly*, (November 1954), **19**, 1, 38.
14. Craig, F. F., Jr.: Discussion of "Combination Method for Predicting Waterflood Performance for Five-Spot Patterns in Stratified Reservoirs," *JPT* (February 1964) 233.

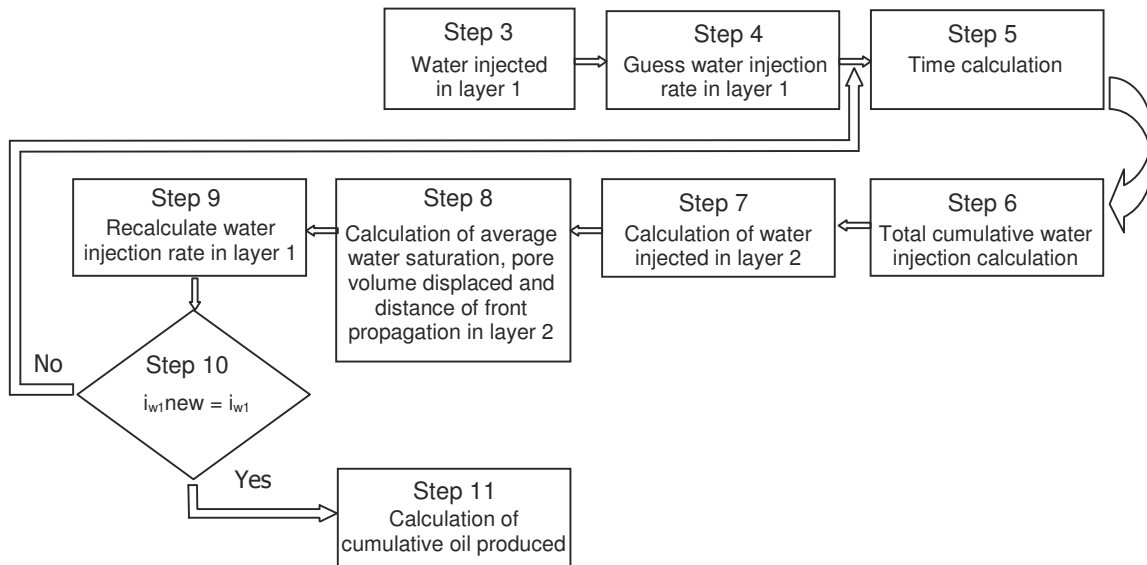
APPENDIX A

Calculation Procedure Flowchart, before Breakthrough



Calculation Procedure Flowchart, after Breakthrough in Layer 1



Calculation Procedure Flowchart, after Breakthrough in Layer 2

APPENDIX B

VBA Program for New Analytical Method

```

Sub DykstraParsonsMod()
Dim x2 As Double, Swav As Double
Dim pv As Double, pv1 As Double, k1 As Double, k2 As Double, h As Double, phi As Double
Dim C As Double, kroe As Double, krwe As Double, no As Double, nw As Double, krw As Double
Dim Sw As Double, Swc As Double, Sor As Double, muo As Double, muw As Double, kro As Double
Dim Wi1 As Double, Wibt As Double, Wi2 As Double, t As Double, iw As Double, fwbt As Double
Dim fwderbt As Double, delSw As Double, m As Double, Bo As Double, Bw As Double, i As Integer
Dim n As Double, So As Double, fw1 As Double, fw2 As Double, L As Double, p As Double, w As Double
Dim MOV As Double, iw1 As Double, Wit As Double, Swav2 As Double, Wi2p As Double, Np As Double
Dim C1 As Double, C2 As Double, Savn As Double, Wipv As Double, fwder1 As Double, Wi1p As Double
Dim Npd As Double, Sw1 As Double, fw3 As Double, fw As Double, Swbt As Double
Dim fwder As Double, fwder2 As Double, Swav1 As Double, pv2 As Double, Wi As Double, kro2 As Double
Dim krw2 As Double, delt As Double, t2 As Double, tn As Double, Np1 As Double, Npn As Double
Dim Win As Double, Wp As Double, Wpi As Double, qw As Double, qo As Double, fwn As Double
Dim Wp2 As Double, Npn2 As Double, Np2 As Double, Win2 As Double, Wpi2 As Double, Npx As Double
Dim Npy As Double, iwx As Double, delWip1 As Double, x1 As Double
Dim Mob As Double

```

With ThisWorkbook.Worksheets("Input")

```

Bo = .Cells(1, 2)
Bw = .Cells(2, 2)
kroe = .Cells(7, 2)
krwe = .Cells(8, 2)
Swc = .Cells(3, 2)
Sor = .Cells(6, 2)
no = .Cells(1, 9)
nw = .Cells(2, 9)

```

```

muo = .Cells(9, 2)
muw = .Cells(10, 2)
L = .Cells(1, 6)
w = .Cells(2, 6)
h = .Cells(4, 6)
phi = .Cells(3, 6)
iw = .Cells(11, 2)
k1 = .Cells(13, 2)
k2 = .Cells(14, 2)
End With

```

```

pv = L * h * w * phi / 5.615
MOV = L * 2 * h * w * phi * (1 - Sor - Swc) / 5.615

```

Call clrcnt

```

With ThisWorkbook.Worksheets("Output2")
    Swbt = 0.5270625
    kro = kroe * (((1 - Swbt) - Swc) / (1 - Sor - Swc)) ^ no
    krw = krwe * ((Swbt - Swc) / (1 - Sor - Swc)) ^ nw
    fwbt = 1 / (1 + kro * muw / (muo * krw))
    fwderbt = (fwbt - fwbt ^ 2) * (no / (1 - Swbt - Sor) + nw / (Swbt - Swc))
    Swav = 1 / fwderbt + Swc
    delSw = ((1 - Sor) - Swbt) / 500
    i = 0
    Sw = Swbt
    fw = fwbt
    fw1 = fwbt
    Sw1 = Swbt + delSw
    fw2 = fwbt
    krw = krwe * ((Swav - Swc) / (1 - Sor - Swc)) ^ nw
    krw2 = krw

```

'Calculations before the breakthrough

```

Wi1p = pv * (Swav - Swc)
iw1 = k1 * krw * h / (k1 * krw * h + k2 * krw2 * h) * iw
Do Until Abs(Wi1p - Wi1) < 0.00001
    delWi1p = pv * (Swav - Swc) / 20
    Wi1 = Wi1 + delWi1p
    Npn = Wi1 / Bo
    iwx = 0
    Do Until Abs(iw1 - iwx) <= 0.00001
        iwx = iw1

```

```

t = Wi1 / iw1
Wit = iw * t
Wi2p = Wit - Wi1
pv1 = Wi1 * fwderbt
x1 = pv1 / (h * w * phi / 5.615)
pv2 = Wi2p * fwderbt
Swav2 = Wi2p / pv2 + Swc
Npx = pv2 * ((1 - Swc) - (1 - Swav2)) / Bo
Npy = Npx + Npn
x2 = pv2 / (h * w * phi / 5.615)
kro = kroe * (((1 - Swav) - Swc) / (1 - Sor - Swc)) ^ no
krw = krwe * ((Swav - Swc) / (1 - Sor - Swc)) ^ nw
kro2 = kroe * (((1 - Swav2) - Swc) / (1 - Sor - Swc)) ^ no
krw2 = krwe * ((Swav2 - Swc) / (1 - Sor - Swc)) ^ nw
iw1 = iw / (1 + (k2 / k1) * ((x1 * muw * kroe + (L - x1) * muo * krw) / (x2 * muw *
kroe + (L - x2) * muo * krw2)))

```

Loop

```

C1 = pv1 * (Swav - Swc) / (1 - Sor - Swc)
C2 = pv2 * (Swav2 - Swc) / (1 - Sor - Swc)
C = (C1 + C2) / (2 * pv)
Np = C * MOV / Bo
Wi = Np * Bo
.Cells(i + 2, 14) = Swav2
.Cells(i + 2, 12) = Wi2
.Cells(i + 2, 11) = Wit
.Cells(i + 2, 9) = iw1
.Cells(i + 2, 10) = t
.Cells(i + 2, 8) = Wi1
.Cells(i + 2, 15) = pv2
.Cells(i + 2, 16) = x
.Cells(i + 2, 17) = C
.Cells(i + 2, 18) = Np
.Cells(i + 2, 22) = Npn
i = i + 1

```

Loop

' **Calculation @ the time of breakthrough**

```

Wi1p = pv * (Swav - Swc)
Npn = pv * (Swav - Swc) / Bo
iwx = 0

```

```

Do Until Abs(iw1 - iwx) <= 0.00001
iwx = iw1

```

```

t = Wi1p / iw1
Wit = iw * t
Wi2p = Wit - Wi1p
pv2 = Wi2p * fwderbt
Swav2 = Wi2p / pv2 + Swc
Npx = pv2 * ((1 - Swc) - (1 - Swav2)) / Bo
Npy = Npx + Npn
x = pv2 / (h * w * phi / 5.615)
kro = kroe * (((1 - Swav) - Swc) / (1 - Sor - Swc)) ^ no
krw = krwe * ((Swav - Swc) / (1 - Sor - Swc)) ^ nw
kro2 = kroe * (((1 - Swav2) - Swc) / (1 - Sor - Swc)) ^ no
krw2 = krwe * ((Swav2 - Swc) / (1 - Sor - Swc)) ^ nw
iw1 = iw / (1 + (L * k2 * kroe * muw / (krw * k1)) * (krw2 / (x * muw * kroe + (L -
x) * muo * krw2)))

```

Loop

'Calculation @ the time of 1stlayer breakthrough

```

C1 = pv * (Swav - Swc) / (1 - Sor - Swc)
C2 = pv2 * (Swav2 - Swc) / (1 - Sor - Swc)
C = (C1 + C2) / (2 * pv)
Np = C * MOV / Bo
Wi = Np * Bo

```

```

.Cells(i, 9) = iw1
.Cells(i, 10) = t
.Cells(i, 14) = Swav2
.Cells(i, 15) = pv2
.Cells(i, 16) = x
.Cells(i, 12) = Wi2
.Cells(i, 11) = Wit
.Cells(i, 17) = C
.Cells(i, 18) = Np

```

```

i = i + 1
Swav = Swav2
Np1 = pv * ((1 - Swc) - (1 - Swav)) / Bo
Np2 = pv * ((1 - Swc) - (1 - Swav2)) / Bo

```

```

tn = t
Wi2p = pv * (Swav2 - Swc)
Wi2 = Wit - Wi1p

```

'After 1st layer broke through

```

Sw = Swbt
Sw2 = Swbt
Sw = Sw + delSw
fw = fwbt
fw1 = fwbt
Sw1 = Swbt + delSw
fw2 = fwbt
krw = krwe * ((Swav - Swc) / (1 - Sor - Swc)) ^ nw
krw2 = krw
Wpi = 0
Do Until Sw = (1 - Sor)
  If Swav >= (1 - Sor) Then
    Exit Do
  End If
  If x <= L Then
    kro = kroe * (((1 - Sw) - Swc) / (1 - Sor - Swc)) ^ no
    krw = krwe * ((Sw - Swc) / (1 - Sor - Swc)) ^ nw
    fw1 = 1 / (1 + kro * muw / (krw * muo))
    fwder = (fw1 - fw1 ^ 2) * (no / (1 - Sw - Sor) + nw / (Sw - Swc))
    Swav = Sw + (1 - fw1) / fwder
    Win = pv * 1 / fwder
    Npn = pv * ((1 - Swc) - (1 - Swav)) / Bo
    iwx = 0
    Do Until Abs(iw1 - iwx) < 0.00001
      iwx = iw1
      tn = Win / iw1
      delt = tn - t
      Wit = iw * tn
      Wp = (Win - Wi1p) * Bw - (Npn - Np1) * Bo
      Wp = Wpi + Wp
      Wi2 = Wi2 + (iw - iw1) * delt
      Wi2 = Wit - Win
      pv2 = Wi2 * fwderbt
      Swav2 = Wi2 / pv2 + Swc
      Npx = pv2 * ((1 - Swc) - (1 - Swav2)) / Bo
      Npy = Npx + Npn
      x = pv2 / (h * w * phi / 5.615)
      kro = kroe * (((1 - Swav) - Swc) / (1 - Sor - Swc)) ^ no
      krw = krwe * ((Swav - Swc) / (1 - Sor - Swc)) ^ nw
      kro2 = kroe * (((1 - Swav2) - Swc) / (1 - Sor - Swc)) ^ no
      krw2 = krwe * ((Swav2 - Swc) / (1 - Sor - Swc)) ^ nw

```

$$iw1 = iw / (1 + (L * k2 * kroe * muw * krw2 / ((krw * k1) * (x * muw * kroe + (L - x) * muo * krw2))))$$

Loop

$$.Cells(i + 6, 12) = Wi2$$

$$.Cells(i + 6, 11) = Wit$$

$$.Cells(i + 6, 8) = Win$$

$$.Cells(i + 6, 14) = Swav2$$

$$.Cells(i + 6, 15) = pv2$$

$$.Cells(i + 6, 16) = x$$

$$t = tn$$

$$C1 = 1 / 2 * ((Swav - Swc) / (1 - Sor - Swc))$$

$$C2 = 1 / 2 * pv2 / pv * ((Swav2 - Swc) / (1 - Sor - Swc))$$

$$C = C1 + C2$$

$$Np = C * MOV / Bo$$

$$Wi = Np * Bo + Wp * Bw$$

$$.Cells(i + 6, 17) = C$$

$$.Cells(i + 6, 18) = Np$$

$$.Cells(i + 6, 11) = Wit$$

$$.Cells(i + 6, 9) = iw1$$

$$.Cells(i + 6, 10) = tn$$

$$.Cells(i + 6, 12) = Wi2$$

$$.Cells(i + 6, 14) = Swav2$$

$$.Cells(i + 6, 15) = pv2$$

$$.Cells(i + 6, 16) = x$$

$$.Cells(i + 6, 21) = qw$$

$$.Cells(i + 6, 22) = Npn$$

‘Calculations after the second layer has broken through

Else

$$fwn = fw2$$

$$Sw2 = Sw2 + delSw$$

$$kro = kroe * (((1 - Sw) - Swc) / (1 - Sor - Swc)) ^ no$$

$$krw = krwe * ((Sw - Swc) / (1 - Sor - Swc)) ^ nw$$

$$fw1 = 1 / (1 + kro * muw / (krw * muo))$$

$$fwder = (fw1 - fw1 ^ 2) * (no / (1 - Sw - Sor) + nw / (Sw - Swc))$$

$$Swav = Sw + (1 - fw1) / fwder$$

$$Win = pv * 1 / fwder$$

$$Npn = pv * ((1 - Swc) - (1 - Swav)) / Bo$$

$$kro2 = kroe * (((1 - Sw2) - Swc) / (1 - Sor - Swc)) ^ no$$

$$krw2 = krwe * ((Sw2 - Swc) / (1 - Sor - Swc)) ^ nw$$

$$fw2 = 1 / (1 + kro2 * muw / (krw2 * muo))$$

$$fwder2 = (fw2 - fw2 ^ 2) * (no / (1 - Sw2 - Sor) + nw / (Sw2 - Swc))$$


```

Swav2 = Sw2 + (1 - fw2) / fwder2
Win2 = pv * 1 / fwder2
Npn = pv * ((1 - Swc) - (1 - Swav)) / Bo
Npn2 = pv * ((1 - Swc) - (1 - Swav2)) / Bo
Npy = Npn + Npn2
iwx = iw / (1 + (L * k2 * kro2 * muw / (krw * k1)) * (krw2 / (L * muw * kro2)))
Do Until Abs(iw1 - iwx) < 0.00001
iwx = iw1
tn = Win / iw1
delt = tn - t
Wit = Win + Win2
Wp = (Win - Wi1p) * Bw - (Npn - Np1) * Bo
Wp2 = (Win2 - Wi2p) * Bw - (Npn2 - Np2) * Bo
Wp = Wpi + Wp
Wp2 = Wpi2 + Wp2
Wi2 = Wi2 + (iw - iw1) * delt
kro = kroe * (((1 - Swav) - Swc) / (1 - Sor - Swc)) ^ no
krw = krwe * ((Swav - Swc) / (1 - Sor - Swc)) ^ nw
kro2 = kroe * (((1 - Swav2) - Swc) / (1 - Sor - Swc)) ^ no
krw2 = krwe * ((Swav2 - Swc) / (1 - Sor - Swc)) ^ nw
iw1 = iw / (1 + (k2 * krw2 / (k1 * krw)))
Loop

```

```

.Cells(i + 6, 12) = Wi2
.Cells(i + 6, 11) = Wit
.Cells(i + 6, 8) = Win
.Cells(i + 6, 14) = Swav2
.Cells(i + 6, 15) = pv2
.Cells(i + 6, 16) = x
t = tn
C1 = 1 / 2 * ((Swav - Swc) / (1 - Sor - Swc))
C2 = 1 / 2 * ((Swav2 - Swc) / (1 - Sor - Swc))
C = C1 + C2
Np = C * MOV / Bo
Wi = Np * Bo + Wp * Bw + Wp2 * Bw

```

```

.Cells(i + 6, 17) = C
.Cells(i + 6, 18) = Np
.Cells(i + 6, 11) = Wit
.Cells(i + 6, 9) = iw1
.Cells(i + 6, 10) = tn
.Cells(i + 6, 12) = Wi2
.Cells(i + 6, 14) = Swav2

```

```
.Cells(i + 6, 15) = pv2  
.Cells(i + 6, 16) = x  
.Cells(i + 6, 21) = qw  
.Cells(i + 6, 22) = Npn  
.Cells(i + 6, 223) = Npn2
```

```
Wpi2 = Wp2  
Np2 = Npn2  
Wi2p = Win2  
End If
```

```
Wpi = Wp  
i = i + 1  
Np1 = Npn  
Wi1p = Win  
Sw = Sw + delSw  
Loop  
End With
```

```
End Sub
```

APPENDIX C

Eclipse 100 Simulation Model, Case 1

RUNSPEC

DIMENS

1 200 2 /

OIL

WATER

FIELD

REGDIMS

2 1 0 0 /

TABDIMS

1 1 30 30 1 30 /

WELLDIMS

2 50 2 5 /

START

1 'JAN' 1983 /

NSTACK

200 /

GRID

=====

DX

400*400

/

DY

20*1 20*2 20*8 20*9 20*10 20*10 20*9 20*8 20*2 20*1

20*1 20*2 20*8 20*9 20*10 20*10 20*9 20*8 20*2 20*1

/

DZ

200*35

200*35

/

PERMX

200*500

200*350

/

PERMY

200*500

200*350

/

PERMZ

200*50

200*35

/

BOX

1 1 1 200 1 1 /

MULTZ

200*0/

ENDBOX

TOPS

200*8000.0 /

BOX

1 1 1 200 1 1 /

PORO

200*.25

/

BOX

1 1 1 200 2 2 /

PORO

200*.25

/

ENDBOX

RPTGRID

1 1 1 1 1 0 0 0 /

GRIDFILE

2 1 /

INIT

PROPS

=====

SWOF

-- Sw	krw	kro	Pcow
0.2	0	0.85	0
0.25	0.000332936	0.683829014	0
0.3	0.0023187	0.538847423	0
0.35	0.007216059	0.414068396	0
0.4	0.016148364	0.308454264	0
0.45	0.030163141	0.220907729	0
0.5	0.050255553	0.150260191	0
0.55	0.07738113	0.095255667	0
0.6	0.112463739	0.054527525	0
0.65	0.15640102	0.0265625	0
0.7	0.210068317	0.009639196	0
0.75	0.274321643	0.001703985	0
0.8	0.35	0	0

/

PVTW

3480 1.00 3.00E-06 .9 0.0 /

PVCDO

3460 1.250 0 8 /

GRAVITY

34.2 1.07

/

ROCK

3460.0 5.0E-06 /

REGIONS

=====

SATNUM

400*1 /

FIPNUM

200*1 200*2 /

SOLUTION

=====

EQUIL

8087 3460 15000 0 0 0 1 0 0 /

RPTSOL

PRESSURE SWAT SGAS SOIL FIP /

RPTRST

BASIC=2 /

SUMMARY

=====

RUNSUM

SEPARATE

RPTONLY

FOPR

FWPR

FWIR

FWCT

ROPR

/

RWIR

/

RWPR

/

WBHP

/

FPR

FOPT

FWPT

FWIT

FOE

FOEW

WPI

/

WPI1

/

FLPR

FLPT

FVPR

FVPT

SCHEDULE

=====

RPTSCHED

FIELD 16:55 18 APR 86

1	0	1	0	0	0	2	2	0	0	0	2	0	0	0	0	0
0	0	0	0	0	0	0	0	0	0	0	0	0	0	0	0	0
0	0	0	0	0	0	0	0	0	0	0	0	0	0	0	0	/

WELSPECS

```
'P' 'G' 1 1 8035 'OIL' /  
'T' 'G' 1 200 8035 'WAT' /  
/  
COMPDAT  
'P' ' ' 1 1 1 2 'OPEN' 1 0 .27 3* X /  
'T' ' ' 1 200 1 2 'OPEN' 1 0 .27 3* X /  
/  
WCONPROD  
'P' 'OPEN' 'RESV' 4* 800 /  
/  
WCONINJ  
'T' 'WAT' 'OPEN' 'RESV' 1* 800 /  
/  
WECON  
P 0 0 .8 /  
/  
TSTEP  
200*3.65/  
TSTEP  
10*36.5/  
TSTEP  
10*365/  
TSTEP  
10*365/  
END
```


Eclipse 100 Simulation Model, Case 2

RUNSPEC

DIMENS

1 100 2 /

OIL

WATER

FIELD

REGDIMS

2 1 0 0 /

TABDIMS

2 1 30 30 1 30 /

WELLDIMS

2 50 2 5 /

START

1 'JAN' 1983 /

NSTACK

200 /

GRID

=====

DX

200*400

/

DY

10*1 10*5 10*16 10*18 10*20 10*20 10*18 10*16 10*5 10*1

10*1 10*5 10*16 10*18 10*20 10*20 10*18 10*16 10*5 10*1

/

DZ

100*35

100*35

/
PERMX
100*500
100*350
/
PERMY
100*500
100*350
/
PERMZ
100*50
100*35
/
BOX
1 1 1 100 1 1 /
MULTZ
100*0/
ENDBOX
TOPS
100*8000.0 /
BOX
1 1 1 100 1 1 /
PORO
100*.25
/
BOX
1 1 1 100 2 2 /
PORO
100*.25

/
 ENDBOX
 RPTGRID
 1 1 1 1 1 0 0 0 /
 GRIDFILE
 2 1 /
 INIT
 PROPS

=====

SWOF

-- Sw	krw	kro	Pcow
0.2	0	0.85	0
0.25	0.000332936	0.683829014	0
0.3	0.0023187	0.538847423	0
0.35	0.007216059	0.414068396	0
0.4	0.016148364	0.308454264	0
0.45	0.030163141	0.220907729	0
0.5	0.050255553	0.150260191	0
0.55	0.07738113	0.095255667	0
0.6	0.112463739	0.054527525	0
0.65	0.15640102	0.0265625	0
0.7	0.210068317	0.009639196	0
0.75	0.274321643	0.001703985	0
0.8	0.35	0	0
/			
0.3	0	0.9	0
0.35	0.01020408	0.56676385	0
0.4	0.04081633	0.32798834	0
0.45	0.09183673	0.16793003	0

0.5 0.16326531 0.07084548 0
 0.55 0.25510204 0.02099125 0
 0.6 0.36734694 0.00262391 0
 0.65 0.5 0 0

/

PVTW

3460 1.00 3.00E-06 .9 0.0 /

PVCDO

3460 1.250 0 8 /

GRAVITY

34.2 1.07 0.7

--0.00 0.00 0.00

/

ROCK

3460.0 5.0E-06 /

REGIONS

=====

SATNUM

100*1 100*2 /

FIPNUM

100*1 100*2 /

SOLUTION

=====

EQUIL

8035 3460 15000 0 0 0 1 0 0 /

RPTSOL

PRESSURE SWAT SGAS SOIL FIP /

RPTRST

BASIC=2 /

SUMMARY

=====

RUNSUM

SEPARATE

RPTONLY

FOPR

FWPR

FWIR

FWCT

ROPR

/

RWIR

/

RWPR

/

WBHP

/

FPR

FOPT

FWPT

FWIT

FOE

FOEW

WPI

/

WPI1

/

FLPR

FLPT

FVPR

FVPT

SCHEDULE

=====

FIELD 16:55 18 APR 86

RPTSCHED 1 0 1 0 0 0 2 2 0 0 0 2 0 0 0 0 0

0 0 0 0 0 0 0 0 0 0 0 0 0 0 0 0 0

0 0 0 0 0 0 0 0 0 0 0 0 0 0 0 0 /

WELSPECS

'P' 'G' 1 1 8035 'OIL' /

'T' 'G' 1 100 8035 'WAT' /

/

COMPDAT

'P' ' ' 1 1 1 2 'OPEN' 1 0 .27 3* X /

'I' ' ' 1 100 1 2 'OPEN' 1 0 .27 3* X /

/

WCONPROD

'P' 'OPEN' 'RESV' 4* 800 /

/

WCONINJ

'I' 'WAT' 'OPEN' 'RESV' 1* 800 /

/

WECON

P 0 0 .8 /

/

TSTEP

200*3.65

/

TSTEP

100*36.5

/

TSTEP

10*365

/

TSTEP

10*365

/

END

Eclipse 100 Simulation Model, Case 3

RUNSPEC

DIMENS

1 200 2 /

OIL

WATER

FIELD

REGDIMS

2 1 0 0 /

TABDIMS

1 1 30 30 1 30 /

WELLDIMS

2 50 2 5 /

START

1 'JAN' 1983 /

NSTACK

200 /

GRID

=====

DX

400*400

/

DY

20*1 20*2 20*8 20*9 20*10 20*10 20*9 20*8 20*2 20*1

20*1 20*2 20*8 20*9 20*10 20*10 20*9 20*8 20*2 20*1

/

DZ

200*50

200*25

/

PERMX

200*500

200*100

/

PERMY

200*500

200*100

/

PERMZ

200*50

200*10

/

BOX

1 1 1 200 1 1 /

MULTZ

200*0/

ENDBOX

TOPS

200*8000.0 /

BOX

1 1 1 200 1 1 /

PORO

200*.25

/

BOX

1 1 1 200 2 2 /

PORO

200*.25

/

ENDBOX

RPTGRID

1 1 1 1 1 0 0 0 /

GRIDFILE

2 1 /

INIT

PROPS

=====

SWOF

-- Sw	krw	kro	Pcow
0.2	0	0.85	0
0.25	0.000332936	0.683829014	0
0.3	0.0023187	0.538847423	0
0.35	0.007216059	0.414068396	0
0.4	0.016148364	0.308454264	0
0.45	0.030163141	0.220907729	0
0.5	0.050255553	0.150260191	0

0.55 0.07738113 0.095255667 0
 0.6 0.112463739 0.054527525 0
 0.65 0.15640102 0.0265625 0
 0.7 0.210068317 0.009639196 0
 0.75 0.274321643 0.001703985 0
 0.8 0.35 0 0

/

PVTW

3460 1.00 3.00E-06 .9 0.0 /

PVCDO

3460 1.250 0 8 /

GRAVITY

34.2 1.07 0.7

/

ROCK

3460.0 5.0E-06 /

REGIONS

=====

SATNUM

400*1 /

FIPNUM

200*1 200*2 /

SOLUTION

=====

EQUIL

8035 3460 15000 0 0 0 1 0 0 /

RPTSOL

PRESSURE SWAT SOIL FIP /

RPTRST

BASIC=2 /

SUMMARY

=====

RUNSUM

SEPARATE

RPTONLY

FOPR

FWPR

FWIR

FWCT

ROPR

/

RWIR

/

RWPR

/

WBHP

/

FPR

FOPT

FWPT

FWIT

FOE

FOEW

WPI

/

WPI1

/

FLPR


```
TSTEP
10*36.5
/
TSTEP
10*365
/
TSTEP
10*365
/
END
```

Eclipse 100 Simulation Model, Case 4

```
RUNSPEC
DIMENS
1 100 2 /
OIL
WATER
FIELD
REGDIMS
2 1 0 0 /
TABDIMS
2 1 30 30 1 30 /
WELLDIMS
2 50 2 5 /
START
1 'JAN' 1983 /
NSTACK
200 /
```

GRID

=====

DX

200*400

/

DY

10*1 10*5 10*16 10*18 10*20 10*20 10*18 10*16 10*5 10*1

10*1 10*5 10*16 10*18 10*20 10*20 10*18 10*16 10*5 10*1

/

DZ

100*50

100*25

/

PERMX

100*500

100*100

/

PERMY

100*500

100*100

/

PERMZ

100*50

100*10

/

BOX

1 1 1 100 1 1 /

MULTZ

100*0/

ENDBOX

TOPS

100*8000.0 /

BOX

1 1 1 100 1 1 /

PORO

100*.25

/

BOX

1 1 1 100 2 2 /

PORO

100*.25

/

ENDBOX

RPTGRID

1 1 1 1 1 0 0 0 /

GRIDFILE

2 1 /

INIT

PROPS

=====

SWOF

-- Sw	krw	kro	Pcow
0.2	0	0.85	0
0.25	0.000332936	0.683829014	0
0.3	0.0023187	0.538847423	0
0.35	0.007216059	0.414068396	0
0.4	0.016148364	0.308454264	0
0.45	0.030163141	0.220907729	0

0.5	0.050255553	0.150260191	0
0.55	0.07738113	0.095255667	0
0.6	0.112463739	0.054527525	0
0.65	0.15640102	0.0265625	0
0.7	0.210068317	0.009639196	0
0.75	0.274321643	0.001703985	0
0.8	0.35	0	0

/

0.3	0	0.9	0
0.35	0.01020408	0.56676385	0
0.4	0.04081633	0.32798834	0
0.45	0.09183673	0.16793003	0
0.5	0.16326531	0.07084548	0
0.55	0.25510204	0.02099125	0
0.6	0.36734694	0.00262391	0
0.65	0.5	0	0

/

PVTW

3460 1.00 3.00E-06 .9 0.0 /

PVCDO

3460 1.250 0 8 /

GRAVITY

34.2 1.07 0.7

--0.00 0.00 0.00

/

ROCK

3460.0 5.0E-06 /

REGIONS

=====

SATNUM

100*1 100*2 /

FIPNUM

100*1 100*2 /

SOLUTION

=====

EQUIL

8035 3460 15000 0 0 0 1 0 0 /

RPTSOL

PRESSURE SWAT SOIL FIP /

RPTRST

BASIC=2 /

SUMMARY

=====

RUNSUM

SEPARATE

RPTONLY

FOPR

FWPR

FWIR

FWCT

ROPR

/

RWIR

/

RWPR

/

WBHP

/

FPR
FOPT
FWPT
FWIT
FOE
FOEW
WPI

/

WPII

/

FLPR

FLPT

FVPR

FVPT

SCHEDULE

=====

RPTSCHED

FIELD 16:55 18 APR 86

1 0 1 0 0 0 2 2 0 0 0 2 0 0 0 0 0
0 0 0 0 0 0 0 0 0 0 0 0 0 0 0 0 0
0 0 0 0 0 0 0 0 0 0 0 0 0 0 0 0 /

WELSPECS

'P' 'G' 1 1 8035 'OIL' /

'T' 'G' 1 100 8035 'WAT' /

/

COMPDAT

'P' ' ' 1 1 1 2 'OPEN' 1 0 .27 3* X /

'I' ' ' 1 100 1 2 'OPEN' 1 0 .27 3* X /

/

```
WCONPROD
'P' 'OPEN' 'RESV' 4* 800 /
/
WCONINJ
'T' 'WAT' 'OPEN' 'RESV' 1* 800 /
/
WECON
P 0 0 .8 /
/
TSTEP
200*3.65
/
TSTEP
100*36.5
/
TSTEP
10*365
/
TSTEP
10*365
/
END
```

Eclipse 100 Simulation Model, Case 5

```
RUNSPEC
DIMENS
1 200 2 /
OIL
```

WATER

FIELD

REGDIMS

2 1 0 0 /

TABDIMS

1 1 30 30 1 30 /

WELLDIMS

2 50 2 5 /

START

1 'JAN' 1983 /

NSTACK

200 /

GRID

=====

DX

400*400

/

DY

20*1 20*2 20*8 20*9 20*10 20*10 20*9 20*8 20*2 20*1

20*1 20*2 20*8 20*9 20*10 20*10 20*9 20*8 20*2 20*1

/

DZ

200*35

200*35

/

PERMX

200*500

200*350

/

PERMY

200*500

200*350

/

PERMZ

200*50

200*35

/

BOX

1 1 1 200 1 1 /

MULTZ

200*0/

ENDBOX

TOPS

200*8000.0 /

BOX

1 1 1 200 1 1 /

PORO

200*.25

/

BOX

1 1 1 200 2 2 /

PORO

200*.25

/

ENDBOX

RPTGRID

1 1 1 1 1 0 0 0 /

GRIDFILE

2 1 /

INIT

PROPS

=====

SWOF

-- Sw	krw	kro	Pcow
0.2	0	0.85	0
0.25	0.000332936	0.683829014	0
0.3	0.0023187	0.538847423	0
0.35	0.007216059	0.414068396	0
0.4	0.016148364	0.308454264	0
0.45	0.030163141	0.220907729	0
0.5	0.050255553	0.150260191	0
0.55	0.07738113	0.095255667	0
0.6	0.112463739	0.054527525	0
0.65	0.15640102	0.0265625	0
0.7	0.210068317	0.009639196	0
0.75	0.274321643	0.001703985	0
0.8	0.35	0	0

/

PVTW

3460 1.00 3.00E-06 .9 0.0 /

PVCDO

3460 1.250 0 8 /

GRAVITY

34.2 1.07 0.7

/

ROCK

3460.0 5.0E-06 /

REGIONS

=====

SATNUM

400*1 /

FIPNUM

200*1 200*2 /

SOLUTION

=====

EQUIL

8035 3460 15000 0 0 0 1 0 0 /

RPTSOL

PRESSURE SWAT SGAS SOIL FIP /

RPTRST

BASIC=2 /

SUMMARY

=====

RUNSUM

SEPARATE

RPTONLY

FOPR

FWPR

FWIR

FWCT

ROPR

/

RWIR

/

RWPR

/

WBHP

/

FPR

FOPT

FWPT

FWIT

FOE

FOEW

WPI

/

WPII

/

FLPR

FLPT

FVPR

FVPT

SCHEDULE

=====

RPTSCHED

FIELD 16:55 18 APR 86

1 0 1 0 0 0 2 2 0 0 0 2 0 0 0 0 0

0 0 0 0 0 0 0 0 0 0 0 0 0 0 0 0

0 0 0 0 0 0 0 0 0 0 0 0 0 0 0 0 /

WELSPECS

'P' 'G' 1 1 8035 'OIL' /

'T' 'G' 1 200 8035 'WAT' /

/

COMPDAT

'P' ' 1 1 1 2 'OPEN' 1 0 .27 3* X /

'T' ' 1 200 1 2 'OPEN' 1 0 .27 3* X /


```
/
WCONPROD
'P' 'OPEN' 'RESV' 4* 1600 /
/
WCONINJ
'T' 'WAT' 'OPEN' 'RESV' 1* 1600 /
/
WECON
P 0 0 .8 /
/
TSTEP
200*3.65
/
TSTEP
10*36.5
/
TSTEP
10*365
/
TSTEP
10*365
/
END
```

Eclipse 100 Simulation Model, Case 6

RUNSPEC

DIMENS

1 200 2 /

OIL

WATER

FIELD

REGDIMS

2 1 0 0 /

TABDIMS

2 1 30 30 1 30 /

WELLDIMS

2 50 2 5 /

START

1 'JAN' 1983 /

NSTACK

200 /

GRID

=====

DX

400*400

/

DY

20*1 20*2 20*8 20*9 20*10 20*10 20*9 20*8 20*2 20*1

20*1 20*2 20*8 20*9 20*10 20*10 20*9 20*8 20*2 20*1

/

DZ

200*35

200*35

/
PERMX
200*500
200*350
/
PERMY
200*500
200*350
/
PERMZ
200*50
200*35
/
BOX
1 1 1 200 1 1 /
MULTZ
200*0/
ENDBOX
TOPS
200*8000.0 /
BOX
1 1 1 200 1 1 /
PORO
200*.25
/
BOX
1 1 1 200 2 2 /
PORO
200*.25

/
 ENDBOX
 RPTGRID
 1 1 1 1 1 0 0 0 /
 GRIDFILE
 2 1 /
 INIT
 PROPS

=====

SWOF

-- Sw	krw	kro	Pcow	
0.2	0		0.85	0
0.25	0.000332936		0.683829014	0
0.3	0.0023187		0.538847423	0
0.35	0.007216059	0.414068396		0
0.4	0.016148364	0.308454264		0
0.45	0.030163141	0.220907729		0
0.5	0.050255553	0.150260191		0
0.55	0.07738113	0.095255667		0
0.6	0.112463739	0.054527525		0
0.65	0.15640102	0.0265625		0
0.7	0.210068317	0.009639196		0
0.75	0.274321643	0.001703985		0
0.8	0.35	0		0
/				
0.3	0	0.9		0
0.35	0.01020408	0.56676385		0
0.4	0.04081633	0.32798834		0
0.45	0.09183673	0.16793003		0

0.5 0.16326531 0.07084548 0
 0.55 0.25510204 0.02099125 0
 0.6 0.36734694 0.00262391 0
 0.65 0.5 0 0

/

PVTW

3460 1.00 3.00E-06 .9 0.0 /

PVCDO

3460 1.250 0 8 /

GRAVITY

34.2 1.07 0.7

/

ROCK

3460.0 5.0E-06 /

REGIONS

=====

SATNUM

200*1 200*2 /

FIPNUM

200*1 200*2 /

SOLUTION

=====

EQUIL

8035 3460 15000 0 0 0 1 0 0 /

RPTSOL

PRESSURE SWAT SGAS SOIL FIP /

RPTRST

BASIC=2 /

SUMMARY

=====

RUNSUM

SEPARATE

RPTONLY

FOPR

FWPR

FWIR

FWCT

ROPR

/

RWIR

/

RWPR

/

WBHP

/

FPR

FOPT

FWPT

FWIT

FOE

FOEW

WPI

/

WPI1

/

FLPR

FLPT

FVPR

FVPT

SCHEDULE

=====

FIELD 16:55 18 APR 86

RPTSCHED 1 0 1 0 0 0 2 2 0 0 0 2 0 0 0 0 0

0 0 0 0 0 0 0 0 0 0 0 0 0 0 0 0 0

0 0 0 0 0 0 0 0 0 0 0 0 0 0 0 0 /

WELSPECS

'P' 'G' 1 1 8035 'OIL' /

'T' 'G' 1 200 8035 'WAT' /

/

COMPDAT

'P' ' ' 1 1 1 2 'OPEN' 1 0 .27 3* X /

'I' ' ' 1 200 1 2 'OPEN' 1 0 .27 3* X /

/

WCONPROD

'P' 'OPEN' 'RESV' 4* 1600 /

/

WCONINJ

'I' 'WAT' 'OPEN' 'RESV' 1* 1600 /

/

WECON

P 0 0 .8 /

/

TSTEP

200*3.65

/

TSTEP

```
100*36.5  
/  
TSTEP  
10*365  
/  
TSTEP  
10*365  
/  
END
```

Eclipse 100 Simulation Model, Case 7

```
RUNSPEC  
DIMENS  
1 200 2 /  
OIL  
WATER  
FIELD  
REGDIMS  
2 1 0 0 /  
TABDIMS  
1 1 30 30 1 30 /  
WELLDIMS  
2 50 2 5 /  
START  
1 'JAN' 1983 /  
NSTACK  
200 /
```


GRID

=====

DX

400*400

/

DY

20*1 20*2 20*8 20*9 20*10 20*10 20*9 20*8 20*2 20*1

20*1 20*2 20*8 20*9 20*10 20*10 20*9 20*8 20*2 20*1

/

DZ

200*50

200*25

/

PERMX

200*500

200*100

/

PERMY

200*500

200*100

/

PERMZ

200*50

200*10

/

BOX

1 1 1 200 1 1 /

MULTZ

200*0/

ENDBOX

TOPS

200*8000.0 /

BOX

1 1 1 200 1 1 /

PORO

200*.25

/

BOX

1 1 1 200 2 2 /

PORO

200*.25

/

ENDBOX

RPTGRID

1 1 1 1 1 0 0 0 /

GRIDFILE

2 1 /

INIT

PROPS

=====

SWOF

-- Sw	krw	kro	Pcow
0.2	0	0.85	0
0.25	0.000332936	0.683829014	0
0.3	0.0023187	0.538847423	0
0.35	0.007216059	0.414068396	0
0.4	0.016148364	0.308454264	0
0.45	0.030163141	0.220907729	0

0.5	0.050255553	0.150260191	0
0.55	0.07738113	0.095255667	0
0.6	0.112463739	0.054527525	0
0.65	0.15640102	0.0265625	0
0.7	0.210068317	0.009639196	0
0.75	0.274321643	0.001703985	0
0.8	0.35	0	0

/

PVTW

3460 1.00 3.00E-06 .9 0.0 /

PVCDO

3460 1.250 0 8 /

GRAVITY

34.2 1.07 0.7

/

ROCK

3460.0 5.0E-06 /

REGIONS

=====

SATNUM

400*1 /

FIPNUM

200*1 200*2 /

SOLUTION

=====

EQUIL

8035 3460 15000 0 0 0 1 0 0 /

RPTSOL

PRESSURE SWAT SGAS SOIL FIP /

RPTRST
BASIC=2 /
SUMMARY

=====

RUNSUM
SEPARATE
RPTONLY
FOPR
FWPR
FWIR
FWCT
ROPR
/
RWIR
/
RWPR
/
WBHP
/
FPR
FOPT
FWPT
FWIT
FOE
FOEW
WPI
/
WPI1
/

FLPR

FLPT

FVPR

FVPT

SCHEDULE

=====

RPTSCHED

FIELD 16:55 18 APR 86

1 0 1 0 0 0 2 2 0 0 0 2 0 0 0 0 0

0 0 0 0 0 0 0 0 0 0 0 0 0 0 0 0 0

0 0 0 0 0 0 0 0 0 0 0 0 0 0 0 0 /

WELSPECS

'P' 'G' 1 1 8035 'OIL' /

'T' 'G' 1 200 8035 'WAT' /

/

COMPDAT

'P' ' ' 1 1 1 2 'OPEN' 1 0 .27 3* X /

'I' ' ' 1 200 1 2 'OPEN' 1 0 .27 3* X /

/

WCONPROD

'P' 'OPEN' 'RESV' 4* 1600 /

/

WCONINJ

'T' 'WAT' 'OPEN' 'RESV' 1* 1600 /

/

WECON

P 0 0 .8 /

/

TSTEP

200*3.65

```
/
TSTEP
100*3.65
/
TSTEP
10*36.5
/
TSTEP
10*365
/
TSTEP
10*365
/
END
```

Eclipse 100 Simulation Model, Case 8

```
RUNSPEC
DIMENS
1 200 2 /
OIL
WATER
FIELD
REGDIMS
2 1 0 0 /
TABDIMS
2 1 30 30 1 30 /
WELLDIMS
2 50 2 5 /
```

START

1 'JAN' 1983 /

NSTACK

200 /

GRID

=====

DX

400*400

/

DY

20*1 20*2 20*8 20*9 20*10 20*10 20*9 20*8 20*2 20*1

20*1 20*2 20*8 20*9 20*10 20*10 20*9 20*8 20*2 20*1

/

DZ

200*50

200*25

/

PERMX

200*500

200*100

/

PERMY

200*500

200*100

/

PERMZ

200*50

200*10

/

BOX

1 1 1 200 1 1 /

MULTZ

200*0/

ENDBOX

TOPS

200*8000.0 /

BOX

1 1 1 200 1 1 /

PORO

200*.25

/

BOX

1 1 1 200 2 2 /

PORO

200*.25

/

ENDBOX

RPTGRID

1 1 1 1 1 0 0 0 /

GRIDFILE

2 1 /

INIT

PROPS

=====

SWOF

-- Sw	krw	kro	Pcow
0.2	0	0.85	0
0.25	0.000332936	0.683829014	0

0.3	0.0023187	0.538847423	0
0.35	0.007216059	0.414068396	0
0.4	0.016148364	0.308454264	0
0.45	0.030163141	0.220907729	0
0.5	0.050255553	0.150260191	0
0.55	0.07738113	0.095255667	0
0.6	0.112463739	0.054527525	0
0.65	0.15640102	0.0265625	0
0.7	0.210068317	0.009639196	0
0.75	0.274321643	0.001703985	0
0.8	0.35	0	0

/

0.3	0	0.9	0
0.35	0.01020408	0.56676385	0
0.4	0.04081633	0.32798834	0
0.45	0.09183673	0.16793003	0
0.5	0.16326531	0.07084548	0
0.55	0.25510204	0.02099125	0
0.6	0.36734694	0.00262391	0
0.65	0.5	0	0

/

PVTW

3460 1.00 3.00E-06 .9 0.0 /

PVCDO

3460 1.250 0 8 /

GRAVITY

34.2 1.07 0.7

/

ROCK

3460.0 5.0E-06 /

REGIONS

=====

-- Specifies the number of saturation regions (only one for this case)

SATNUM

200*1 200*2 /

FIPNUM

200*1 200*2 /

SOLUTION

=====

EQUIL

8035 3460 15000 0 0 0 1 0 0 /

RPTSOL

PRESSURE SWAT SGAS SOIL FIP /

RPTRST

BASIC=2 /

SUMMARY

=====

RUNSUM

SEPARATE

RPTONLY

FOPR

FWPR

FWIR

FWCT

ROPR

/

RWIR

/
 RWPR
 /
 WBHP
 /
 FPR
 FOPT
 FWPT
 FWIT
 FOE
 FOEW
 WPI
 /
 WPI1
 /

FLPR
 FLPT
 FVPR
 FVPT
 SCHEDULE

=====

RPTSCHED FIELD 16:55 18 APR 86

1 0 1 0 0 0 2 2 0 0 0 2 0 0 0 0 0
 0 0 0 0 0 0 0 0 0 0 0 0 0 0 0 0
 0 0 0 0 0 0 0 0 0 0 0 0 0 0 0 0 /

WELSPECS

'P' 'G' 1 1 8035 'OIL' /
 'T' 'G' 1 200 8035 'WAT' /

```
/
COMPDAT
P ' 1 1 1 2 'OPEN' 1 0 .27 3* X /

I ' 1 200 1 2 'OPEN' 1 0 .27 3* X /
/
WCONPROD
P ' 'OPEN' 'RESV' 4* 1600 /
/
WCONINJ
T 'WAT' 'OPEN' 'RESV' 1* 1600 /
/
WECON
P 0 0 .8 /
/
TSTEP
200*3.65
/
TSTEP
100*36.5
/
TSTEP
10*365
/
TSTEP
10*365
/
END
```

Eclipse 100 Simulation Model, Case 9

RUNSPEC

DIMENS

1 200 2 /

OIL

WATER

FIELD

REGDIMS

2 1 0 0 /

TABDIMS

1 1 30 30 1 30 /

WELLDIMS

2 50 2 5 /

START

1 'JAN' 1983 /

NSTACK

200 /

GRID

=====

DX

400*400

/

DY

20*1 20*2 20*8 20*9 20*10 20*10 20*9 20*8 20*2 20*1

20*1 20*2 20*8 20*9 20*10 20*10 20*9 20*8 20*2 20*1

/

DZ

200*35

200*35

/

PERMX

200*500

200*350

/

PERMY

200*500

200*500

/

PERMZ

200*50

200*50

/

BOX

1 1 1 200 1 1 /

MULTZ

200*0/

ENDBOX

TOPS

200*8000.0 /

BOX

1 1 1 200 1 1 /

PORO

200*.25

/

BOX

1 1 1 200 2 2 /

PORO

200*.25

/

ENDBOX

RPTGRID

1 1 1 1 1 0 0 0 /

GRIDFILE

2 1 /

INIT

PROPS

=====

SWOF

-- Sw	krw	kro	Pcow
0.2	0	0.85	0
0.25	0.000332936	0.683829014	0
0.3	0.0023187	0.538847423	0
0.35	0.007216059	0.414068396	0
0.4	0.016148364	0.308454264	0
0.45	0.030163141	0.220907729	0
0.5	0.050255553	0.150260191	0
0.55	0.07738113	0.095255667	0
0.6	0.112463739	0.054527525	0
0.65	0.15640102	0.0265625	0
0.7	0.210068317	0.009639196	0
0.75	0.274321643	0.001703985	0
0.8	0.35	0	0

/

PVTW

3460 1.00 3.00E-06 .9 0.0 /

PVCDO

3460 1.250 0 8 /

GRAVITY

34.2 1.07 0.7

/

ROCK

3460.0 5.0E-06 /

REGIONS

=====

SATNUM

400*1 /

FIPNUM

200*1 200*2 /

SOLUTION

=====

EQUIL

8035 3460 15000 0 0 0 1 0 0 /

RPTSOL

PRESSURE SWAT SGAS SOIL FIP /

RPTRST

BASIC=2 /

SUMMARY

=====

RUNSUM

SEPARATE

RPTONLY

FOPR

FWPR

FWIR

FWCT


```

    0 0 0 0 0 0 0 0 0 0 0 0 0 0 0 0 /
WELSPECS
'P' 'G'  1  1  8035 'OIL' /
'T' 'G'  1 200 8035 'WAT' /
/
COMPDAT
'P'  '  1  1  1  2 'OPEN'  1  0  .27 3* X /
'I'  '  1 200  1  2 'OPEN'  1  0  .27 3* X /
/
WCONPROD
'P' 'OPEN' 'RESV' 4* 800 /
/
WCONINJ
'T' 'WAT' 'OPEN' 'RESV' 1* 800 /
/
WECON
P 0 0 .8 /
/
TSTEP
200*3.65
/
TSTEP
10*36.5
/
TSTEP
10*365/
TSTEP
10*365/
END

```

VITA

Name: Rustam Rauf Gasimov

Address: Nasimi 22, apt.32, Baku, Azerbaijan

Email: kasimov_rustam@yahoo.com

Education: B. S., Petroleum Engineering, Azerbaijan State Oil Academy, Baku,
Azerbaijan (July 2001)

M.S., Petroleum Engineering, Texas A&M University, College Station,
TX 77843-3116, U.S.A. (August 2005)